

平成 26 年度  
環境研究総合推進費補助金 研究事業  
総合研究報告書

破碎・凝結プロセスを伴う生物スラッジの  
超高圧圧搾脱水法の開発  
(3K123005)

平成 27 年 3 月

名古屋大学 入谷 英司

補助事業名 環境研究総合推進費補助金研究事業（平成 24 年度～平成 26 年度）

所管 環境省

国庫補助金 33,332,000 円

研究課題名 破碎・凝結プロセスを伴う生物スラッジの超高压圧搾脱水法の開発

研究期間 平成 24 年 6 月 8 日～平成 27 年 3 月 31 日

研究代表者名 入谷英司（名古屋大学）

研究分担者 片桐誠之（名古屋大学）

## 目 次

総合研究報告書概要 .....	1
本文	
1. 研究背景と目的 .....	6
1.1 研究背景 .....	6
1.2 研究目的 .....	13
2. 研究方法 .....	15
2.1 実験試料 .....	16
2.2 破砕・凝結プロセスの確立 .....	17
2.3 低圧圧搾（濾過）脱水法の確立 .....	19
2.4 超高压圧搾脱水法の確立 .....	22
3. 結果と考察 .....	24
3.1 下水余剰汚泥の破砕・凝結処理 .....	24
3.2 低圧圧搾（濾過） .....	30
3.3 超高压圧搾 .....	32
3.4 新規圧搾モデルの提案 .....	38
3.5 実用化への検討 .....	51
4. 結論 .....	56
5. 参考文献 .....	57
6. 研究発表 .....	58
論文発表	
学会等発表	
※「国民との科学・技術対話」の実施	
7. 知的財産権の取得状況 .....	96
研究概要図 .....	97
英文概要 .....	98

## 環境研究総合推進費補助金 研究事業 総合研究報告書概要

研究課題名：破砕・凝結プロセスを伴う生物スラッジの超高压圧搾脱水法の開発

研究番号：3K123005

国庫補助金清算所要額：33,332,000 円

研究期間：平成24年6月8日～平成27年3月31日

研究代表者名：入谷英司（名古屋大学）

研究分担者：片桐誠之（名古屋大学）

### 研究目的

産業廃棄物の中で最大の排出量割合を占める汚泥を減量化するための高効率な脱水法の開発が切望されている。濾過や圧搾等の省エネルギー的な機械的分離操作は、有望な手法であり、下水余剰汚泥や消化汚泥等の難脱水性生物スラッジを対象として、強固で粗大なフロックを形成する高性能な高分子凝集剤の開発による脱水速度の向上、あるいは圧搾における操作圧の増大による脱水度の向上（ケーキ含水率の低減化）が取り組まれてきた。しかしながら、高分子凝集剤を使用すると高压を作用させても強固なフロック内の水分の除去は困難で低含水率ケーキは得られないという致命的な欠点をもつ。一方、凝集剤を使用せずに高压を作用させると、ケーキの高い圧縮性のため脱水速度は低压下より減少することもあり、現在の技術では難脱水性生物スラッジの高効率な脱水は困難な状況にある。

本研究では、両者の欠点を克服する革新的な技術として、破砕・凝結プロセスを伴う超高压圧搾脱水法を提案し、その有効性を明らかにする。本手法は、提案する破砕・凝結プロセ

スにより、フロックを一端崩壊させてフロック内の束縛水を放出させると共に、スラッジ表面の特性をコントロールし、凝集剤フリーで緩く凝結したフロックを形成させて高速脱水を行い、ステップ超高压圧搾で凝結フロックを崩壊しつつ高度脱水するものであり、汚泥による環境負荷を低減させることを目指す。破碎・凝結プロセスによる脱水速度の向上とステップ超高压圧搾による脱水度の向上が生じるそれぞれの機構を解明し、得られた成果に立脚して、両者を融合することによって初めて達成される最も効率的な脱水性能を得るための設計指針を提示することを目的とする。

## 研究方法

代表的な難脱水性生物スラッジである下水余剰汚泥を対象に、高压圧搾速度と高脱水度を達成するために適した破碎・凝結プロセス及びステップ超高压圧搾の手法と操作条件を明らかにし、より高効率の高速脱水法の設計指針を提示する。破碎・凝結プロセスについては、超音波照射、ビーズミル、ホモジナイザー、エレクトロポレーションを用いる手法について検討を行い、その作用効果を比較し、より優れた破碎・凝結の手法と操作条件を探求する。破碎操作により一端フロックを崩壊させ、フロック内の束縛水を放出させるとともに、スラッジ表面の特性を変化させ、スラリー中のイオン、ポリマー等を利用して凝集剤を添加することなく形成する緩い自己凝結フロックに関する基礎特性を把握して低圧圧搾での脱水速度の増大への寄与を明らかにし、破碎・凝結プロセスの指針を得る。また、破碎・凝結プロセスが超高压圧搾操作でのフロックの崩壊や達成される脱水ケーキの最終脱水度に及ぼす影響について検討し、ステップ超高压圧搾に適した破碎・凝結の手法と操作条件を見出すとともに、圧搾圧力とケーキ脱水度との関係を明らかにし、超高压圧搾操作の指針を得る。現象をより科学的に解明するため、実際の汚泥と併せてモデル汚泥を用いた検討も行い、破碎・凝結プロセスや超高压圧搾の機構解明に挑み、最適操作法の確立のための指針を得る。

## 結果と考察

代表的な難脱水性生物スラッジである下水余剰汚泥を対象に、本研究で提案する破碎・凝結プロセスとステップ超高压圧搾とを融合した脱水法の適用の可能性を検討した。提案するプロセスのコンセプトは、スラッジを破碎して、一端フロックを崩壊させることによりフロック内の束縛水を放出させると共に、破碎方法によりスラッジ表面の特性をコントロールし、スラリー中のイオン、ポリマー等を利用して凝集剤を添加することなく緩く自己凝結した粗大フロックを形成させ、低压圧搾操作で迅速に汚泥中の多量の水分を除去した後、引き続いて行う超高压圧搾操作による圧縮作用によって、生成濾過ケーキ内の凝集フロックが崩壊し、直ちにケーキの低含水率化が行われるというものである。

### <下水余剰汚泥の破碎・凝結処理>

超音波照射、ビーズミル、ホモジナイザー、エレクトロポレーションによる下水余剰汚泥の破碎・凝結操作を試みたところ、特に超音波を照射した場合に顕著な効果が見られた。超音波照射により汚泥フロックが破碎されるため、フロック径は一旦減少するが、その後に緩速攪拌を行うと増大するようになり、自己凝結フロックが形成されることを粒度分布測定と顕微鏡観察により確認した。

### <低压圧搾（濾過）>

破碎・凝結プロセスを経た汚泥懸濁液の低压圧搾を窒素ガスにて加圧する形式の定圧濾過にて行った。汚泥原液と比較して破碎・凝結プロセス後の汚泥では濾過抵抗が増大したが、これは自己凝結フロックに取り込まれない微細粒子が僅かではあるがスラリー中に存在するためである。遠心分離により上澄液中の微細粒子を除去することで、濾過抵抗を著しく小さくすることができた。低压圧搾の前工程として濃縮槽を設置し、微細粒子を含む上澄液については水処理工程における曝気槽に戻して生分解処理することにより、低压圧搾速度の向上と破碎汚泥の減量化が図れる。

### <超高压圧搾>

低圧圧搾した汚泥ケーキを 10 ～ 50 MPa の超高压で圧搾したところ、含水率が 27 ～ 47%と、既存技術と比較して極めて小さい脱水汚泥を得ることができた。含水率が最も小さくなった条件では、脱水時間 1 分で含水率は約 40%、1 時間で約 30%となり、コンポスト化、焼却、炭化、熔融など以後の汚泥処理法に合わせて適切な条件設定を行うことで効率的な脱水が実現できる。微生物細胞内の水分が 70 ～ 80 %であることを考えると、単にフロックの崩壊による汚泥粒子間の自由水や粒子表面の付着水だけでなく、細胞内に含まれる束縛水も除去されていると考えられる。なお、下水余剰汚泥の脱水特性は採取する時期によって変化したが、破碎・凝結プロセスを経ること、また圧力を大きくすることによる含水率の減少は明確であり、本手法の有用性が確認できた。また、汚泥の圧搾脱水挙動のモデル化を行い、修正 Terzaghi-一般化 Voigt モデルにて脱水挙動の推算が可能であることを明らかにした。

### 環境政策への貢献

本研究で提案する難脱水性生物スラッジの高速減量化技術が確立されれば、産業廃棄物の中で最も大きな排出量割合を占め、水分含量が高い汚泥を、現存技術では想定できないほどの極めて低い含水率に、最も省エネルギー的な機械的固液分離操作によって高速で処理でき、「スラッジによる環境負荷の低減」に繋がる。また、以後の焼却等の操作の負荷低減にも結び付くことから、「地球温暖化に関する取り組み」への貢献も期待できる。脱水汚泥は、凝集剤フリーで処理されるため、薬品が含まれず、「再資源化」への用途も大きく拡がり、「物質循環の確保と循環型社会構築のための取組」への貢献が極めて大きい。また、本技術は、エネルギー利用の観点から注目される消化スラッジや食品廃棄物スラッジ等にも適用でき、その再資源化のキーテクノロジーであることから、環境問題と資源・エネルギー問題との密接な関係を念頭においた環境経済の政策研究の趣旨とも一致している。さらに、「水環境の保全」とともに「水の循環再利用」を促進するために行われる、様々な廃水を対象とした高度処理においても、大量の生物スラッジが発生し、その適切な処理が必要とされることから、水循環の確保においても本技術の果たす役割は大きい。

## 研究成果の実現可能性

本手法は、凝集剤を用いることなく、破碎・凝結操作により自己凝結フロックを形成させ、ステップ超高压により下水余剰汚泥の含水率を極めて小さくすることが可能である。脱水汚泥の含水率は 27 ～ 47% となり、コンポスト化、焼却、炭化、熔融など以後の汚泥処理法に合わせて適切な条件設定を行うことで効率的な脱水が実現できる。破碎・凝結プロセスや超高压脱水機で必要となるエネルギーは、現状プロセスにおける汚泥の乾燥工程よりも著しく小さく、汚泥の含水率を 40% にすることを想定すると、超音波照射式破碎を導入した場合の所要エネルギーは、脱水・乾燥を行う現状プロセスの 8% 程度であり、省エネルギーでの操作が可能である。また、凝集剤を用いないため再資源化への用途が広がり、実用化のメリットは大きい。なお、検討課題となった自己凝結フロックに取り込まれない微細粒子については、濃縮槽を設置することで、圧搾操作で排出される搾液とともに廃水に混合させ、曝気槽での処理が可能である。超高压下での使用が可能で汚泥の漏れの小さい濾布の選定は済ませており、超高压脱水機の大型化と余剰汚泥の連続的な破碎・凝結を行うための装置のライン化が今後の課題となるが、本研究成果の実現可能性は十分に期待できる。

## 結論

破碎・凝結プロセスとステップ超高压圧搾とを融合した脱水法を提案し、脱水時間と脱水度の両面から、現存技術に比べ格段に優れていることを実証した。難脱水性生物スラッジとして下水余剰汚泥を例にとり、超音波照射と緩速攪拌による破碎・凝結操作と 10 ～ 50 MPa の超高压圧搾とを組み合わせた脱水操作により、含水率が 27 ～ 47% と、既存技術と比較して極めて小さい脱水汚泥を得ることができた。圧密脱水速度も著しく向上し、含水率が最も小さくなった条件では、コンポスト化を想定した場合の含水率 60% は超高压圧搾脱水時間 1 秒、焼却や炭化の場合の含水率 40% は 1 分、熔融の場合の含水率 30% は 1 時間で達成した。下水余剰汚泥の脱水特性は採取する時期によって変化したが、破碎・凝結プロセスを経ること、また圧力を大きくすることによる含水率の減少は明確であり、本手法の有用性を示すことができた。

## 1. 研究背景と目的

### 1. 1 研究背景

本研究の開始前年にあたる平成 23 年度における産業廃棄物の排出量に関するデータによると、Fig. 1 に示すようにほぼ半数にあたる 43.6 %を汚泥が占めている<sup>1)</sup>。したがって、難脱水性生物スラッジの高効率な脱水法の開発は、汚泥の減量化や脱水汚泥の資源としての有効利用の見地から現在急務とされている課題である。

代表研究者が長年にわたり研究を続けている濾過、圧搾等の機械的固液分離が最も省エネルギー的であることから、現在も国の内外で機械的分離に関して多くの研究や技術開発が行われている<sup>2)</sup>。これらのほとんどは、Fig. 2 に示すように強固で粗大なブロックを形成する高性能な高分子凝集剤の開発による脱水速度の向上、あるいは圧搾における操作圧の増大による脱水度の向上（ケーキ含水率の低減化）を目指すものである。しかし、高分子凝集剤を使用すると高圧を作用させても強固なブロック内の水分の除去は困難で低含水率ケーキは得られないという致命的な欠点をもつ。一方、凝集剤を使用せずに高圧を作用させると、ケーキの高い圧縮性のため脱水速度は低圧下より減少することもあり、現在の技術では難脱水性有機汚泥の高効率な脱水は困難な状況にある。

本研究では、両者の欠点を克服する革新的な技術として、Fig. 3 に示す破碎・凝結プロセスを伴う超高压圧搾脱水法を提案して、その有効性を検証し、脱水機構の解明に基づき最適な操作法を提示する。Fig. 4 に示すように、破碎・凝結プロセスにより、汚泥ブロックを一端崩壊させてブロック内の束縛水を放出させると共に、スラッジ表面の特性をコントロールし、スラリー中のイオン、ポリマー等を利用して凝集剤フリーで緩く凝結したブロックを形成させて高速脱水を行い、次いで圧力をステップ状に増加させて超高压を作用させ、ケーキ内に残存する束縛水を機械的圧力で可能な限界まで除去する。高い脱水速度と高い脱水度の両者を同時に満足する省エネルギー的な脱水プロセスの確立が期待できる。



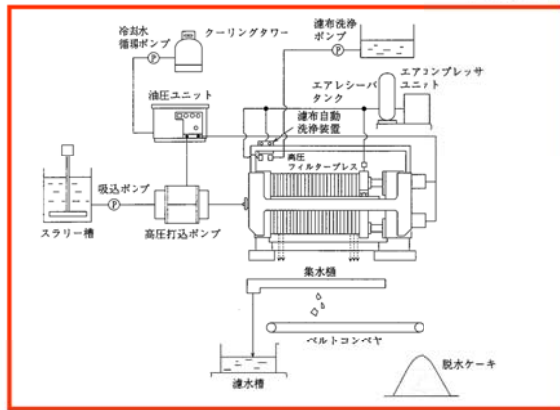
# 現状技術の限界

- 優れた高分子凝集剤の開発

→ 脱水速度の向上

- 高圧フィルタープレスの開発  
(圧力: 3.9 MPa)

条辺ら: 新日鉄技報,  
372, 67 (1999)より



下水余剰スラッジ  
消化スラッジ  
食品廃棄物スラッジ  
畜産スラッジ  
など

高分子凝集剤を使用する → 強固なフロックのため、  
低含水率ケーキが得られない  
高分子凝集剤を使用しない → 脱水速度が小さい

現状技術では、難脱水性生物スラッジの高効率な高度脱水は困難

Fig. 2 機械的脱水法における現状技術の限界

# 提案する技術

## 破碎・凝結プロセスを伴う超高压圧搾脱水法

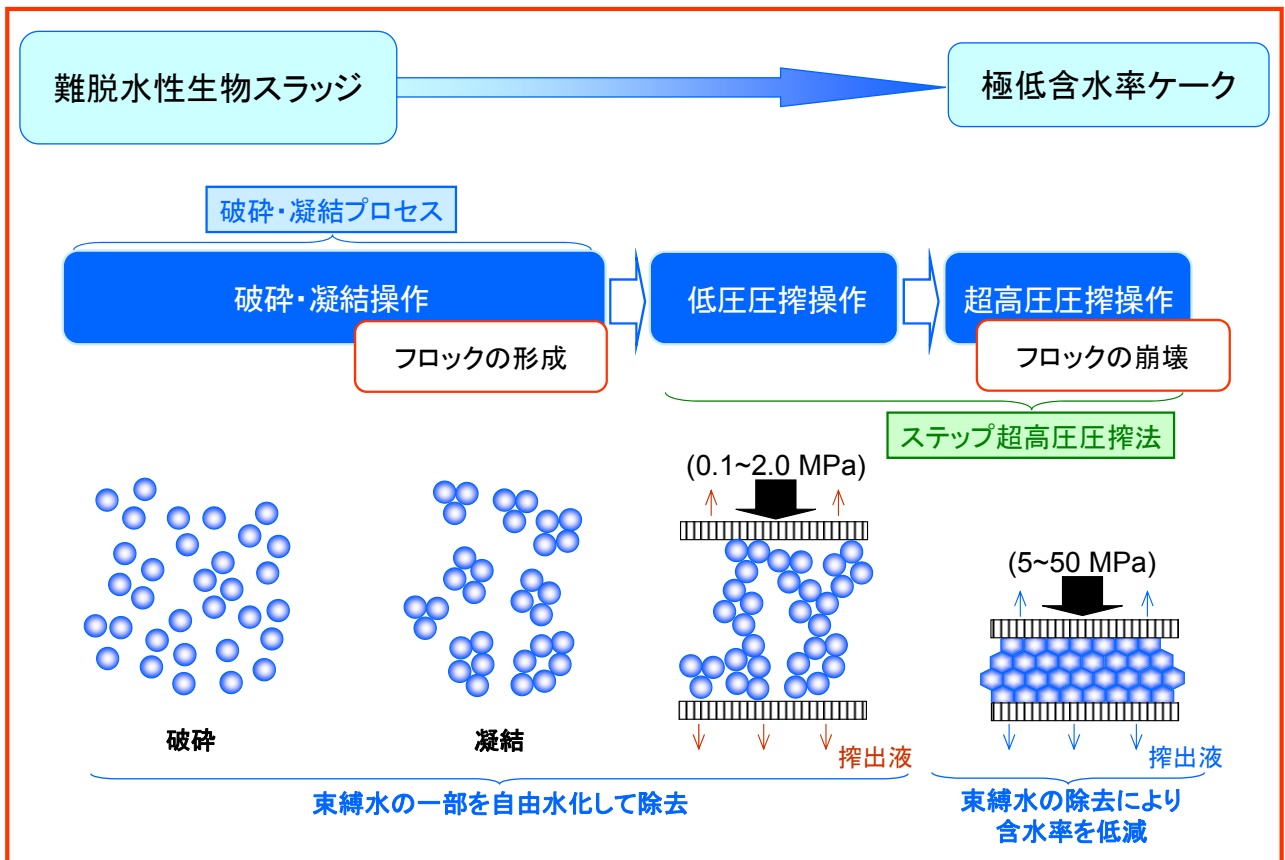


Fig. 3 本研究で提案する高効率高速脱水法

# 破砕・凝結操作の意図

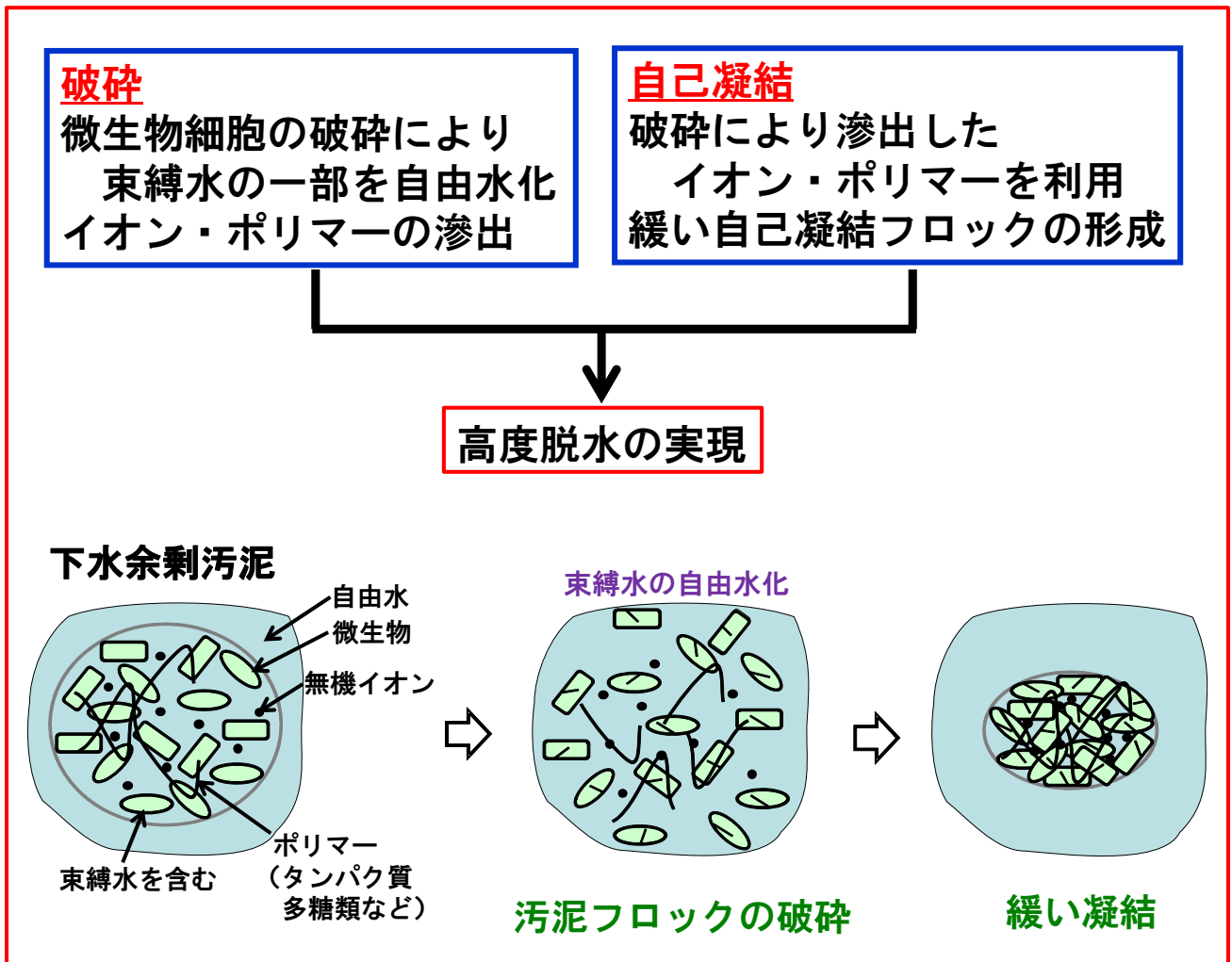


Fig. 4 破砕・凝結プロセス導入の意図

## <現存脱水技術>

汚泥の減量化において、最も省エネルギー的な操作である機械的固液分離には、種々のタイプの脱水機が使用されている。また、脱水機による汚泥の高度な脱水は、圧搾操作によってもたらされる。現存技術である主な脱水機を以下に示す。

### ○脱水機

有機汚泥に対して用いられている脱水機として、真空脱水機、加圧脱水機（フィルタープレス）、ベルトプレス、遠心脱水機、圧入式スクリーンプレスなどがある。各脱水機の長所と短所を以下に示す。

#### ・真空脱水機

真空圧により脱水を行う装置。

長所：連続運転でメンテナンスが容易。

短所：脱水ケーキの含水率が大きい。消費電力が大きい。濾布の交換が必要。

#### ・加圧脱水機（フィルタープレス）

加圧により脱水を行う装置で、真空圧よりも大きな圧力を作用させることができる。

長所：脱水ケーキの含水率が小さい。

短所：バッチ運転。補機が多く、機器設置面積が大きい。濾布の交換が必要。

#### ・ベルトプレス

2枚のベルト間にスラリーを挟んで、多数のロールの間をベルトにより屈曲移送させて脱水を行う装置。

長所：脱水ケーキの含水率が小さい。連続運転でメンテナンスが容易。

短所：多量の濾布洗浄水が必要。濾布の交換が必要。

- ・遠心脱水機

高速回転による遠心力により脱水を行う装置。

長所：脱水ケーキの含水率が小さい。連続運転でメンテナンスが容易。

短所：消費電力が大きい。高速回転のため振動・騒音対策が必要。

- ・圧入式スクリープレス

固定された外筒のバレルとその中で回転するスクリー軸からなり、スクリー軸の回転によってスラリーを出口方向へ送って次第に狭げき部へ押し込み、その際に受ける高圧によって脱水を行う装置。

長所：脱水ケーキの含水率が小さい。連続運転でメンテナンスが容易。

短所：スクリーンの交換が必要。回収率が小さい。

最近では、3.9 MPa の高圧フィルタープレスが開発され、更なる高圧化への取り組みがなされつつあり、実用スケールにおける超高圧圧搾操作に利用できる。なお、現存技術における下水汚泥脱水ケーキの含水率の最高水準は 60～70 % である。

## 1. 2 研究目的

本研究では、現在の機械的固液分離技術では高効率な脱水が困難な下水スラッジ、消化スラッジ、食品廃棄物スラッジ、畜産スラッジなどの難脱水性生物スラッジを対象に、高速減量化を実現できる手法の提案を行い、その有効性を明らかにするとともに、操作の設計指針を得ることを目的とする。

本手法は、提案する破碎・凝結プロセスにより、凝集剤フリーで緩く凝結したフロックを形成させて高速脱水を行い、ステップ超高压圧搾で凝結フロックを崩壊しつつ高度脱水するものであり、従来の技術では不可能な脱水度の低含水率ケーキを高速度で得て、スラッジによる環境負荷を低減させることを目指す。破碎・凝結プロセスと超高压圧搾による脱水速度および脱水度の向上が生じる機構を解明し、得られた成果に立脚して、最も効率的な脱水性能を得るための設計指針を提示することを最終目的とする。

難脱水性生物スラッジである下水余剰汚泥を対象に、Fig. 5 に示す研究計画に沿って、破碎・凝結プロセスとステップ超高压圧搾とを融合した高効率の高速脱水法の適用の可能性を脱水速度と脱水度の両面から探求する。破碎・凝結プロセスでは、超音波照射、ビーズミル、ホモジナイザー等による破碎法を検討し、一端フロックを崩壊させることによりフロック内の束縛水を放出させるとともに、破碎によりスラッジ表面の特性を変化させ、スラリー中のイオン、ポリマー等を利用して凝集剤を添加することなく緩い凝結フロックを形成させる。フロック内の束縛水の放出量、表面特性の変化、凝結の程度等、それらの優劣を検討して第一段階の低圧圧搾で脱水速度を最大にするために最も効果的な操作法と操作条件を見出す。ステップ超高压圧搾では、フロックの崩壊が容易な破碎・凝結プロセスの操作指針を得るとともに、超高压作用下で達成できる脱水ケーキの含水率の限界値を汚泥性状と関連付けて明らかにし、超高压圧搾の最適操作条件を見出す。

# 研究計画

	破碎・凝結	低圧圧搾	超高压圧搾
H24年度	破碎・凝結プロセスの確立(超音波照射法, ビーズミル, せん断ホモジナイザー) 担当: 片桐, 入谷		
	破碎・凝結操作による低圧圧搾の高性能化 担当: 片桐		超高压圧搾の高性能化 担当: 入谷
H25年度	破碎・凝結プロセスの確立(超音波照射法, ビーズミル, せん断ホモジナイザー, エレクトロポーレーション法, ジェット噴流法) 担当: 片桐, 入谷		
			破碎・凝結の手法に応じた 超高压圧搾の手法の開発 担当: 入谷
H26年度	破碎・凝結プロセスの確立 担当: 片桐, 入谷		超高压脱水法の確立 担当: 入谷
	破碎・凝結とステップ超高压圧搾の融合によるプロセスの最適化 担当: 入谷, 片桐		

Fig. 5 研究目的達成のための研究計画と実施担当者

## 2. 研究方法

代表的な難脱水性生物スラッジである下水余剰汚泥を対象に、破碎・凝結プロセスとステップ超高压圧搾とを融合した高効率の高速脱水法の適用の可能性を、脱水速度と脱水度の両面から探求する。

破碎・凝結プロセスでは、Fig. 6 に示す超音波照射、ビーズミル、ホモジナイザー等による破碎法を検討し、一端フロックを崩壊させることによりフロック内の束縛水を放出させると共に、破碎によりスラッジ表面の特性を変化させ、スラリー中のイオン、ポリマー等を利用して凝集剤を添加することなく形成する緩い自己凝結フロックに関する基礎特性を把握して低圧圧搾での脱水速度の増大への寄与を明らかにし、破碎・凝結プロセスの指針を得る。また、汚泥粒子やその凝結・崩壊フロックへの水の様々な結合状態を調べるとともに、圧搾圧力とケーキ脱水度との関係を明らかにし、破碎・凝結プロセスを伴う脱水法における超高压圧搾操作のための指針を得る。現象をより科学的に解明するため、実際の汚泥と併せてモデル汚泥を用いた検討も行い、破碎・凝結プロセスや超高压圧搾の機構解明に挑み、最適操作法の確立のための指針を得る。

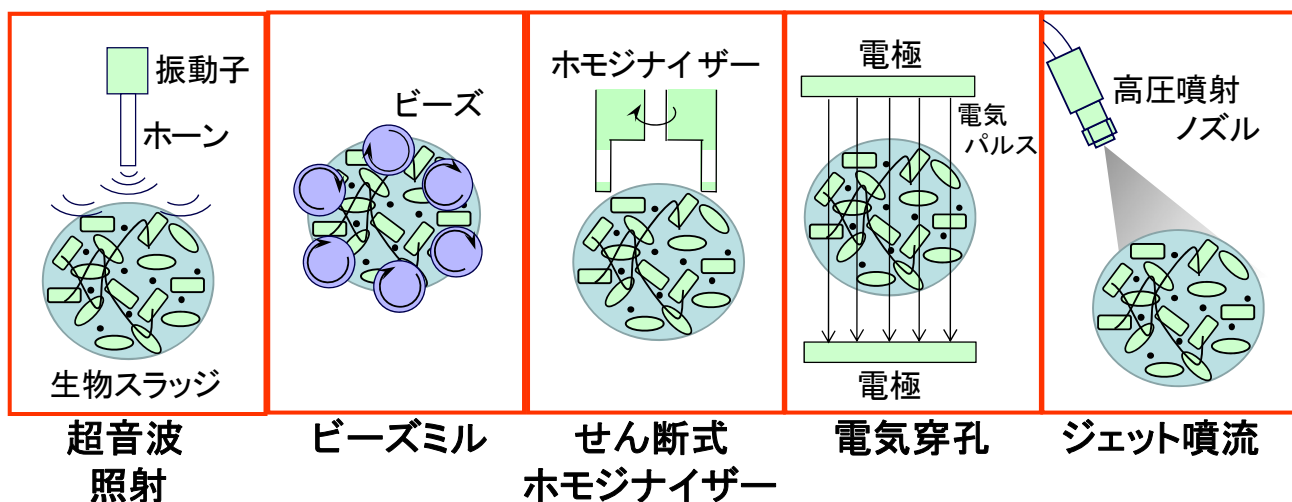


Fig. 6 種々の破碎法

## 2. 1 実験試料

### 生物スラッジ（活性汚泥）

活性汚泥とは、種々の細菌を含有したゼラチン状（高分子有機体）を主体とした「フロック（flocs）」とその周りに棲息している原生動物をいう。浄化を行う細菌類が粘性物質を分泌して無生物のフロックを形成し、その中に細菌類は棲息する。そのフロックの主成分は多糖類、タンパク質、核酸であるといわれている。活性汚泥では、このフロック形成能（floc forming）をもつ細菌集団のみが活性汚泥に定着することができる。なぜなら、フロックは重力をもつので、フロックの中に棲んでいれば、沈殿槽で上澄液と沈降分離して、曝気槽へ返送され、その菌数を一定に保つことができるからである。フロック形成能のない細菌群は曝気槽から沈殿槽へ行ったとき、上澄液中に懸濁し、処理水と一緒に流される。正常な活性汚泥は 1 mL 中  $10^7 \sim 10^8$  の細菌密度で棲息している<sup>3)</sup>。

本実験では、名古屋市上下水道局植田水処理センターから採取した活性汚泥（余剰汚泥）を用いた。乾燥濃度測定の結果、汚泥濃度は 4000～5000 mg/L で、ピクノメーターを用いた密度測定の結果、汚泥密度  $\rho_s = 1.451 \text{ g/cm}^3$  であった。4℃の冷蔵庫内における 20 時間のデカンテーションで濃縮し、質量濃度  $s = 0.005$  に調整したものを実験試料とした。

## 2. 2 破碎・凝結プロセスの確立

超音波ホモジナイザー (UP-200S, Dr. Hielscher 製)、ビーズミル (ビーズビーター11079-S, Hamilton Beach 製; ビーズクラッシャー $\mu$ T-12, タイテック製; サンプルクラッシャー TK-AM5, タイテック製)、せん断式ホモジナイザー (T-25, IKA 製)、エレクトロポレーター (Gene Pulser Xcell, BIO-RAD 製) による下水余剰汚泥の破碎と攪拌機 (BL600, 新東科学製) を用いた緩速攪拌による凝結の操作方法を検討した。

Fig. 7 には、破碎・凝結効果が顕著であった超音波照射による破碎と攪拌による凝結の操作方法を示した。汚泥懸濁液を 100 mL ビーカーに 80 mL 取り出し、超音波ホモジナイザーのホーンの先端を試料の上端から約 3 分の 1 まで入れ、0.5 s 周期で断続照射した。装置の最大出力は 200 W で、その 20 ~ 100%、すなわち 40 ~ 200W の出力で照射が可能である。照射条件としては、出力  $P = 40, 80, 120$  W、実照射時間  $t = 5, 15, 35, 60$  s で実験を行った。なお実照射時間は、0.5 s 周期の断続照射のため、実際の操作時間の半分となる。超音波照射後、50 rpm で緩速攪拌を行い、活性汚泥フロックの自己凝結を促した。

破碎および凝結効果の評価は、レーザー回折式粒度分布測定 (SALD2200, 島津製作所製)、顕微鏡観察 (デジタルマイクロスコープ BA210E, 島津理化製)、また内径 2.9 cm のアクリル製沈降管を用いた重力沈降試験により行った。

## ～破碎・凝結操作～

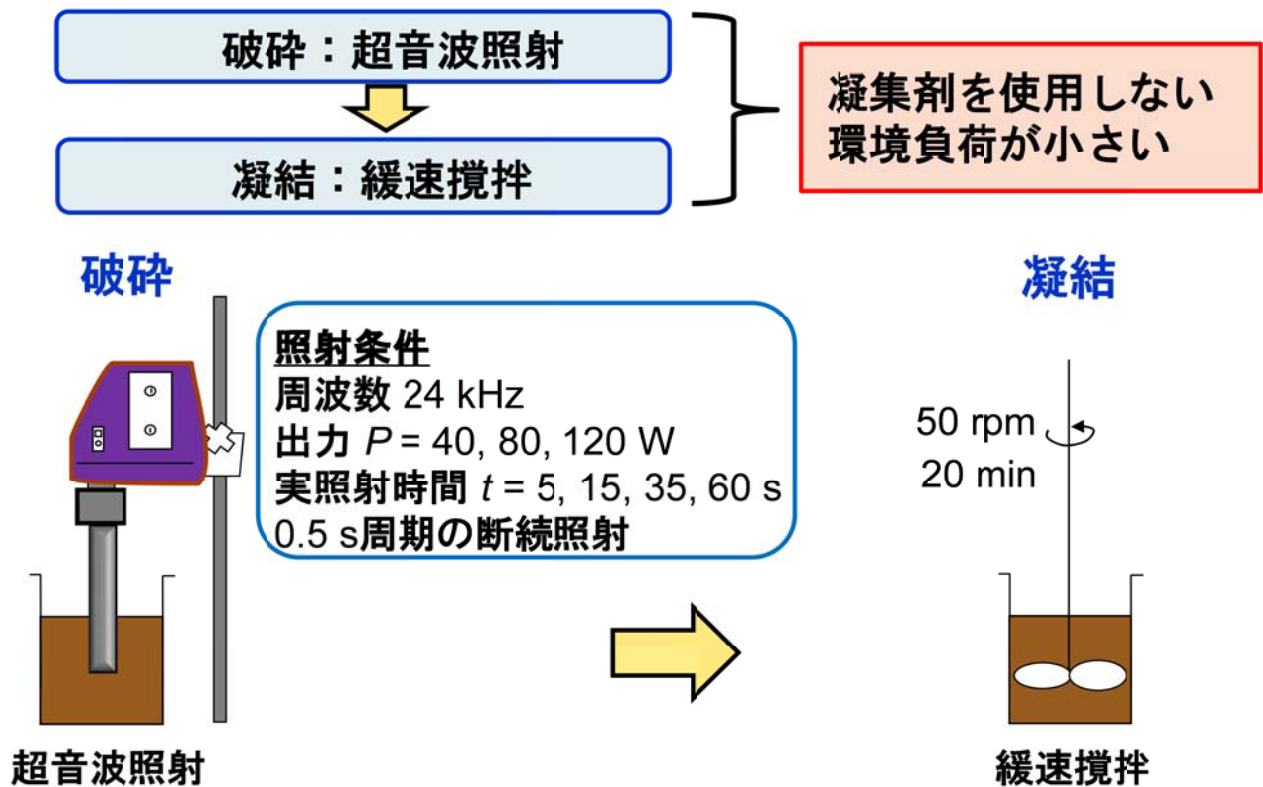


Fig. 7 超音波照射と緩速攪拌による汚泥フロクの破碎・凝結

### 2. 3 低圧圧搾（濾過）脱水法の確立

Fig. 8 には、本研究において設計・製作した超高压圧搾セルを示す。ステンレス製、セル内径 3.50 cm、セル断面積 9.62 cm<sup>2</sup> で、窒素加圧による低圧圧搾（濾過）と材料試験機による超高压圧搾の両操作が可能である。この超高压圧搾セルを用いて Fig. 9 に示すシステム<sup>4)</sup>により、圧力  $p_f = 98$  kPa で汚泥の低圧圧搾（濾過）を行い、脱水量  $v$  の経時変化を測定した。濾材には、濾布 TRG803K（岡山中尾フィルター製）を用いた。Table 1 に濾布の物性値を示す。

Table 1 濾布の物性値

型番	TRG803K
厚み [mm]	0.34
質量 [g/m <sup>2</sup> ]	324
通気性 [cm <sup>3</sup> /cm <sup>2</sup> /s]	0.3 以下
糸の形態	スパン

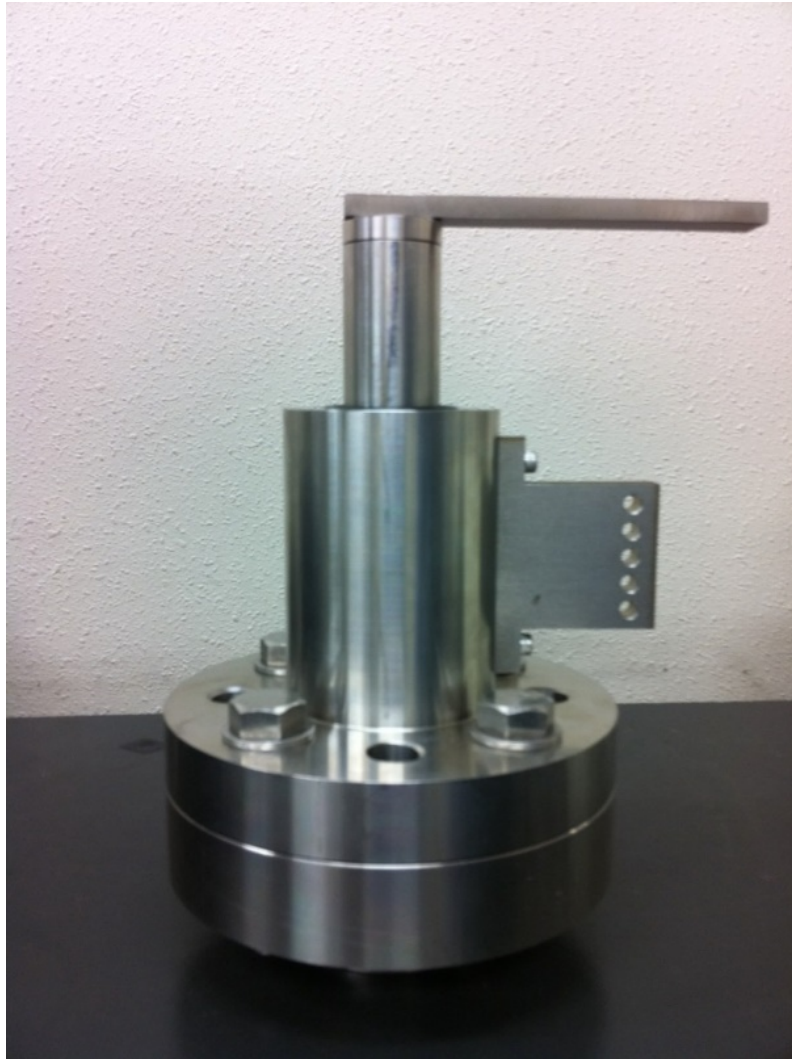
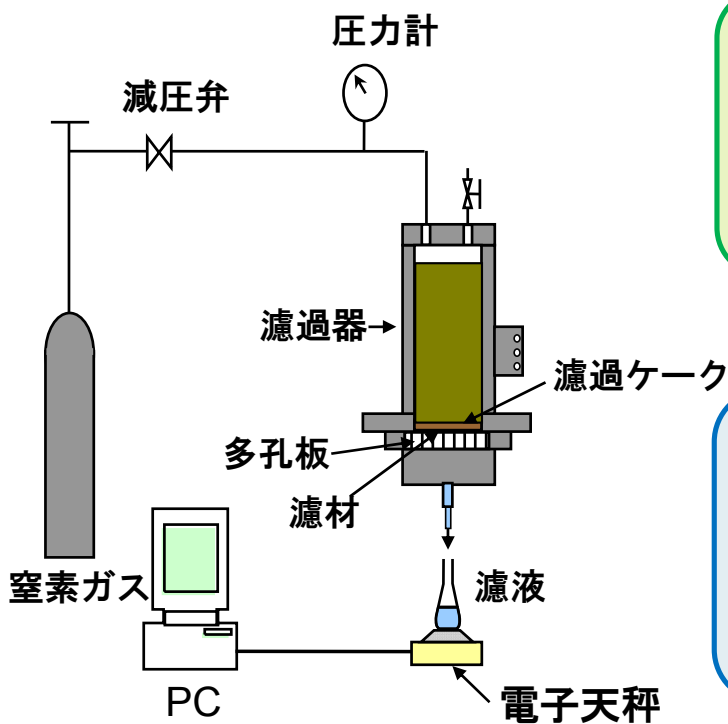


Fig. 8 超高压压搾セル

# ～低圧圧搾(濾過)～

## 濾過装置



### 実験条件

濾過圧力  $p_f = 98 \text{ kPa}$

濾過面積  $A = 9.62 \text{ cm}^2$

### 濾材

濾布 TRG803K  
(岡山中尾フィルター製)

通気性  $0.3 \text{ cm}^3/(\text{cm}^2 \cdot \text{s})$

Fig. 9 脱水（低圧圧搾）装置の概略図

## 2. 4 超高压压搾脱水法の確立

低压压搾（濾過）終了後、压搾セルの上部フランジを外してピストンと付け替え、また下部フランジに接続されたステンレス製の管とネジを付け替えて、Figs. 10, 11 に示すように材料試験機（SC-50H, 東京試験機製）にて定压压搾<sup>5)</sup>を行った。はじめに、压力  $p_1 = 98 \text{ kPa} \sim 2 \text{ MPa}$  で予压密した後、压力を上げて压搾压力  $p_2 = 10 \sim 50 \text{ MPa}$  で両面排水にて压搾を行い、超高压压搾セルに取り付けたダイヤルゲージにてケーキ厚さ  $L$  の経時変化を測定した。

# ～超高压压搾～

## 压搾装置

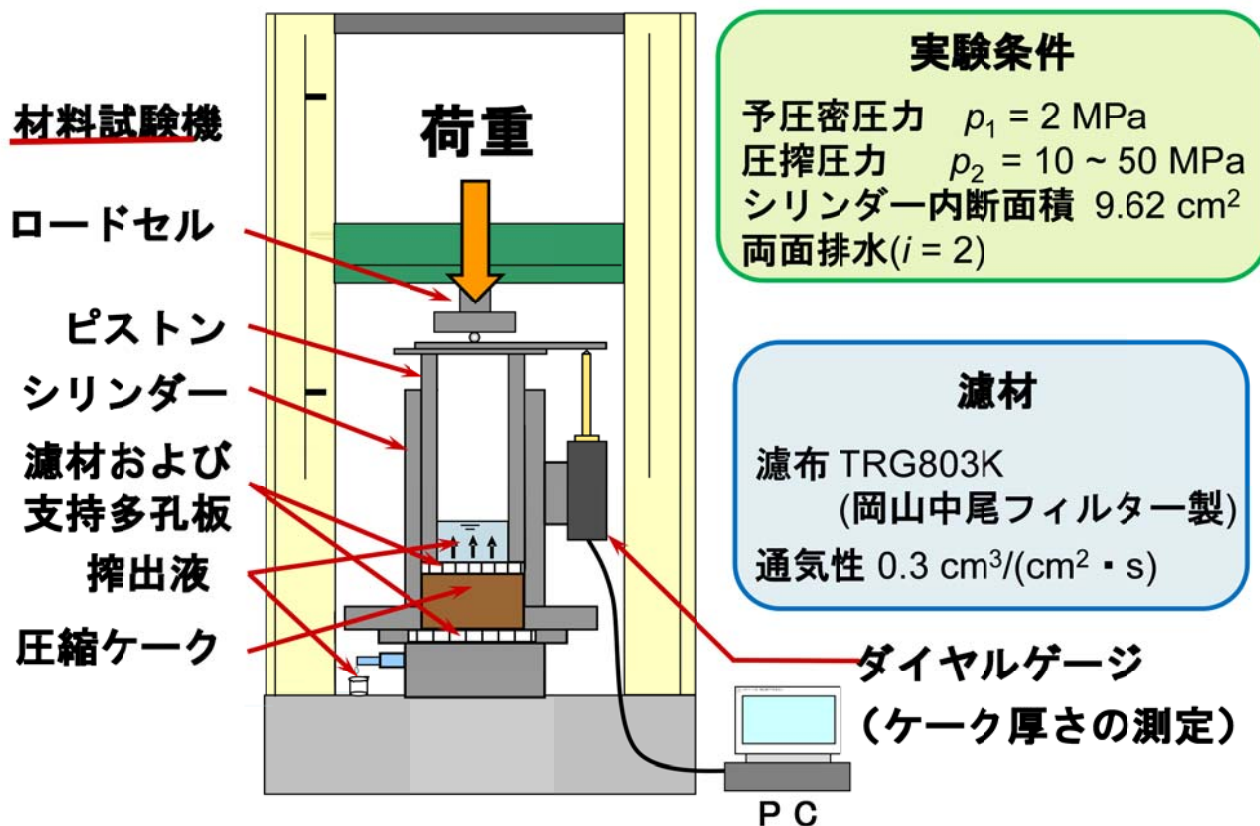


Fig. 10 脱水（超高压压搾）装置の概略図

圧搾終了後、ケーキ含水率を乾燥機（DS610, ヤマト科学製）あるいは赤外線式水分計（FD-720, Kett 製）にて測定した。また、走査電子顕微鏡（JCM-5000, 日本電子製）にて圧搾脱水後のケーキ表面の電顕写真を撮影した。

## 超高压圧搾装置

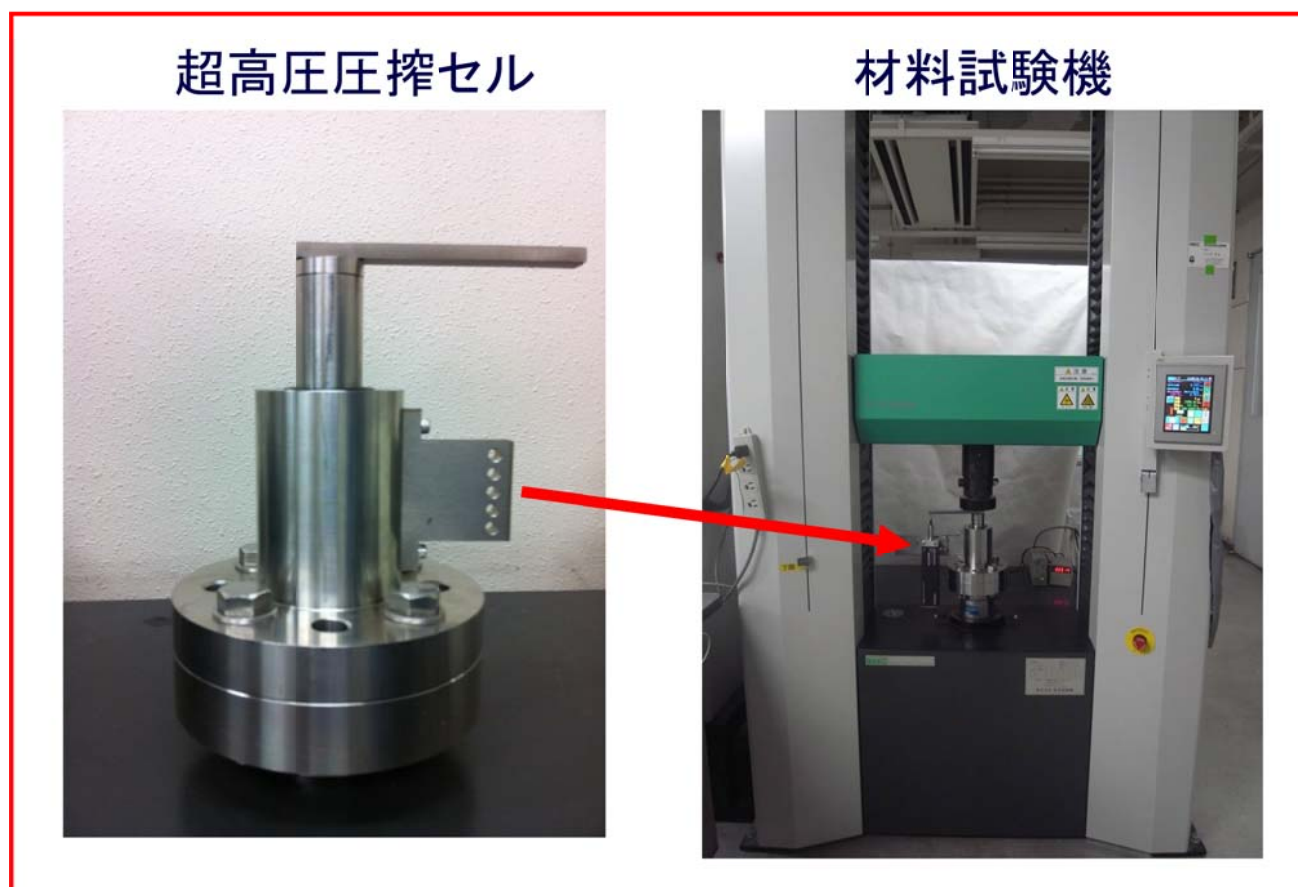


Fig. 11 脱水（超高压圧搾）装置の写真

### 3. 結果と考察

#### 3. 1 下水余剰汚泥の破碎・凝結処理

超音波ホモジナイザー、ビーズミル、せん断式ホモジナイザー、エレクトロポレーションによる下水余剰汚泥の破碎・凝結操作を試みたところ、Fig. 12 に示す代表的な結果からわかるように、いずれの方法においても条件を適切に設定することにより、フロック破碎後の自己凝結現象が観察されたが、特に超音波を照射した場合に顕著な効果が見られた。そこで超音波照射と緩速攪拌による破碎・凝結効果の検討を詳細に行った。

超音波の出力を 40 W、実照射時間を 15 s として破碎・凝結操作を行った場合の汚泥フロックの顕微鏡写真を Fig. 13 に、また照射時間を変化させた時のフロックの面積平均径  $d_s$  の変化を Fig. 14 に示した。超音波照射によりフロック径が減少し、その後緩速攪拌を行うことでフロック径が増大することがわかる。照射時間を大きくすると、破碎が進行するが、いずれの条件でも自己凝結フロックが形成された。破碎・凝結操作後のフロックは、汚泥原液よりも大きなフロックも認められるが、面積平均径の値に大きな差はなかった。しかしながら、一旦、フロックを破碎し、その後に緩く凝結しているため、圧搾時に崩壊しやすいことが期待される。

なお、破碎が進行するとフロックに取り込まれない微細粒子が増加する様子が観察された。重力沈降試験を行うと上澄液が若干濁っており、低圧圧搾の際の抵抗増大の要因となることが考えられる。スラリーに NaCl を添加したところ、一価のイオンであるため汚泥原液にはほとんど影響を及ぼさなかったが、破碎後の凝結に及ぼす影響は顕著で、Fig. 15 に示すように沈降速度が著しく増大した<sup>6)</sup>。Fig. 16 の顕微鏡写真から、フロックの凝結に及ぼす超音波照射と塩添加の相乗効果は明確である。

## 破碎・凝結効果の評価 (破碎法の比較)

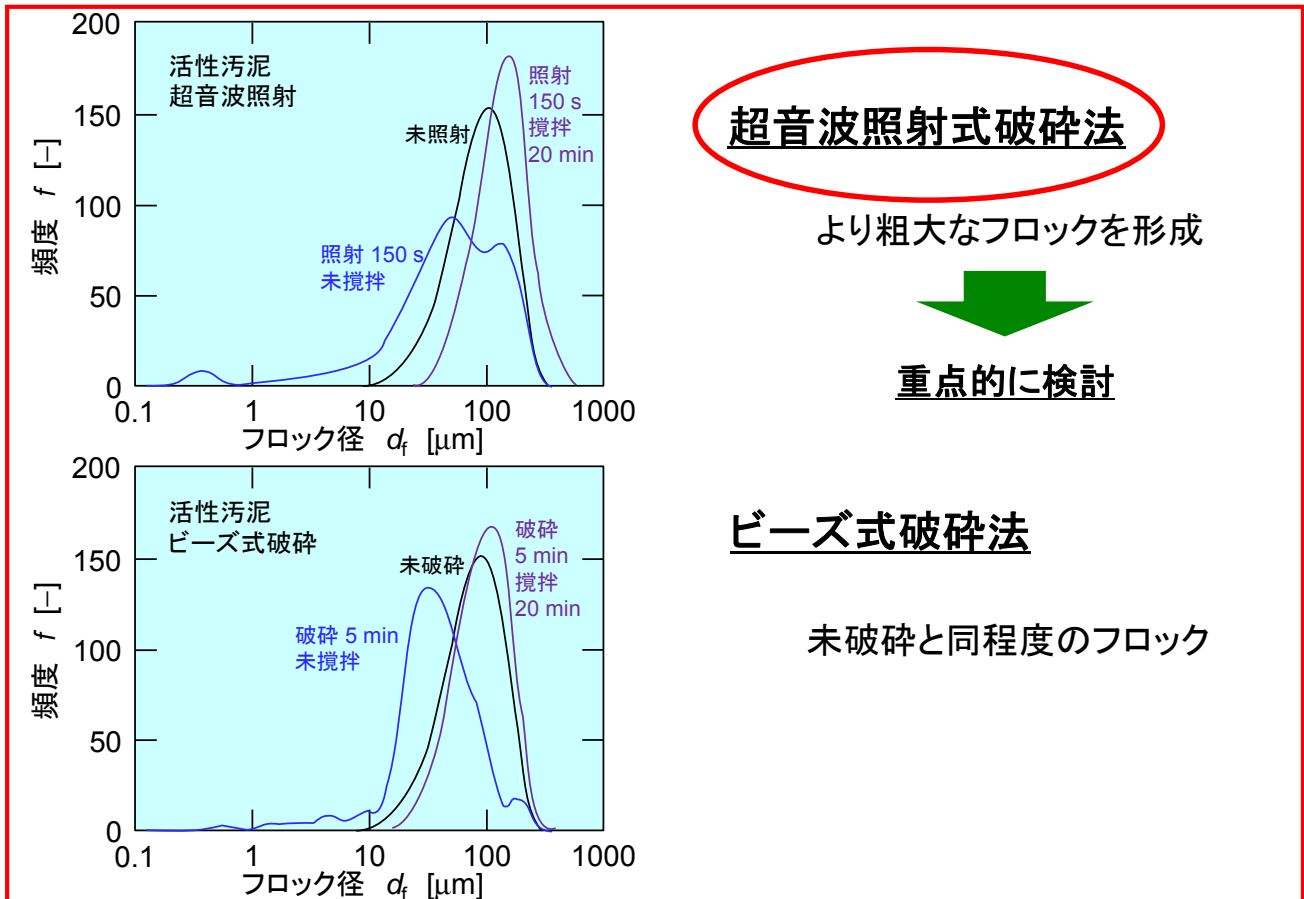


Fig. 12 破碎・凝結効果の評価 (破碎法の比較)

# 破砕・凝結効果の評価

## 顕微鏡写真

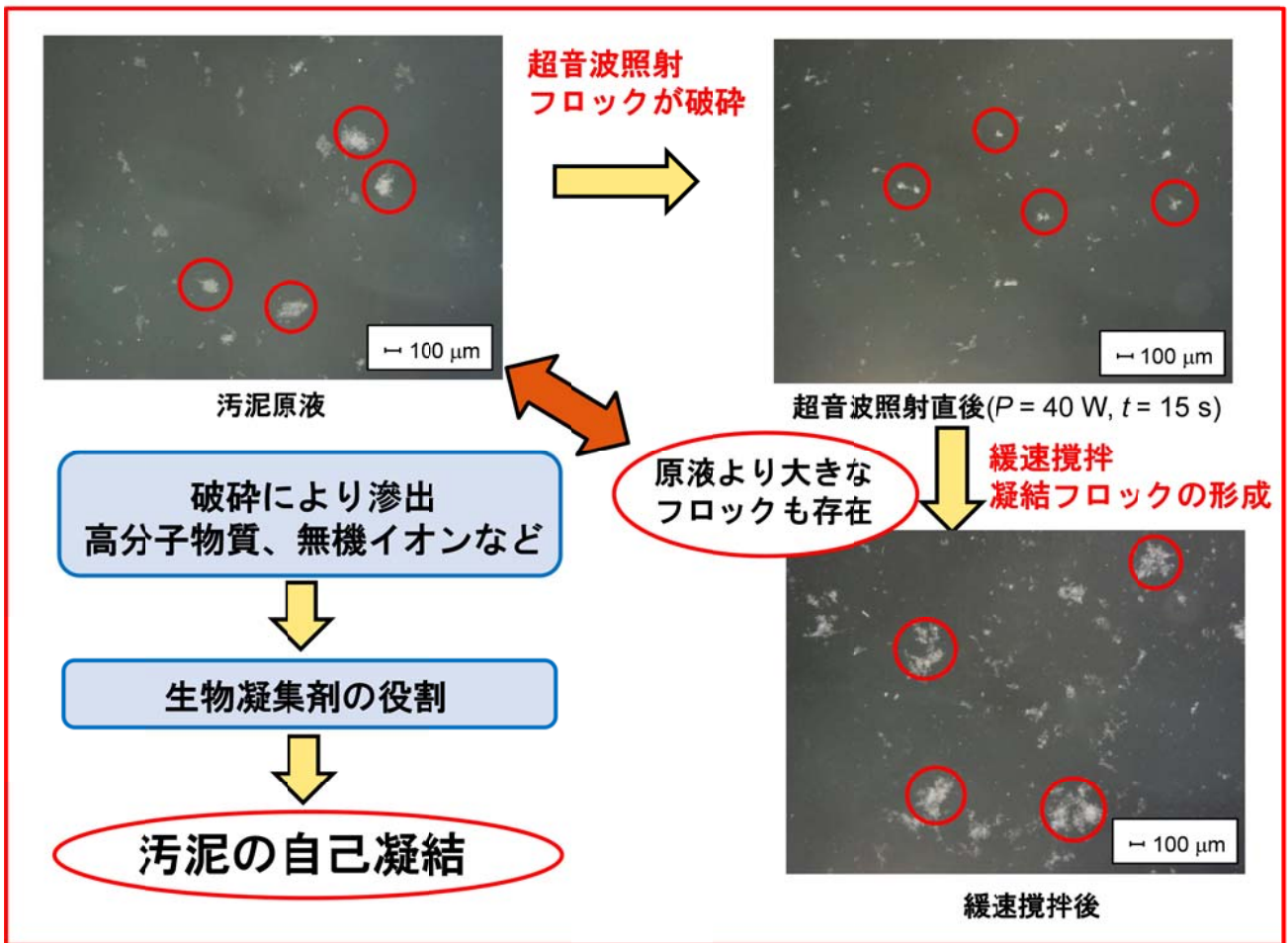


Fig. 13 顕微鏡写真による破砕・凝結効果の評価

# 破碎・凝結効果の評価

## 粒度分布

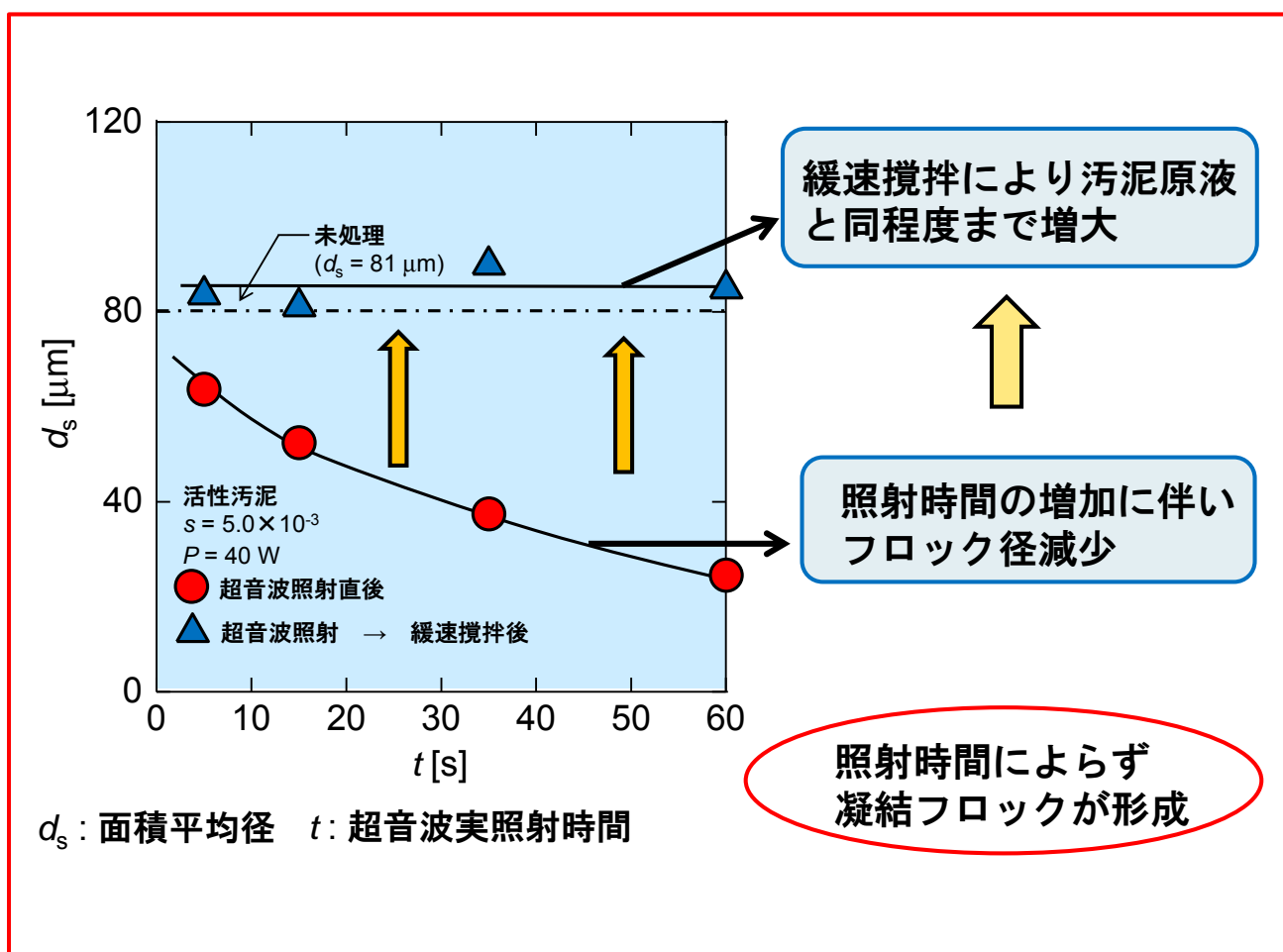


Fig. 14 粒度分布による破碎・凝結効果の評価

## 沈降試験による評価

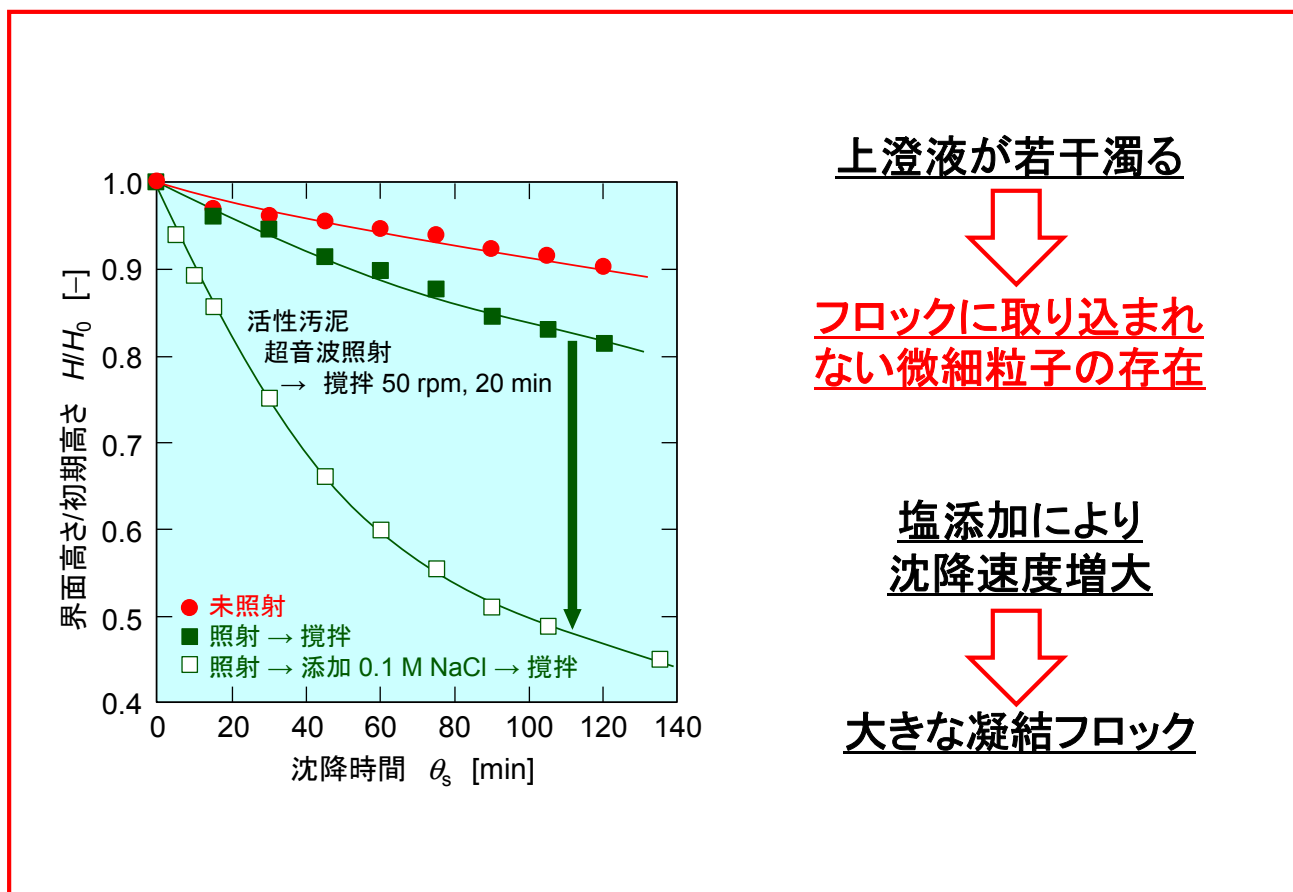
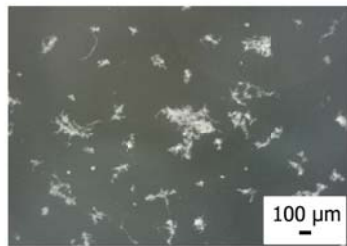
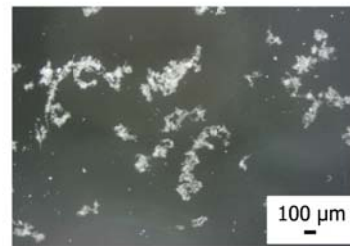


Fig. 15 重力沈降試験による破碎・凝結効果の評価

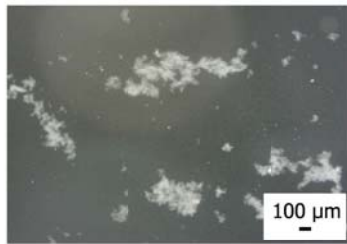
## 超音波照射と塩添加の相乗効果



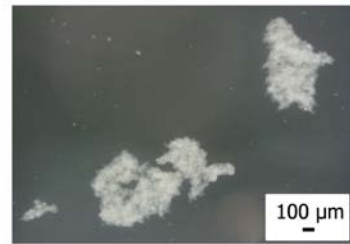
未照射(原液)



未照射→塩添加(0.1 M NaCl)  
→攪拌



超音波照射→攪拌



超音波照射→塩添加(0.1 M NaCl)  
→攪拌

Fig. 16 超音波照射と塩添加の相乗評価

### 3. 2 低圧圧搾（濾過）

超音波照射後に緩速攪拌を行う破砕・凝結プロセスを経た汚泥懸濁液の低圧圧搾を窒素ガスで加圧する形式の定圧濾過にて行った。Fig. 17 に示すように、濾過抵抗の指標となる濾過速度の逆数  $d\theta/dv$  と単位濾過面積あたりの濾液量  $v$  との関係は、超音波を照射することで変化し、破砕・凝結プロセス後の汚泥では未照射の汚泥原液と比較して濾過抵抗が増大した。顕微鏡観察や重力沈降試験によりフロックに取り込まれない微細粒子が僅かではあるが存在することが明らかであり、濾過抵抗増大の要因となることが考えられた。そこで、遠心分離により上澄液中の微細粒子を除去したところ、Fig. 17 に示すように濾過抵抗が著しく小さくなった。このことから、破砕・凝結操作において微細粒子を発生させない試みが必要であること、また発生が防げない場合には、除去して水処理工程における曝気槽に戻すなどの対策が必要であることがわかった。なお、余剰汚泥を超音波処理することで生分解性が向上することが知られており<sup>7)</sup>、曝気槽に戻す汚泥量が小さければ負荷増大による影響も小さいものと考えられる。また、Fig. 17 では、遠心分離を導入した結果を示したが、重力沈降により同様な効果が期待できることを確認しており、破砕・凝結プロセス後に一般的な汚泥処理場で導入されている濃縮槽を設けることで対策が可能である。

# 低圧圧搾(濾過)

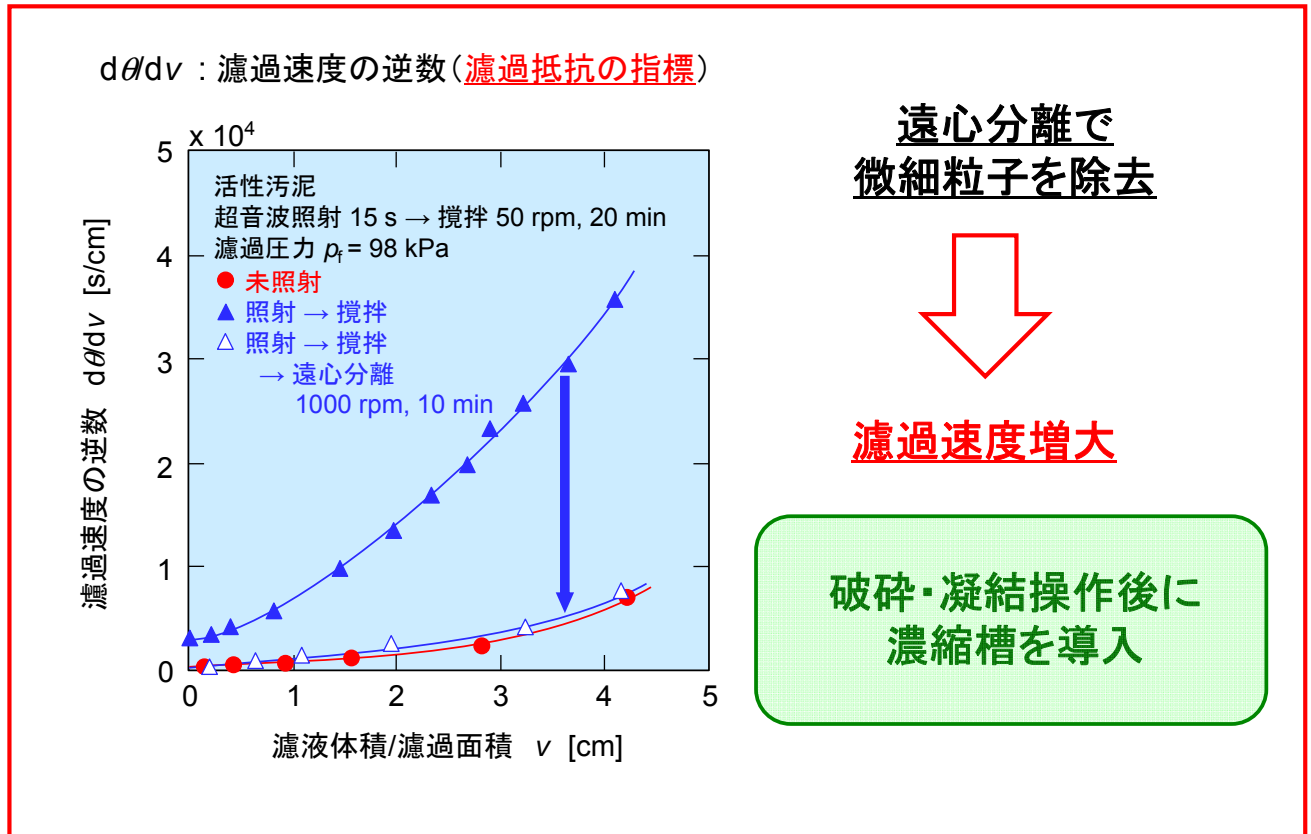


Fig. 17 下水余剰汚泥の濾過挙動

### 3. 3 超高压圧搾

Fig. 18 には、低圧圧搾後の汚泥ケーキを 10 MPa で超高压圧搾した場合のケーキ含水率  $R$  の経時変化を示した。破碎・凝結プロセスを経た汚泥では、処理時間 1 分でケーキ含水率は約 40 %、1 時間で約 30 %、24 時間で 27 % となった。この結果は、現存技術の最高水準である 60 ~ 70 % を遙かに凌いでおり、併せて脱水速度の観点からも満足のいくものであった。減量化の程度で数値化すると、99.3 % の減量化が達成されている。微生物細胞内の水分が 70 ~ 80 % であることを考えると、この 27 % という極めて低い含水率は、単にフロックの崩壊による汚泥粒子間の自由水や粒子表面の付着水だけでなく、細胞内に含まれる束縛水も除去されていることを示している。未処理の汚泥については、24 時間の処理で含水率は 41.4% まで低下した。モデル試料の圧搾実験により、代表的なバクテリアの大腸菌は 1 MPa 程度、パン酵母は 5 MPa 程度で菌体が破裂することが明らかとなり<sup>8)</sup>、超高压による脱水効果が大きいことがわかった。しかしながら、本手法を用いることで、より短時間で、より含水率の小さい汚泥ケーキが得られることから、破碎・凝結プロセスを経ることの重要性が確認された。なお、図中の実線は、後述する本研究での提案圧搾モデルである修正 Terzaghi-一般化 Voigt モデルを用いて求めた計算値であり、プロットの実験値と良好に一致していることから脱水挙動の推算が可能である。

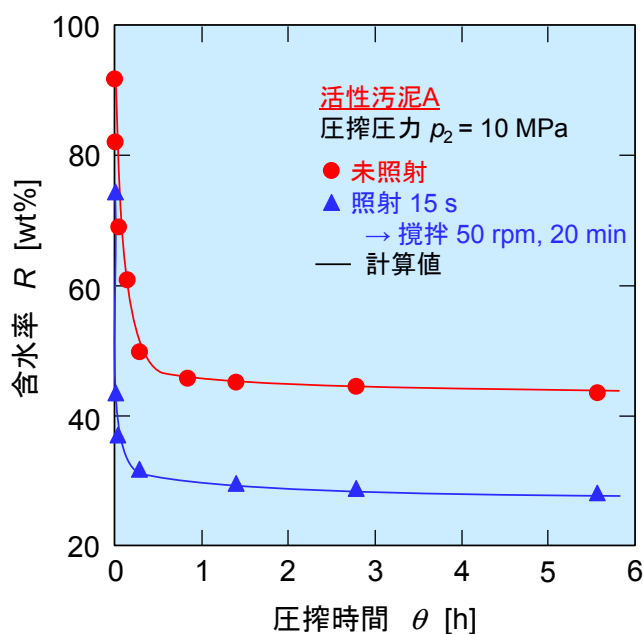
Fig. 19 は、Fig. 18 (活性汚泥 A) とは異なる時期に採取した余剰汚泥 (活性汚泥 B) を用いて行った実験結果であり、超音波の照射時間と出力を変化させた場合の含水率の経時変化である。超音波破碎条件による影響はわずかであるが、いずれの条件においても未処理の汚泥原液と比較して顕著な含水率低下が観察された。破碎操作を行うと、超高压作用下でフロックが容易に崩壊し、含水率が著しく減少することがわかる。既述したように、破碎が進行すると自己凝結時にフロックに取り込まれない微細粒子が増えるため、超音波出力を小さめに設定して、わずかな時間、照射する方法がエネルギー的な観点も含め、有用であると判断される。

Fig. 20 には、圧搾圧  $p_2$  が脱水ケーキの最終含水率  $R_e$  に及ぼす影響を示した。圧力の増加とともに最終含水率は顕著に減少し、いずれの圧力においても破碎処理した汚泥ケーキの方が汚泥原液から得たケーキより含水率が大きく低減した。なお、未処理汚泥の場合でも、含水率の低下が認められ、超高压の作用効果が確認された。圧搾圧力を大きくすることで、更なる含水率の低下が見込めることも明らかである。

以上のように、試料となる汚泥の状態によって脱水効果が異なるが、いずれの条件においても未処理の場合よりも著しく含水率が小さくなることは確実であり、本手法の有用性が確認された。

Fig. 21 には、超音波照射法による破碎・凝結操作後の自己凝結ブロックと超高压圧搾後の下水余剰汚泥の電顕（走査電子顕微鏡 JCM-500, 日本電子製）写真を示した。自己凝結ブロックを見ると微生物の形状は保たれており、様々な微生物が集まってブロックを形成していることがわかる。一方、超高压圧搾後の電顕写真では、微生物の形状が確認できない。このことから、超高压圧搾により微生物細胞が破壊されることが推察され、またモデル試料の圧搾実験からも超高压により微生物菌体が破裂することが確認されていることから、細胞内の束縛水も除去され含水率の著しい低下に繋がったものと考えられる。

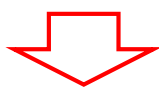
# 超高压压搾



微生物細胞内水分 70~80wt%  
 ↓  
 束縛水の除去

従来技術  
 含水率 80wt%前後  
 最新技術  
 含水率 60~70wt%  
**本研究**  
 含水率 27wt%

**超高压で  
 破碎・凝結フロックが崩壊**



**含水率の著しい低下**

**破碎操作で  
 フロック強度が低下**



**脱水速度の著しい向上**

用途	目標含水率	脱水時間	
		未照射	照射
コンポスト化	60wt%	8 min	1 s
焼却・炭化	40wt%	24 h	1 min
溶融	30wt%	x	1 h

Fig. 18 超高压压搾による下水余剰汚泥の脱水挙動

# 超高压圧搾

## 破碎条件の影響

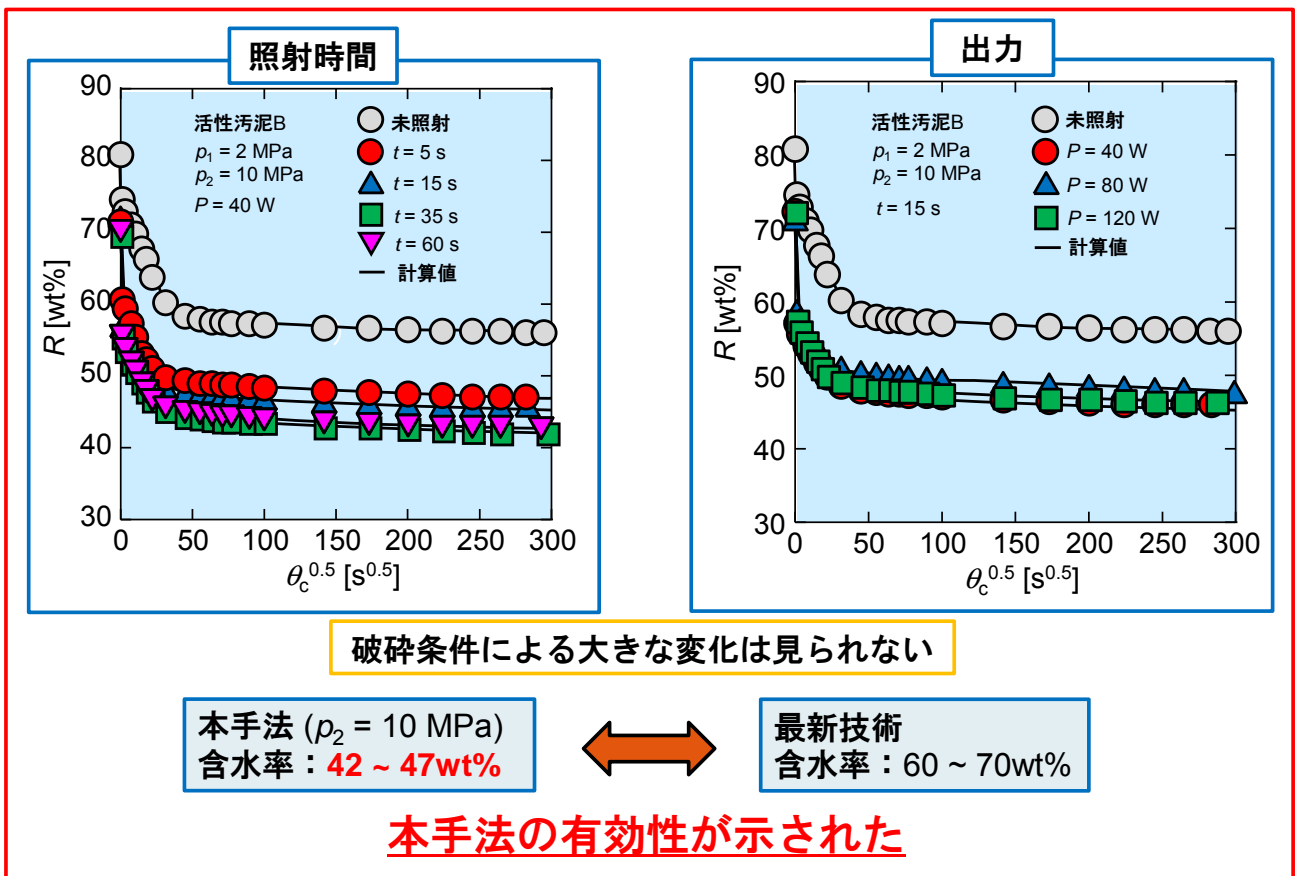


Fig. 19 脱水汚泥ケーキの含水率に及ぼす超音波照射時間・出力の影響

# 超高压压搾

## 压搾圧力の影響

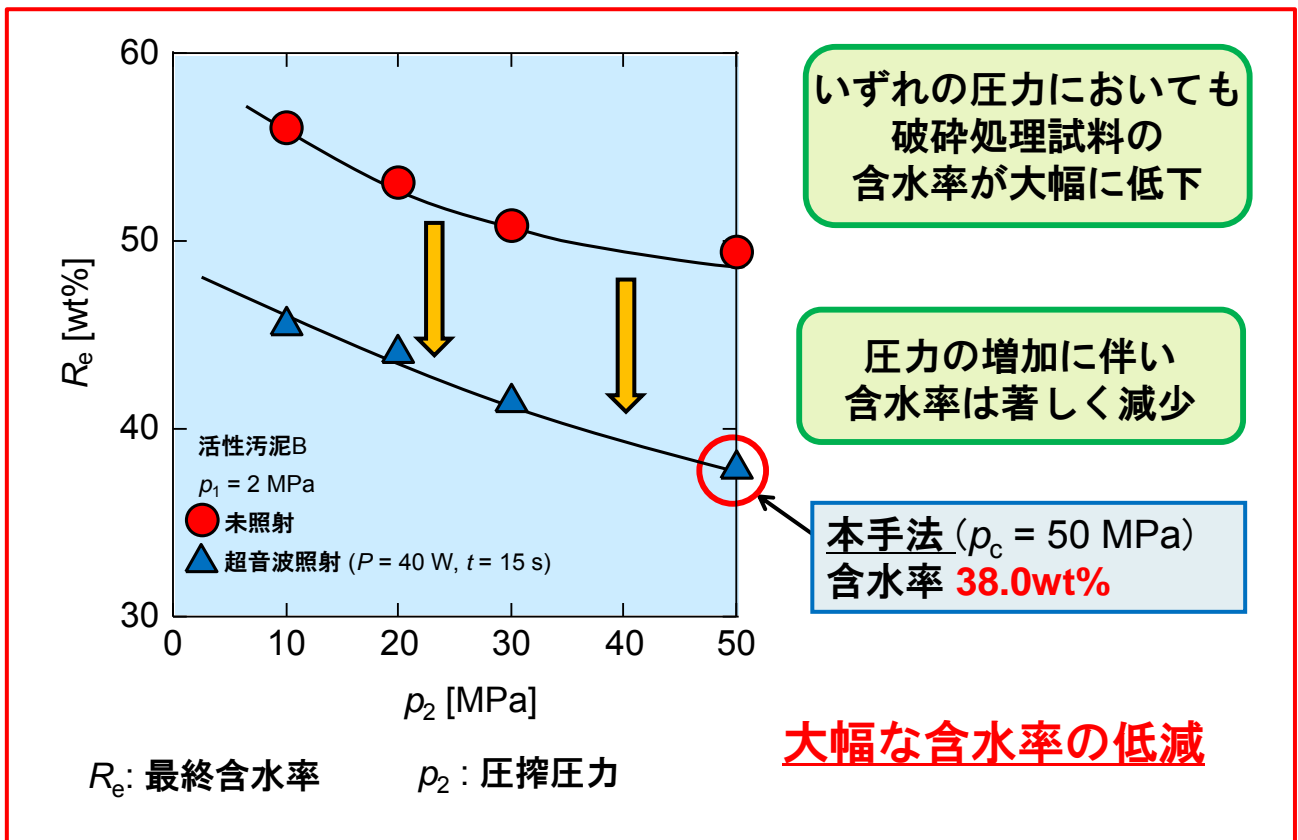


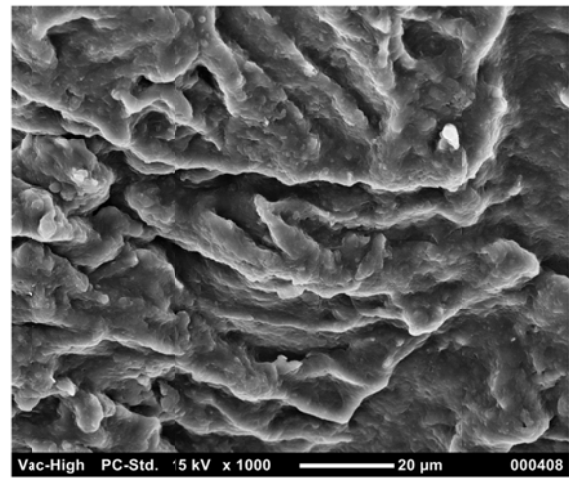
Fig. 20 脱水汚泥ケーキの含水率に及ぼす压搾圧力の影響

## 脱水操作前後の電顕写真



超音波照射法による  
破碎・凝結フロック

様々な微生物が集まって  
凝結フロックを形成



超高圧圧搾後

微生物の形状が確認できない  
超高圧圧搾により微生物細胞が破壊  
→含水率の低下

Fig. 21 下水余剰汚泥の電顕写真

### 3. 4 新規圧搾モデルの提案

#### <新規圧搾モデル圧搾理論>

本研究では、圧搾操作により生物スラッジの減量化を試みた。圧搾および圧搾操作による脱水挙動の解析方法について以下に示す。

一般に、圧搾によるスラリーの固液分離過程は濾過期間とそれに続く圧密期間とに分けることができ、前者は濾過理論、後者は土質力学における Terzaghi の圧密理論を修正した、修正 Terzaghi モデルにより解析される。なお、圧密期間において、粒子のクリープ的塑性変形による二次圧密が存在する場合には、これを考慮した理論解析が行われる。

#### <修正 Terzaghi モデル><sup>9)</sup>

圧密進行中のケーキ内部では、液体だけではなく固体粒子も濾材方向に移動し、圧密によって搾出される液体の流速は、液体の真の移動速度と固体の移動速度との速度差で表される。このような系においては、位置を表す座標として固定座標を用いると、内部の液体および固体粒子の移動を記述する運動方程式と物質収支式との関係、および境界条件などが複雑となり、基礎式の解を得るのが困難となる。

時間によって変化しない量、例えば Fig. 22 に示すように固定された濾材面上から測った単位断面積当たりの固体体積 $\omega$ を位置座標として採用することにより、基礎方程式が簡単化され、また境界面を固定することができる。

圧縮ケーキ内のある位置 $\omega$  (Fig. 22 (b))におけるケーキ部分比抵抗を $\alpha$ とおけば、位置 $\omega$ における微小薄層を過ぎる液体の固体粒子に対する見掛け相対速度  $u$  は、式(1)で表すことができる。

$$u = \frac{1}{\mu\alpha\rho_s} \cdot \frac{\partial p_L}{\partial \omega} = -\frac{1}{\mu\alpha\rho_s} \cdot \frac{\partial p_s}{\partial \omega} \quad (1)$$

ここに、 $p_s$ は固体圧縮圧力、 $p_L$ は液圧である。

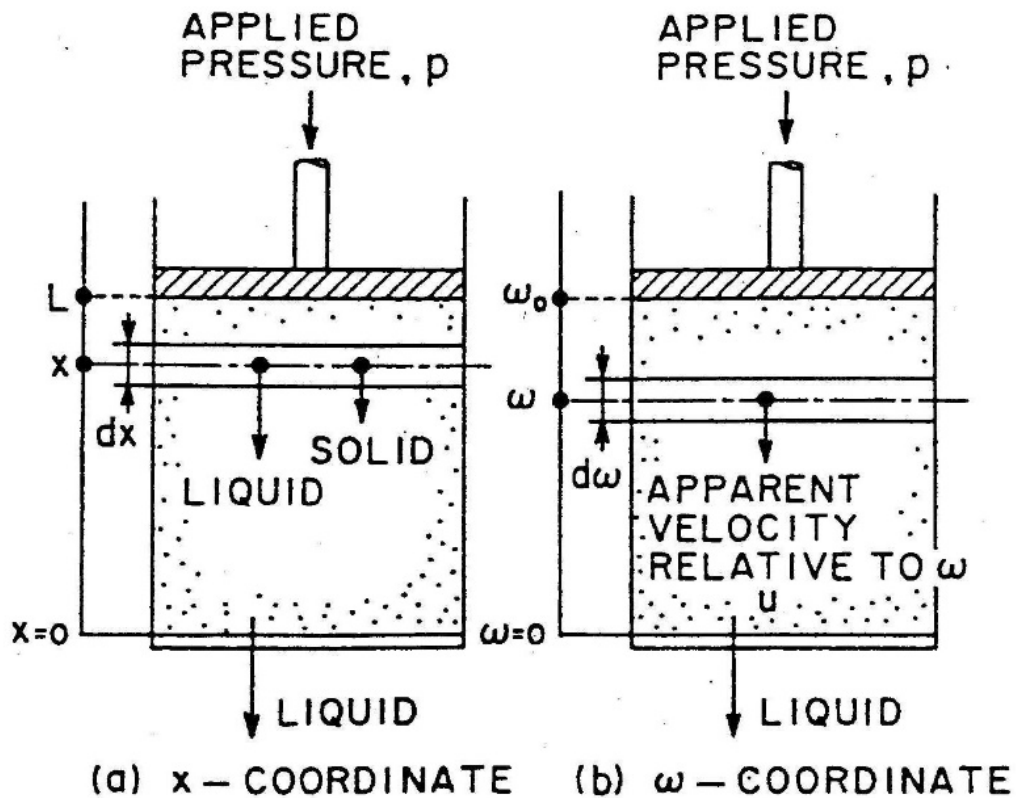


Fig. 22 (a)  $x$  座標と(b)  $\omega$ 座標

ケーキ微小薄層  $d\omega$ における液体の物質収支式は式(2)で与えられる。

$$\frac{\partial e}{\partial \theta_c} = \frac{\partial u}{\partial \omega} \quad (2)$$

ここに、 $e$ は空隙比、 $\theta_c$ は圧密時間である。なお、固定座標  $x$ を用いると、液体および固体についての物質収支式が必要となる。式(1)を(2)に代入し次式を得る。

$$\frac{\partial e}{\partial \theta_c} = \frac{\partial}{\partial \omega} \left( -\frac{1}{\mu \alpha \rho_s} \cdot \frac{\partial p_s}{\partial \omega} \right) \quad (3)$$

ここに、 $\mu$ は溶液の粘度、 $\rho_s$ は固体の真密度である。圧密期間中の $\alpha$ の平均値をとり、一定とし、また、空隙比 $e$ が固体圧縮圧力 $p_s$ に対して直線関係にあると仮定すると、式(3)は修正圧密方程式(4)となる。

$$\frac{\partial p_s}{\partial \theta_c} = C_e \cdot \frac{\partial^2 p_s}{\partial \omega^2} \quad \text{または} \quad \frac{\partial e}{\partial \theta_c} = C_e \cdot \frac{\partial^2 e}{\partial \omega^2} \quad (4)$$

$$C_e \equiv -\frac{1}{\mu \alpha \rho_s (-de/dp_s)} \quad (5)$$

Terzaghi が導いた圧密方程式は固体粒子の移動を無視し固定座標 $x$ を用いているが、式(4)では Terzaghi 式のこの欠点が修正されている。また、式(5)で与えられる $C_e$ は修正圧密係数である。

修正圧密係数 $C_e$ の値に圧密開始時と終了時の平均値を用いることとし、式(4)を圧搾圧力 $p$ が一定（定圧圧搾）の下で解くと、圧密の進行状態を表す平均圧密比 $U_c$ が以下のように得られる。

スラリー原料の圧密

$$U_c = \frac{L_1 - L}{L_1 - L_\infty} = 1 - \exp\left(-\frac{\pi^2}{4} \cdot \frac{i^2 C_e \theta_c}{\omega_0^2}\right) \quad (6)$$

均質な半固体状原料の圧密

$$U_c = \frac{L_1 - L}{L_1 - L_\infty} = 1 - \sum_{n=1}^{\infty} \frac{8}{(2n-1)^2 \pi^2} \exp\left\{-\frac{(2n-1)^2 \pi^2}{4} \cdot \frac{i^2 C_e \theta_c}{\omega_0^2}\right\} \quad (7)$$

ここに、 $L_1$ 、 $L$ 、 $L_\infty$ はそれぞれ圧密初期、時間 $\theta_c$ 、圧密平衡時のケーキ厚さ、 $i$ は排水面数、 $\omega_0$ は単位断面積毎の固体体積である。平均圧密比 $U_c$ は、圧密開始時に0、終了時に1となる。

<二次圧密を考慮した Terzaghi-Voigt モデル><sup>10)</sup>

Terzaghi モデルでは、粒子構造の力学的挙動をスプリングで表しており、固体圧縮圧力  $p_s$  が増加すると粒子構造が  $p_s$  に対応した状態まで瞬間的に圧縮されると仮定している。しかし、実際に粒子構造が圧縮される場合は、変形にある程度の時間経過が必要である。材料中の微小要素における粒子構造のこのようなレオロジー的性質を考慮するため、空隙容積の減少が圧力  $p_s$  の増加に即応して変化する部分（一次圧密）と時間的に遅れて変化する部分（二次圧密またはクリープ変形）の二つから成り立っていると仮定し、Fig. 23 に示すように、後者のクリープ特性をスプリングとダッシュポットを並列結合した Voigt 要素で近似し、これをスプリング 1 個からなる Terzaghi 要素とを直列結合したのが Terzaghi-Voigt モデルである。

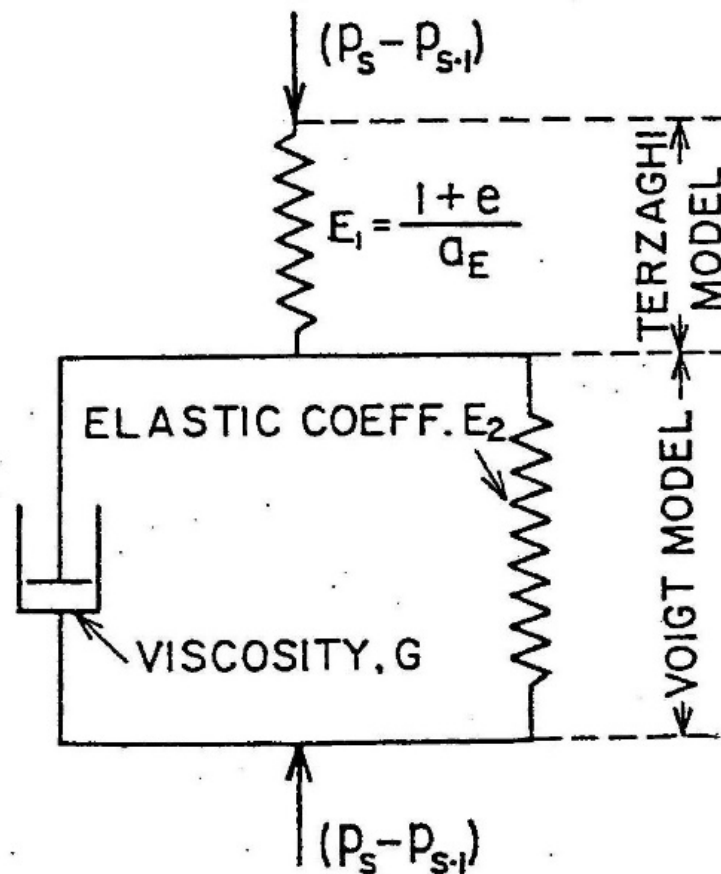


Fig. 23 圧密に対するレオロジーモデル

Terzaghi-Voigt モデルでは、平均圧密比  $U_c$  は次のように表される。

スラリー原料の圧密

$$U_c = (1-B) \left\{ 1 - \exp \left( -\frac{\pi^2}{4} \cdot \frac{i^2 C_e \theta_c}{\omega_0^2} \right) \right\} + B \{ 1 - \exp(-\eta \theta_c) \} \quad (8)$$

均質な半固体状原料の圧密

$$U_c = (1-B) \left[ 1 - \sum_{n=1}^{\infty} \frac{8}{(2n-1)^2 \pi^2} \exp \left\{ -\frac{(2n-1)^2 \pi^2}{4} \cdot \frac{i^2 C_e \theta_c}{\omega_0^2} \right\} \right] + B \{ 1 - \exp(-\eta \theta_c) \} \quad (9)$$

ここに、 $B$  は全圧密量に対する二次圧密の割合、 $\eta$  はクリープの進行速度を表す定数（遅延時間の逆数）である。

<新規圧搾モデル>

一般に圧搾挙動は、上述した従来モデルである修正 Terzaghi モデルあるいは修正 Terzaghi-Voigt モデルで記述できる。しかしながら、下水余剰汚泥、その他にもバクテリアや酵母といった微生物の破裂を伴う圧搾や豆腐、おから、ニンジンなどの有機質モデル試料では、特徴的な圧搾挙動を示し、従来モデルでの解析が不可能であった。そこで、Fig. 24 に示す修正 Terzaghi モデルに Voigt モデルを複数個直列に接続した修正 Terzaghi—一般化 Voigt モデルを提案し、本圧搾解析に適用した。平均圧密比  $U_c$  は、次式のように表される。

$$U_c = \left( 1 - \sum_{k=1}^K B_k \right) \left[ 1 - \sum_{n=1}^{\infty} \frac{8}{(2n-1)^2 \pi^2} \cdot \exp \left\{ -\frac{(2n-1)^2 \pi^2}{4} \cdot \frac{i^2 C_e \theta_c}{\omega_0^2} \right\} \right] + \sum_{k=1}^K B_k \{ 1 - \exp(-\eta_k \theta_c) \} \quad (10)$$

ここに、 $i$  は排水面数、 $C_e$  は修正圧密係数、 $\theta_c$  は圧密時間、 $\omega_0$  は単位断面積毎の固体体積、 $B_k$  は全圧密量に対する各クリープ圧密の割合、 $\eta_k$  は各クリープの進行速度を表す定数（遅延時間の逆数）である。

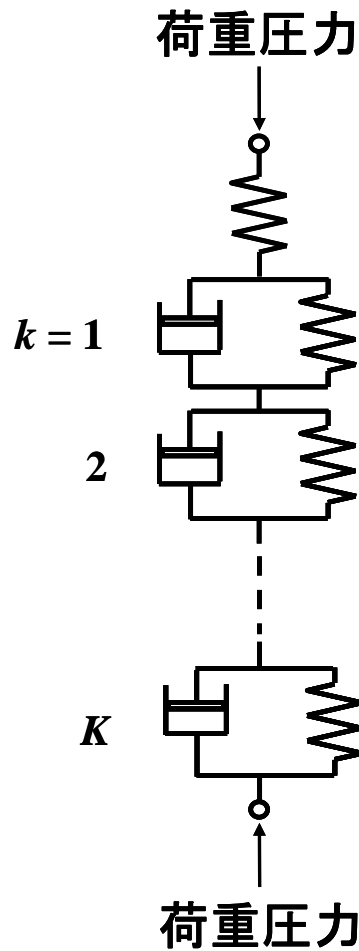


Fig. 24 Terzaghi—一般化 Voigt モデル

段階的に発生するクリープ挙動は、式(10)に基づき Fig. 25 左図のように  $(1 - U_c)$  対  $\theta_c$  の片対数プロットの直線性から決定でき、下水余剰汚泥の場合、三段階で近似できることから、四次圧密までを考慮する必要があることがわかった。Fig. 25 右図は、下水余剰汚泥の圧密挙動を平均圧密比  $U_c$  の経時変化として示した。実線は、式(10)で四次圧密 ( $k = 3$ ) まで考慮し、フィッティングにより得た修正圧密係数や各クリープ定数を用いて求めた計算値であり、プロットの実験値と精度良く一致していることから、脱水過程をモデル化できたと判断される。また、一次から四次までの各圧密量の割合  $A, B_1, B_2, B_3$  を図中に示した。A の値が最も

大きく、一次圧密が全圧密量の 60 %を占めることがわかった。このような生物スラッジの特徴的な圧密挙動は、その物質のレオロジー特性と密接に関係していると考えられ、今後圧密特性とレオロジー特性との関係について詳細な検討が必要となる。超高压圧搾におけるケーキ脱水挙動のモデル化ができたことにより、今後予定している種々の操作条件における脱水性能の推算に寄与するものと期待される。

Fig. 26 には、ケーキの空隙率 $\epsilon_{av}$ と含水率 $R$ の経時変化について、代表的な実験データをプロットで、また新規圧搾モデルに基づく計算値を実線で示した。ケーキの空隙率 $\epsilon_{av}$ と含水率 $R$ はそれぞれ式(11), (12)で表され、式 (10)の $U_c$ の経時変化を用いると、それぞれの経時変化が推算できる。図に示すように実験値と推算値は良好に一致しており、式 (10)の $\omega_0$ が単位断面積当たりの汚泥体積になることから、汚泥の処理量に変化した場合にも適用可能で、本提案モデルにより脱水時間を予測することができる。

$$\epsilon_{av} = 1 - \frac{\omega_0}{L_1 - U_c(L_1 - L_\infty)} \quad (11)$$

$$R = \frac{100\epsilon_{av}\rho}{\epsilon_{av}\rho + (1 - \epsilon_{av})\rho_s} \quad (12)$$

ここに、 $\omega_0$ は単位断面積毎の固体体積、 $L_1$ 、 $L_\infty$ はそれぞれ圧密初期、圧密平衡時のケーキ厚さ、 $\rho$ は搾出液の密度、 $\rho_s$ は固体の真密度である。

次に、モデル式による解析を進め、汚泥の圧密脱水特性を評価する。破碎処理した凝結汚泥を、種々の圧搾圧 $p_2$ で超高压圧搾した際の平均圧密比 $U_c$ の経時変化を Fig. 27 に示した。超高压を作用させた瞬間に汚泥ケーキは著しく圧密され、その傾向は、圧力が大きいほど顕著なことがわかる。

Fig. 28 には、モデル式による解析で求めた全圧密量に対する一次圧密の割合  $A$  と二次から四次までの各クリープ圧密の割合  $B_k$  ( $k = 1, 2, 3$ ) の値と圧力の関係を示した。破碎処理した凝結汚泥では、一次圧密の割合  $A$  が最も大きく、その傾向は圧力の増加とともに顕著となり、一方、それに対応して二次圧密の割合  $B_1$  は圧力の増加とともに小さくなった。なお、三次および四次圧密の割合は極めて小さかった。

Fig. 29 には、比較のために、未処理の汚泥および凝集剤としてポリ塩化アルミニウム (PACl) を用いて凝集処理した汚泥を 10 MPa で圧搾した場合の各圧密量の割合を、破碎・凝結処理した汚泥の結果と併せて示した。汚泥原液との相違は明確で、破碎処理した汚泥は三次圧密の割合  $B_2$  が小さく、一次圧密の割合  $A$  が大きくなっていることがわかる。これは超音波処理によって汚泥が圧密脱水されやすくなっているためと推察される。なお、凝集剤を添加した場合には、二次圧密の割合  $B_1$  が小さく、三次圧密の割合  $B_2$  が大きくなっており、自由水まで取り込んだ強固なブロックを形成するために圧密が進行しにくくなっているものと考えられる。

# 圧搾のモデル化による解析

$$U_c = \frac{L_1 - L}{L_1 - L_\infty}$$

$U_c$ : 平均圧密比,  $L_1$ : 初期ケーキ厚さ  
 $L$ : ケーキ厚さ,  $L_\infty$ : 平衡ケーキ厚さ

## Terzaghi-一般化Voigtモデル

$$U_c = \left(1 - \sum_{k=1}^K B_k\right) \left[1 - \sum_{n=1}^{\infty} \frac{8}{(2n-1)^2 \pi^2} \exp\left\{-\frac{(2n-1)^2 \pi^2 i^2 C_e \theta_c}{4 a_0^2}\right\}\right] + \sum_{k=1}^K B_k \{1 - \exp(-\eta_k \theta_c)\}$$

$C_e$ : 修正圧密係数  
 $B_k$ : 各クリープ量の割合  
 $\eta_k$ : 各圧密速度定数

一次圧密

多段クリープ

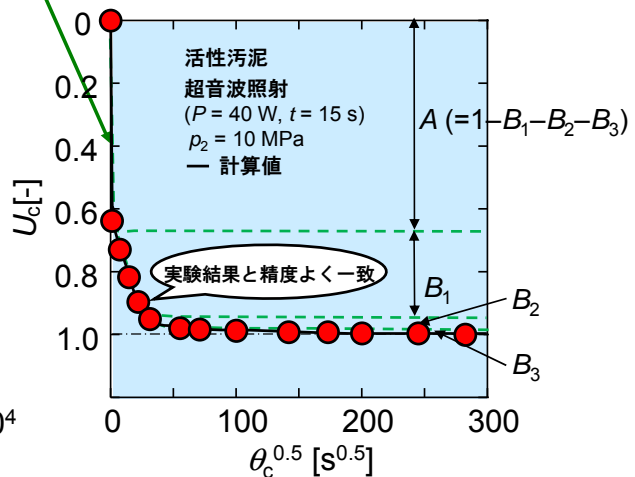
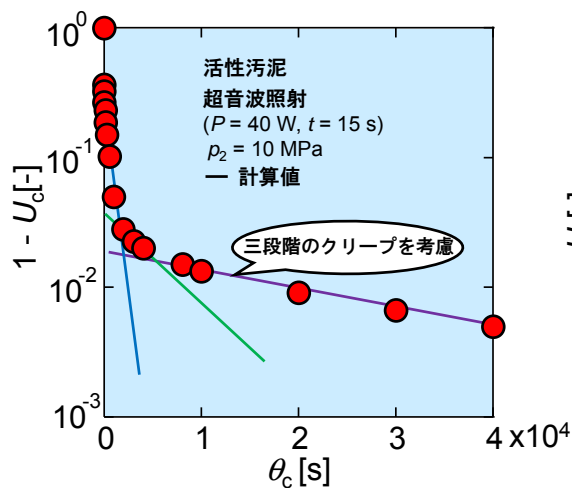


Fig. 25 多段クリープモデルによる下水余剰汚泥の超高压圧搾挙動の解析

## 圧搾のモデル化による解析

$$U_c = \left(1 - \sum_{k=1}^K B_k\right) \left[1 - \sum_{n=1}^{\infty} \frac{8}{(2n-1)^2 \pi^2} \exp\left\{-\frac{(2n-1)^2 \pi^2 i^2 C_c \theta_c}{4 \omega_0^2}\right\}\right] + \sum_{k=1}^K B_k \{1 - \exp(-\eta_k \theta_c)\}$$

$$\varepsilon_{av} = 1 - \frac{\omega_0}{L_1 - U_c (L_1 - L_{\infty})}$$

$\varepsilon_{av}$ : 平均空隙率  $R$ : 含水率

$$R = \frac{100 \varepsilon_{av} \rho}{\varepsilon_{av} \rho + (1 - \varepsilon_{av}) \rho_s}$$

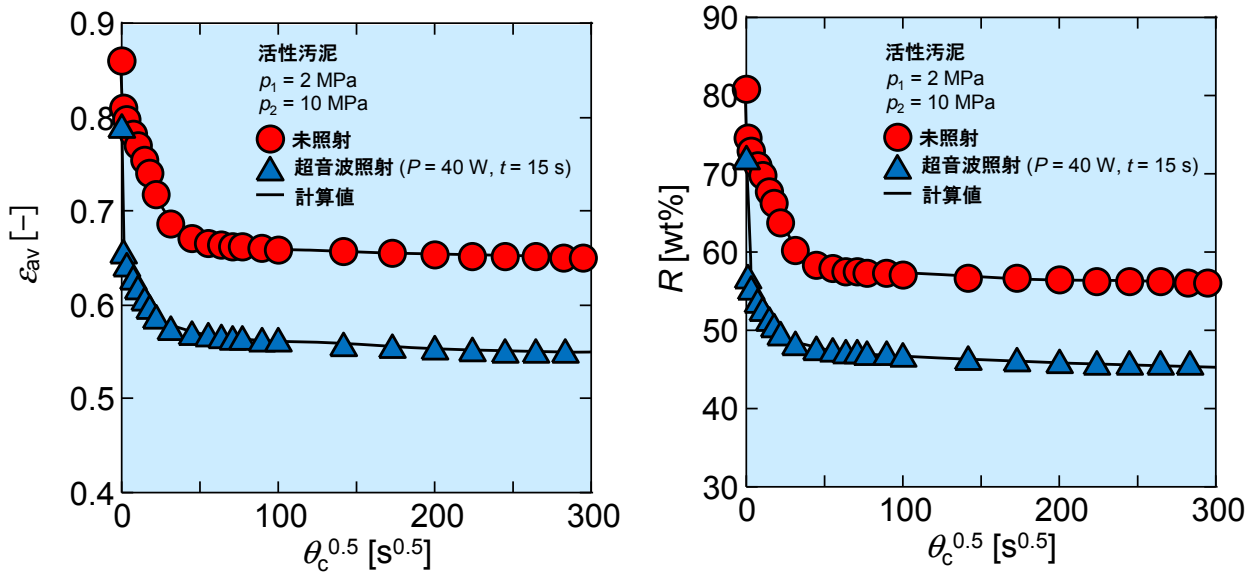


Fig. 26 多段クリープモデルによる脱水挙動の推算

# 平均圧密比 $U_c$ の経時変化

## 圧搾圧力による影響

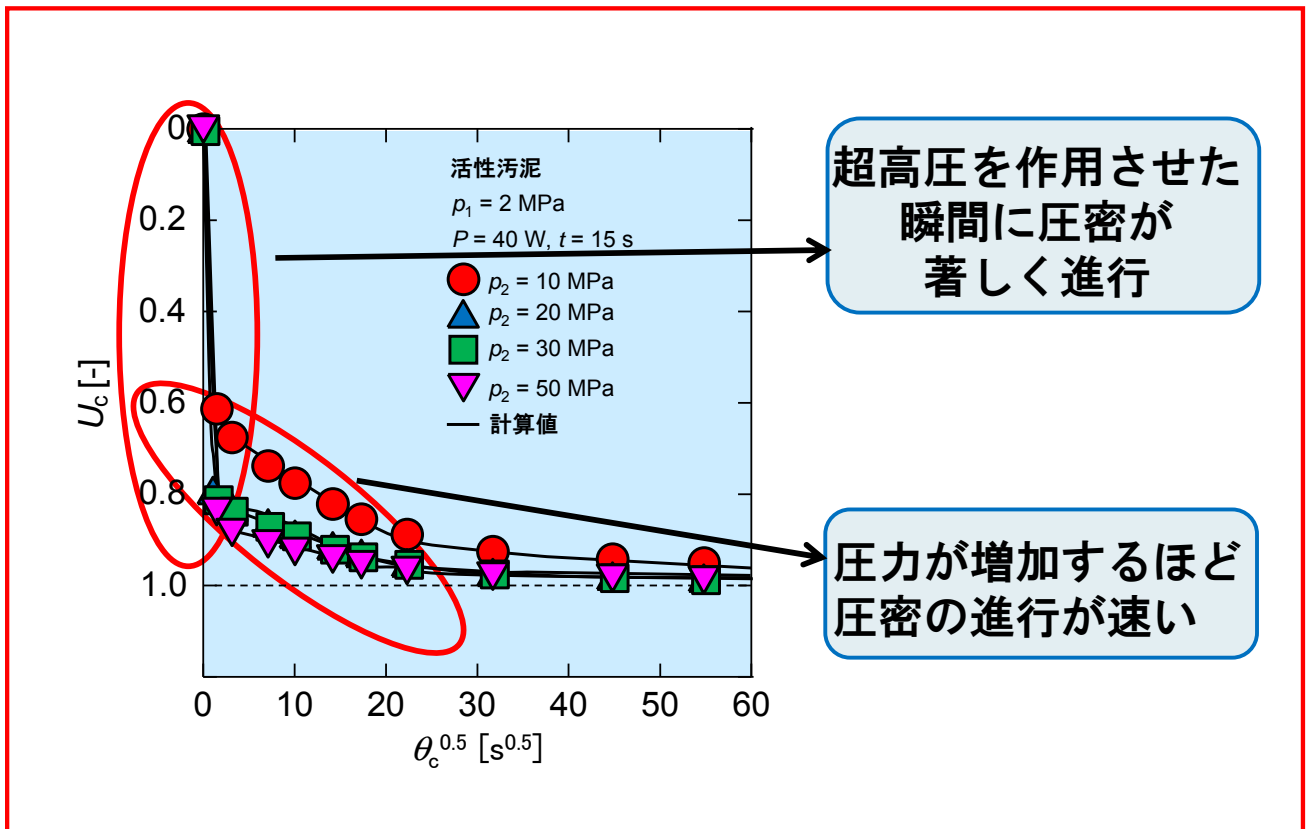


Fig. 27 多段クリープモデルによる解析 (圧搾圧力の影響)

# 圧密脱水特性の評価

## 各圧密量と圧搾圧力の関係

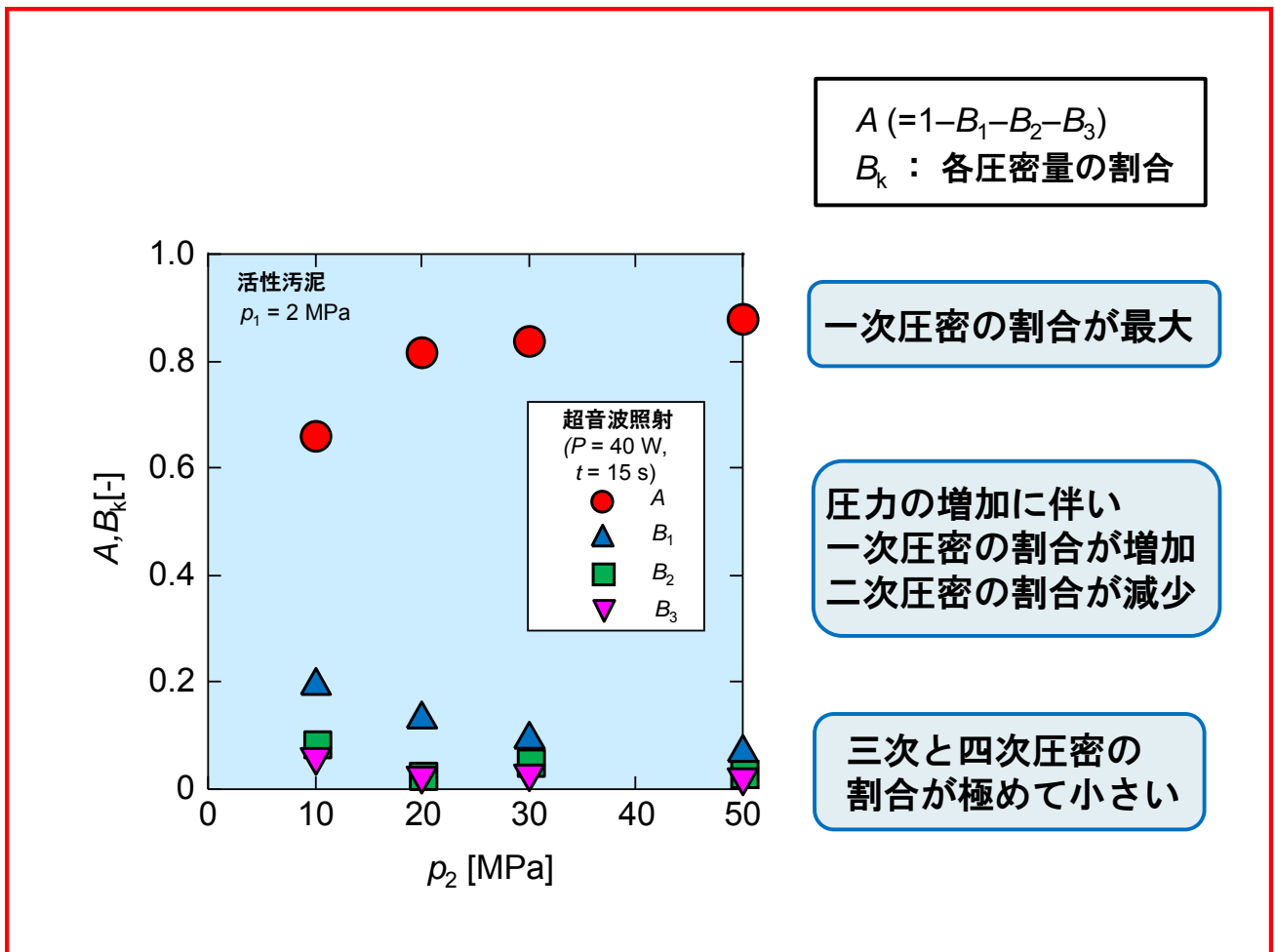


Fig. 28 圧密量と圧搾圧力の関係

# 圧密脱水特性の評価

## 前処理の影響

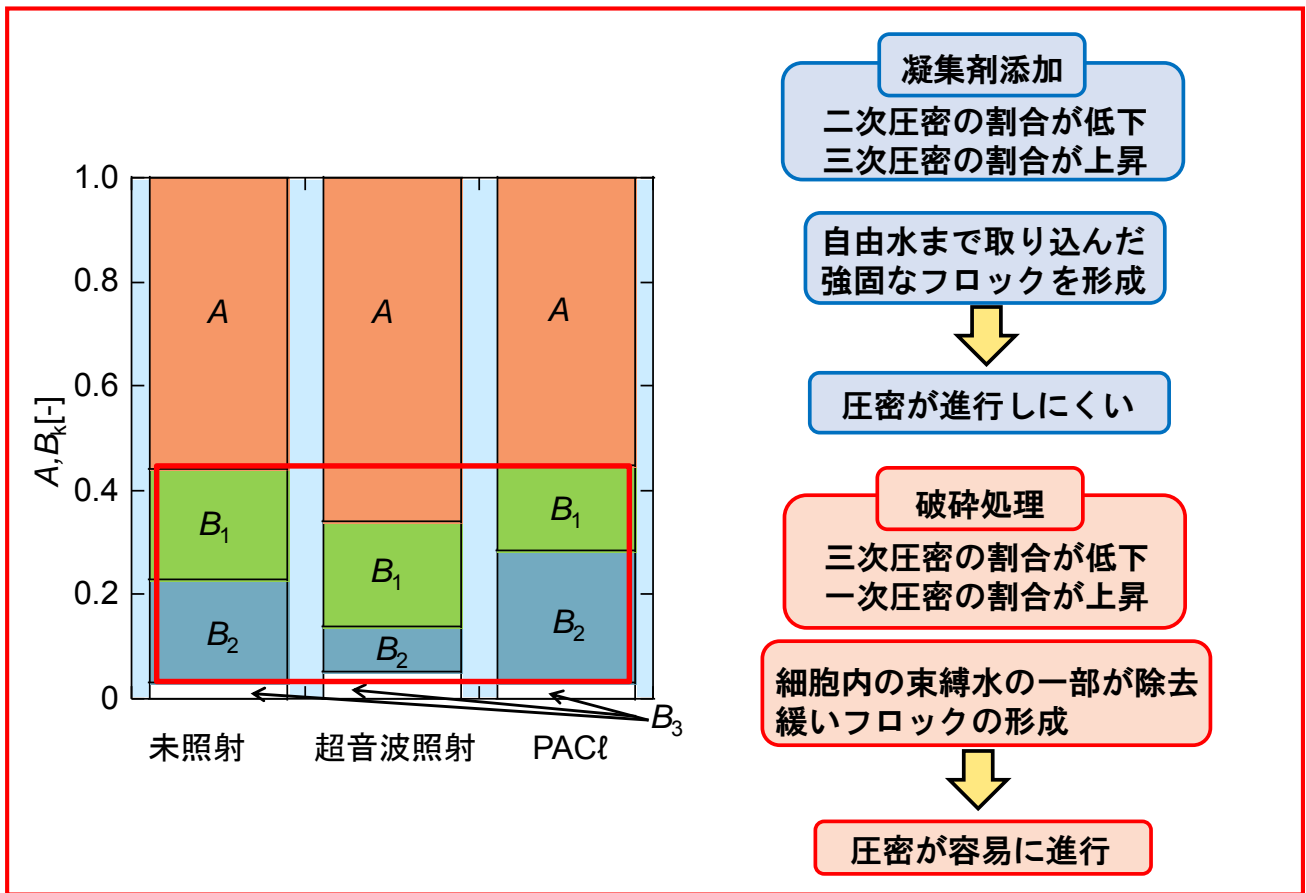


Fig. 29 圧密脱水特性の評価

### 3. 5 実用化への検討

本研究で提案する難脱水性生物スラッジの高速減量化技術が実用化されれば、産業廃棄物の中で最も大きな排出量割合を占め、水分含量が高い汚泥を、現存技術では想定できないほどの極めて低い含水率に、最も省エネルギー的な機械的脱水操作によって高速で処理できるようになり、後段の熱的操作による負荷を小さくし、汚泥処理システム全体のエネルギー削減に繋がる。

Fig. 30 では、一連の研究成果に基づき、本開発技術を導入した汚泥処理プロセスを廃水処理も含めた一連のプロセスとして提案する。排水の流量・水質、余剰汚泥の発生量・汚泥濃度、濃縮汚泥の汚泥濃度および処理水質については、本研究での実験試料（余剰汚泥）を採取した植田水処理センターおよび柴田汚泥処理場のデータを用いた。脱水ケーキの含水率、搾出液の水質および濃縮槽における上澄液の水質は、実験データに基づいており、処理場のデータと併せて汚泥量等を計算した。課題である自己凝結フロックに取り込まれない微細粒子についても、濃縮槽を設置することで、圧搾操作で排出される搾出液とともに排水と混合し、負荷を上げることなく曝気槽での処理が可能となる。

次に、エネルギー的観点からの評価を行った。本手法は、凝集剤を用いることなく、破碎・凝結操作により自己凝結フロックを形成させ、ステップ超高压により下水余剰汚泥の含水率を極めて小さくすることが可能である。脱水汚泥の含水率は27～47%となり、コンポスト化、焼却、炭化、溶融など以後の汚泥処理法に合わせて適切な条件設定を行うことで効率的な脱水が実現できる。仮に、汚泥の含水率を40%にすることを想定すると、超音波照射式破碎を導入し、10 MPaでの超高压圧搾を行う本手法での所要エネルギーは、Fig. 31に示すように脱水・乾燥を行う現状プロセスの8%程度であり、省エネルギーでの操作が可能である。また、凝集剤を用いないため再資源化への用途が広がり、実用化のメリットは大きい。

Fig. 32 には、近年注目されている汚泥の燃料化を想定した場合の本手法導入による優位性を示した。炭化された下水汚泥は、石炭火力発電所における石炭代替燃料としての利用が期待されており、有価物になることから汚泥処理コストが低減でき、導入が進められている。本提案プロセスでは、脱水後の汚泥の含水率が極めて小さいため、一般的に行われている乾燥の工程を経ることなく炭化を行うことが想定でき、熱エネルギーが不要という点において優位性がある。また、凝集剤を用いないという点から、その分についてもコスト削減が可能で、現状プロセスはもちろんのこと、固形燃料化プロセスと比較しても、その有用性は明らかである。

以上より、本手法導入のメリットは大きく、脱水法の操作条件を適切に設定するとともに、汚泥の再利用用途に合わせて脱水をどの程度まで行うかといった設定についても適切にすることで、処理時間も考慮した省エネルギー的で効率的な廃棄汚泥処理が可能となるものと考えられる。なお、超高压下での使用が可能で汚泥の漏れの小さい濾布の選定は済ませており、今後の課題として、超高压脱水機の大型化と余剰汚泥の連続的な破碎・凝結を行うための装置のライン化があげられるが、本研究成果の実現可能性は十分に期待できる。

# 本手法を導入したプロセス

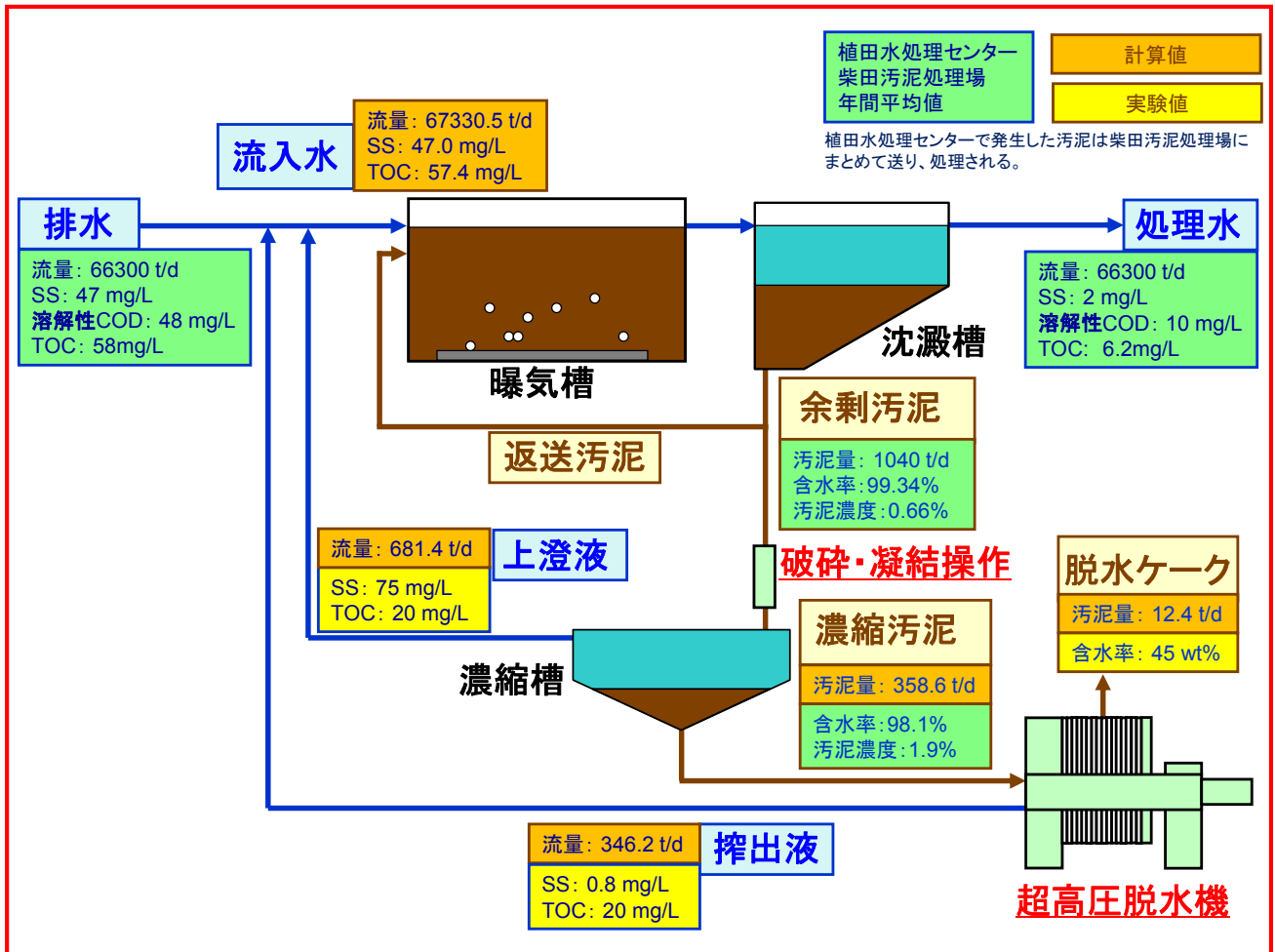


Fig. 30 本手法を導入したプロセス

# エネルギー的観点での優位性

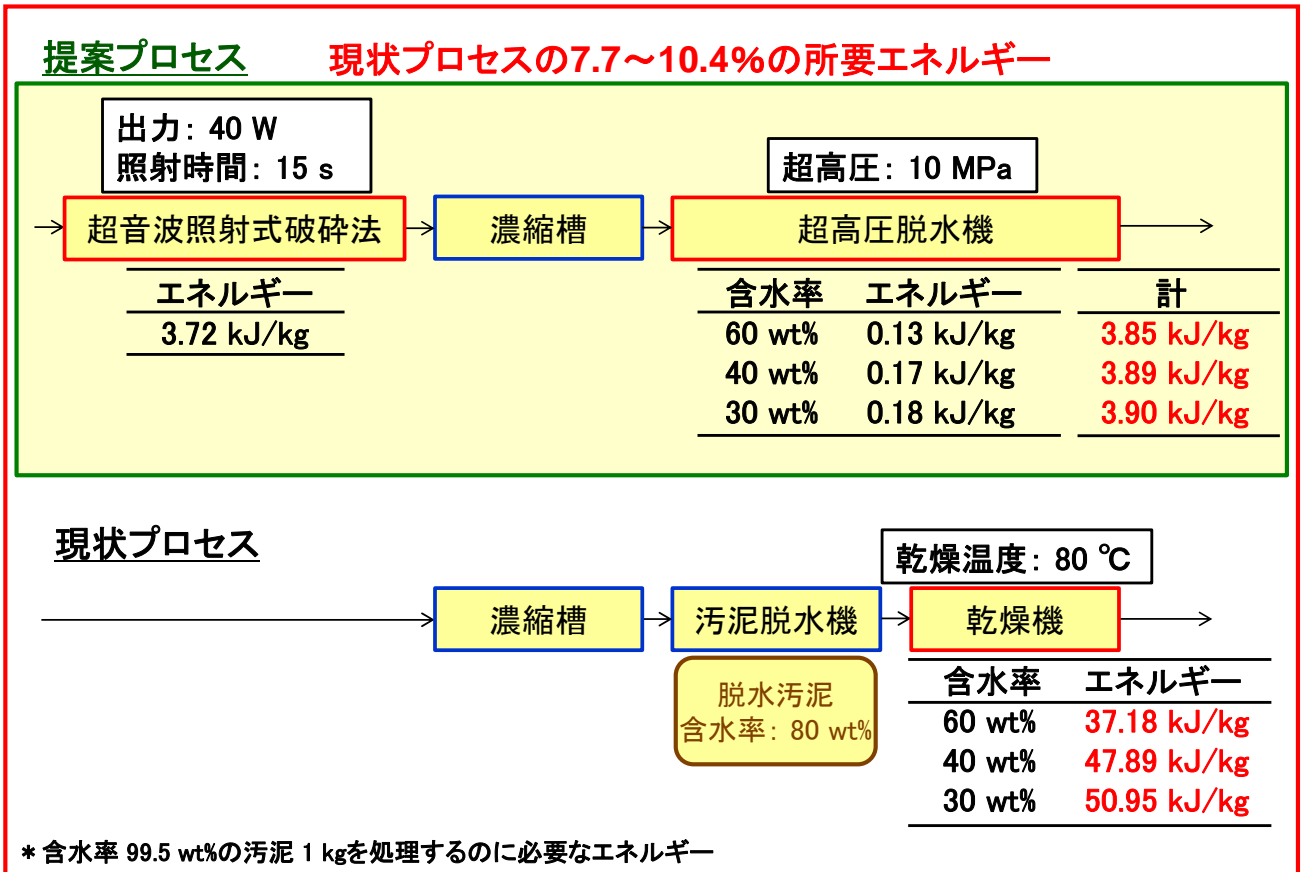


Fig. 31 エネルギー的観点での評価

# 実用化への検討

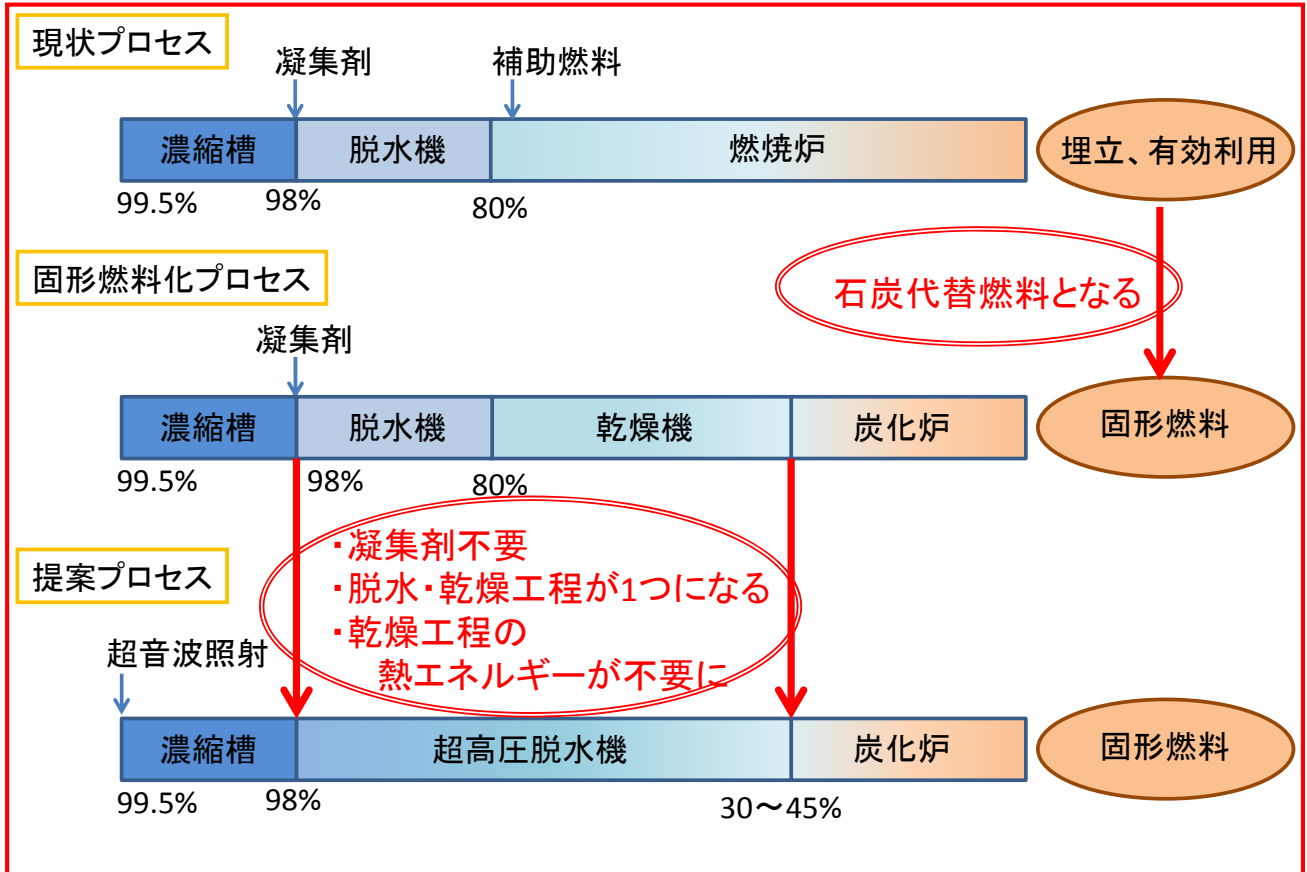


Fig. 32 汚泥の燃料化を想定した場合の提案プロセスの優位性

## 4. 結論

破碎・凝結プロセスとステップ超高压圧搾とを融合した脱水法を提案し、脱水時間と脱水度の両面から、現存技術に比べ格段に優れていることを実証した。難脱水性生物スラッジとして下水余剰汚泥を例にとり、種々の方法で破碎・凝結効果を確認したところ、超音波照射と緩速攪拌の組み合わせが最適であることを示した。さらに、低圧圧搾およびその後の超高压圧搾における脱水速度と脱水度への影響を総合的に考慮すると、超音波照射時間の適切な設定による破碎程度の制御が必要不可欠であることがわかった。採取した汚泥の性状が脱水効果に影響を及ぼすものの、超音波照射と緩速攪拌による破碎・凝結操作と 10 ～ 50 MPa の超高压圧搾とを組み合わせた脱水操作により、含水率が 27 ～ 47% と、既存技術と比較して極めて小さい脱水汚泥を得ることができた。本成果は、機械的脱水では不可能であった汚泥細胞内水分が脱水されたことを示している。圧密脱水速度も著しく向上し、含水率が最も小さくなった条件では、ケーキ含水率は脱水時間 1 分で約 40 %、1 時間で約 30 %、24 時間で 27% まで低減された。汚泥原液を基準とすると、99.3 % もの減量化を実現した。コンポスト化、焼却、炭化、熔融など以後の汚泥処理法に合わせて適切な条件設定を行うことで効率的な脱水が実現できるものと考えられる。

破碎・凝結プロセスや超高压脱水機で必要となるエネルギーは、現状プロセスにおける汚泥の乾燥工程よりも著しく小さく、汚泥の含水率を 40% にすることを想定すると、超音波照射式破碎を導入した場合の所要エネルギーは、脱水・乾燥を行う現状プロセスの 8% 程度であり、省エネルギーでの操作が可能である。また、凝集剤を用いないため再資源化への用途が拡がり、実用化のメリットは大きい。超高压下での使用が可能で汚泥の漏れの小さい濾布の選定は済ませており、超高压脱水機の大型化と余剰汚泥の連続的な破碎・凝結を行うための装置のライン化が今後の課題となるが、本研究成果の実現可能性は大きく、現在の汚泥処理問題への貢献が期待できる。

## 5. 参考文献

- 1) 環境省廃棄物・リサイクル対策；産業廃棄物の排出及び処理状況等(平成 23 年度実績), <http://www.env.go.jp/recycle/waste/sangyo.html>
- 2) 条辺大策, 内山茂幸, 瓜正俊次, 下田雅夫, 末松伸平; 高圧フィルタープレスの開発と商品化, 新日鉄技報, **372**, 67-72 (1999)
- 3) 中塩真喜夫; 廃水の活性汚泥処理, 恒星社厚生閣, 164-165 (1996)
- 4) Iritani, E., N. Katagiri, T. Washizu and K.J. Hwang; High-Level Deliquoring of Activated Sludge by Ultrahigh-Pressure Expression Combined with Flocculation, *Chem. Eng. Sci.*, **112**, 1-9 (2014)
- 5) Iritani, E., N. Katagiri, Y. Wakamatsu and J.H. Cho; Influence of Ultrasonic Pretreatment on Deliquoring Properties in Expression of Carrots, *J. Chem. Eng. Japan*, **47**(12), 869-875 (2014)
- 6) Iritani, E., M. Nishikawa, N. Katagiri and K. Kawasaki; Synergy Effect of Ultrasonication and Salt Addition on Settling Behaviors of Activated Sludge, *Sep. Purif. Technol.*, **144**, 177-185 (2015)
- 7) Mohammadi, A.R., N. Mehrdadi, G.N. Bidhendi and A. Torabian; Excess Sludge Reduction Using Ultrasonic Waves in Biological Wastewater Treatment, *Desalination*, **275**, 67-73 (2011)
- 8) 片桐誠之, 河原広隆, 入谷英司; 微生物ケーキの圧密特性の評価, 化学工学会第 79 年会講演要旨集, 岐阜大学 (岐阜県), H118 (2014)
- 9) Shirato, M., T. Murase, H. Kato and S. Fukaya; Studies on Expression of Slurries under Constant Pressure, *Kagaku Kogaku*, **31**(11), 1125-1131 (1967)
- 10) Shirato, M., T. Murase, A. Tokunaga and O. Yamada; Calculations of Consolidation Period in Expression Operations, *J. Chem. Eng. Japan*, **7**(3), 229-231 (1974)

## 6. 研究発表

### <論文発表>

- 1) Iritani, E., N. Katagiri, and S. Kanetake; Determination of Cake Filtration Characteristics of Dilute Suspension of Bentonite from Various Filtration Tests, *Sep. Purif. Technol.*, **92**, 143-151 (2012)
- 2) Iritani, E., N. Katagiri, Y. Murakami and D. Nakano; Measurements of Growth Rate of Filter Cake in Vertical Single-Pass Ultrafiltration Using Hollow Fiber Membrane Module, *Sep. Sci. Technol.*, **47**(16), 2281-2289 (2012)
- 3) 入谷英司, 片桐誠之, 新庄加苗; BSA およびデキストラン溶液の限外濾過における濾過ケーキの成長と溶質の膜透過の動的挙動, 化学工学論文集, **38**(4), 250-254 (2012)
- 4) 曹達啓, 入谷英司, 片桐誠之; 上向流デッドエンド定圧濾過による O/W エマルションの膜濾過特性の評価, 化学工学論文集, **38**(6), 378-383 (2012)
- 5) Hwang, K.J., P.C. Tsai, E. Iritani and N. Katagiri; Effect of Polysaccharide Concentration on the Membrane Filtration of Microbial Cells, *J. Appl. Sci. Eng.*, **15**(4), 323-332 (2012)
- 6) Cao, D.Q., E. Iritani and N. Katagiri; Properties of Filter Cake Formed during Dead-End Microfiltration of O/W Emulsion, *J. Chem. Eng. Japan*, **46**(9), 593-600 (2013)
- 7) Iritani, E., N. Katagiri, M. Tsukamoto and K.J. Hwang; Determination of Cake Properties in Ultrafiltration of Nano-Colloids Based on Single Step-up Pressure Filtration Test, *AIChE J.*, **60**(1), 289-299 (2014)
- 8) Iritani, E., N. Katagiri, R. Nakajima, K.J. Hwang and T.W. Cheng; Cake Properties of Nanocolloid Evaluated by Variable Pressure Filtration Associated with Reduction in Cake Surface Area, *AIChE J.*, **60**(11), 3869-3877 (2014)
- 9) Iritani, E., N. Katagiri, T. Washizu and K.J. Hwang; High-Level Deliquoring of Activated Sludge by Ultrahigh-Pressure Expression Combined with Flocculation, *Chem. Eng. Sci.*, **112**, 1-9 (2014)
- 10) Iritani, E., N. Katagiri, Y. Wakamatsu and J.H. Cho; Influence of Ultrasonic Pretreatment on Deliquoring Properties in Expression of Carrots, *J. Chem. Eng. Japan*, **47**(12), 869-875 (2014)

- 11) 入谷英司, 片桐誠之, 鷺津拓也, 黄國楨, 鄭東文; 活性汚泥の圧搾による高度脱水における可逆凝集と超高压の複合効果, 化学工学論文集, **40**(5), 396-403 (2014)
- 12) Iritani, E., M. Nishikawa, N. Katagiri and K. Kawasaki; Synergy Effect of Ultrasonication and Salt Addition on Settling Behaviors of Activated Sludge, *Sep. Purif. Technol.*, **144**, 177-185 (2015)

<学会発表>

・国際学会

- 1) Iritani, E., N. Katagiri and T. Washizu; High-Level Deliquoring of Activated Sludge by Step-Up Ultrahigh-Pressure Expression Combined with Reversible Flocculation, Proceedings of the 11th World Filtration Congress (WFC11), Graz (Austria), CD-ROM (2012)
- 2) Iritani, E., N. Katagiri and M. Tsukamoto; Determination of Pressure Dependence of Average Specific Cake Resistance Based on Single Step-Up Pressure Filtration Test, Proceedings of the 11th World Filtration Congress (WFC11), Graz (Austria), CD-ROM (2012)
- 3) Katagiri, N., D. Nakano and E. Iritani; Analysis of Mechanism of Inclined Dead-End Ultrafiltration of Protein Solution, Proceedings of the 11th World Filtration Congress (WFC11), Graz (Austria), CD-ROM (2012)
- 4) Katagiri, N., H. Kawahara and E. Iritani; Evaluation of Filter Cake Properties in Microfiltration of Microbial Suspensions, Proceedings of Filtech 2013, Wiesbaden (Germany), CD-ROM (2013)
- 5) Katagiri, N., T. Washizu and E. Iritani; High-Level Sludge Dewatering by Step-up Ultrahigh-Pressure Expression Combined with Reversible Flocculation, Proceedings of the 1st International IWA Conference on Holistic Sludge Management (HSM2013), Västerås (Sweden), CD-ROM (2013)
- 6) Iritani, E., N. Katagiri, R. Nakajima and M. Tsukamoto; Evaluation of Filtration Characteristics Based on a Variety of Filtration Tests, Proceedings of Filtration and Separation Symposium 2013, Tokyo (Japan), 72-77 (2013)
- 7) Katagiri, N., H. Kawahara and E. Iritani; Effect of Cell Morphology on Microfiltration Properties of Microbial Suspensions, Proceedings of Filtration and Separation Symposium 2013, Tokyo (Japan), 151-156 (2013)

- 8) Cao. D.Q., E. Iritani and N. Katagiri; Determination of Cake Properties in Membrane Filtration of O/W Emulsion, Proceedings of the 9th World Congress of Chemical Engineering (WCCE9), Seoul (Korea), CD-ROM (2013)
- 9) Katagiri, N., H. Kawahara and E. Iritani; Evaluation of Compression-Permeability Characteristics of Microbial Cake Based on Microfiltration Data, Proceedings of European Conference on Fluid-Particle Separation (FPS) 2014, Lyon (France), 11-12 (2014)
- 10) Iritani, E., N. Katagiri, R. Nakajima and M. Tsukamoto; Cake Properties of Nano-Colloids in Variable Pressure Filtration, Proceedings of European Conference on Fluid-Particle Separation (FPS) 2014, Lyon (France), 13-14 (2014)
- 11) Katagiri, N., R. Nakajima and E. Iritani; Evaluation of Cake Properties Based on Variable Pressure Ultrafiltration Associated with Reduction in Cake Surface Area, Proceedings of the 10th International Conference on Separation Science and Technology (ICSST14), Nara (Japan), USB-Memory (2014)
- 12) Yamada, M., N. Katagiri and E. Iritani; Ultrahigh-Pressure Expression Assisted with Self-Coagulation of Sewage Sludge Arising from Disruption Operation, Proceedings of the 10th International Conference on Separation Science and Technology (ICSST14), Nara (Japan), USB-Memory (2014)
- 13) Nakajima, R., N. Katagiri and E. Iritani; Measurement of Cake Properties Based on Variable Pressure Ultrafiltration, Proceedings of Particle Separation 2014, Sapporo (Japan), USB-Memory (2014)

・国内学会

- 1) 曹達啓, 入谷英司; O/W エマルションの膜濾過におけるケーキ特性新規評価法の開発, 化学工学会第 44 回秋季大会講演要旨集, 東北大学 (宮城県), W118 (2012)
- 2) 高橋宏紀, 片桐誠之, 入谷英司; 微生物代謝多糖類の膜分離特性の評価, 化学工学会第 44 回秋季大会講演要旨集, 東北大学 (宮城県), W119 (2012)
- 3) 塚本昌利, 入谷英司; シングル・圧カステップ状濾過によるナノコロイドの濾過特性の迅速決定法の提案, 化学工学会第 44 回秋季大会講演要旨集, 東北大学 (宮城県), W120 (2012)
- 4) 河原広隆, 片桐誠之, 入谷英司; 微生物懸濁液の精密濾過で形成されるケーキ特性の解析, 化学工学会第 44 回秋季大会講演要旨集, 東北大学 (宮城県), W122 (2012)

- 5) 山内一也, 片桐誠之, 入谷英司; 嫌気廃水処理における活性汚泥の有機酸産生と膜分離特性の評価, 化学工学会第 44 回秋季大会講演要旨集, 東北大学 (宮城県), W125 (2012)
- 6) 片桐誠之, 鷺津拓也, 入谷英司; 下水汚泥のステップ超高压圧搾における無機・有機系凝集剤の作用効果, 化学工学会第 78 年会講演要旨集, 大阪大学 (大阪府), R308 (2013)
- 7) 若松祐太, 入谷英司; 野菜試料の圧搾脱液特性に及ぼす前処理効果, 化学工学会第 78 年会講演要旨集, 大阪大学 (大阪府), R313 (2013)
- 8) 山内一也, 片桐誠之, 入谷英司; 嫌気活性汚泥の膜濾過特性に及ぼす廃水組成の影響, 化学工学会第 45 回秋季大会講演要旨集, 岡山大学 (岡山県), O106 (2013)
- 9) 河原広隆, 片桐誠之, 入谷英司; 精密濾過試験に基づく微生物ケーキの圧縮透過特性の評価, 化学工学会第 45 回秋季大会講演要旨集, 岡山大学 (岡山県), O107 (2013)
- 10) 中嶋亮太, 入谷英司; 濾過面積急縮小と変圧変速濾過を融合させた限外濾過ケーキの特性評価, 化学工学会第 45 回秋季大会講演要旨集, 岡山大学 (岡山県), O120 (2013)
- 11) 山田将大, 入谷英司; 破碎・凝結プロセスを導入した下水余剰汚泥の超高压圧搾脱水, 化学工学会第 45 回秋季大会講演要旨集, 岡山大学 (岡山県), O206 (2013)
- 12) 片桐誠之, 河原広隆, 入谷英司; 微生物ケーキの圧密特性の評価, 化学工学会第 79 年会講演要旨集, 岐阜大学 (岐阜県), H118 (2014)
- 13) 山田将大, 入谷英司; 破碎操作による下水汚泥の自己凝集を利用した超高压圧搾脱水, 化学工学会第 46 回秋季大会講演要旨集, 九州大学 (福岡県), F104 (2014)
- 14) 笹川崇光, 片桐誠之, 入谷英司; 微生物代謝多糖およびタンパク質の精密濾過特性の評価, 化学工学会第 46 回秋季大会講演要旨集, 九州大学 (福岡県), F204 (2014)
- 15) 藤井岳, 入谷英司; 破碎処理した酵母スラリーの精密濾過特性, 化学工学会第 46 回秋季大会講演要旨集, 九州大学 (福岡県), F205 (2014)
- 16) 片桐誠之, 山内一也, 入谷英司; 嫌気活性汚泥の有機酸産生と膜濾過特性に及ぼす廃水処理条件の影響, 化学工学会第 80 年会講演要旨集, 芝浦工業大学 (東京都), A224 (2015)
- 17) 片桐誠之, 西川匡子, 入谷英司; 活性汚泥の沈降特性に及ぼす超音波照射と塩添加の相乗効果, 化学工学会第 80 年会講演要旨集, 芝浦工業大学 (東京都), A225 (2015)

<図書>

- 1) 入谷英司; 濾過・圧搾, 「製造プロセスのスケールアップ 正しい進め方とトラブル対策事例集」, 第4章 分離操作設備のスケールアップファクターとその活用ノウハウ, 5節, 技術情報協会, 166-173 (2012)
- 2) 入谷英司; ろ過・圧搾, 粉体工学会編「粉体工学ハンドブック」, 3.9, 朝倉書店, 417-427 (2014)
- 3) 入谷英司; 高吸水性ゲル粒子充填層の圧密・膨張特性, 「ゲルテクノロジーハンドブック」, 第3章 環境浄化, 3節, エヌ・ティー・エス, 614-619 (2014)

※「国民との科学・技術対話」の実施

- 1) 高校生を対象とした実験講習会「テクノサイエンスセミナー」にて成果紹介（主催：名古屋大学工学部、平成24年8月9日、入谷研究室、参加者12名）
- 2) 高校生を対象とした実験講習会「名古屋大学化学・生物実験講習会」にて成果紹介（主催：名古屋大学工学部、平成25年8月6日、入谷研究室、参加者12名）



Contents lists available at ScienceDirect

Chemical Engineering Science

journal homepage: [www.elsevier.com/locate/ces](http://www.elsevier.com/locate/ces)



# High-level deliquoring of activated sludge by ultrahigh-pressure expression combined with flocculation



Eiji Iritani<sup>a,\*</sup>, Nobuyuki Katagiri<sup>a</sup>, Takuya Washizu<sup>a</sup>, Kuo-Jen Hwang<sup>b</sup>

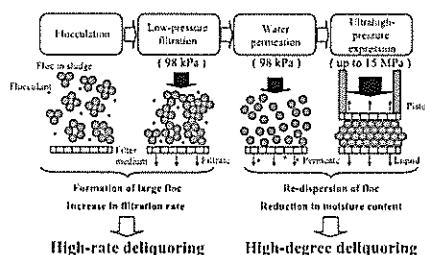
<sup>a</sup> Department of Chemical Engineering, Nagoya University, Furo-cho, Chikusa-ku, Nagoya 464-8603, Japan

<sup>b</sup> Department of Chemical and Materials Engineering, Tamkang University, 151, Yingzhuang Rd., Tamsui, New Taipei City 25137, Taiwan

## HIGHLIGHTS

- Efficient deliquoring process of municipal activated sludge was proposed.
- Low-pressure filtration combined with flocculation led to high-rate deliquoring.
- Expression combined with water permeation resulted in high-degree deliquoring.
- Relation between porosity and compressive pressure was described by a power function.
- Cake moisture content was reduced to 31 wt% at expression pressure of 15 MPa.

## GRAPHICAL ABSTRACT



## ARTICLE INFO

### Article history:

Received 16 January 2014

Received in revised form

4 March 2014

Accepted 8 March 2014

Available online 15 March 2014

### Keywords:

Expression

Ultrahigh pressure

Activated sludge

Moisture content

Deliquoring

Consolidation

## ABSTRACT

The efficient deliquoring process has been developed for achieving high-rate and high-degree deliquoring of municipal excess activated sludge, which exhibits relatively low dewaterability. In the method developed, low-pressure filtration combined with flocculation led to high-rate deliquoring of sludge due to the formation of large flocs. Subsequently, ultrahigh-pressure expression combined with water permeation through the filter cake which promoted the re-dispersion of flocs in the cake resulted in high-degree deliquoring of the cake. It should be noted that the moisture content in the compressed cake was finally reduced to 31 wt% by expression operation under action of an ultrahigh pressure of 15 MPa. This extremely low value of the cake moisture content implies that the liquid contained within the microorganism cells was partially removed by the mechanical pressure when the ultrahigh pressure is applied to the cake in the course of expression. The relation between the equilibrium porosity in the compressed cake and solid compressive pressure was empirically represented by a power function. The kinetics of ultrahigh-pressure expression such as the time variation of the moisture content in the compressed cake was accurately described by combining the multi-stage creep model with the modified Terzaghi model describing the primary consolidation.

© 2014 Elsevier Ltd. All rights reserved.

## 1. Introduction

Sludge accounts for over 40% of industrial waste in Japan, and thus it is of the utmost importance to reduce the waste volume as much as possible from the viewpoint of increased transport costs,

\* Corresponding author. Tel.: +81 52 789 3374; fax: +81 52 789 4531.  
E-mail address: [iritani@nuce.nagoya-u.ac.jp](mailto:iritani@nuce.nagoya-u.ac.jp) (E. Iritani).

a serious shortage of the remaining landfill capacity, and more severe environmental regulations. Deliquoring by mechanical expression of residual sludge arising from wastewater treatment has become increasingly important owing to the relatively low energy consumption compared to thermal drying which follows in the process sequences. It is desirable to remove the maximum feasible amount of liquid by mechanical expression prior to drying and incineration. There has been considerable research on the expression mechanism of sludge in recent decades (Kawasaki et al., 1990b, 1996; Kang et al., 1990a, 1990b; Yoshida, 1993; Chang and Lee, 1998; Chu et al., 1998; La Heij et al., 1996a, 1996b; Lee and Wang, 2000; Mihoubi et al., 2003; Christensen and Keiding, 2007; Huang et al., 2010; Grimi et al., 2010; Petryk and Vorobiev, 2013). Among them, Kawasaki et al. (1990b, 1996) analyzed the expression characteristics of freeze/thaw conditioned excess activated sludge, and examined the effect of bound water, which cannot be easily removed by mechanical expression, on the expression performance. Kang et al. (1990a, 1990b) examined the role of extracellular polymer in expression of activated sludge. Chang and Lee (1998) modified the conventional Terzaghi–Voigt model (Shirato et al., 1974) by considering the ternary consolidation appeared in the final phase of expression in order to accurately evaluate the expression characteristics of sludge (Chu et al., 1998). However, there is not much information on expression characteristics, especially cake moisture content, of excess activated sludge under ultrahigh-pressure expression conditions more than 10 MPa (Bergins, 2004; Venter et al., 2007).

Unfortunately, the deliquoring rate and moisture content of the compressed cake produced by mechanical expression of biological sludge are currently unsatisfactory. The relative effect of expression pressure on decreasing moisture content of the compressed cake and decreasing permeability is fundamental to develop a promising deliquoring method. Although it is to be expected that the increase in the expression pressure leads to the decrease in the moisture content of the compressed cake, the deliquoring rate is unsatisfactory because of the formation of highly compactible filter cake (Tiller and Yeh, 1987; Tiller et al., 1999). In contrast, whilst the deliquoring rate is significantly improved with the advent of high-performance polymer flocculants, the moisture content of the compressed cake is insufficient due to the highly aggregated structure of flocs in the cake. In any case, it is difficult to sufficiently reduce the sludge volume at high rate.

In the present article, a deliquoring method which combined reversible flocculation with ultrahigh-pressure expression is developed as an innovative technique to overcome the defects of

the conventional mechanical deliquoring methods. The effectiveness of the method is examined from the viewpoint of the achievement of high-rate and high-level deliquoring using excess activated sludge discharged from a municipal waste water treatment plant, and the kinetics of ultrahigh-pressure expression is revealed on the basis of the multi-stage creep model combined with the modified Terzaghi model.

## 2. Deliquoring process developed

The outline of the deliquoring process developed in this research is schematically shown in Fig. 1. Inorganic flocculants are initially added to sludge to form large flocs, which enhance the filtration rate in the subsequent low-pressure filtration. After cake formation is completed in the filtration process, water permeation through the filter cake is performed to re-disperse flocs in the cake on the basis of the principle of reversible flocculation achieved by washing out the flocculants. As a result, the cake structure undergoes the substantial change, and thus the denser cake is produced due to the floc breakage in the cake. Finally, the moisture content of the compressed cake is dramatically reduced by expression under action of ultrahigh pressure. Low-pressure filtration combined with flocculation leads to high-rate deliquoring of sludge, and ultrahigh-pressure expression combined with water permeation through the filter cake results in the high degree of deliquoring of the cake.

## 3. Experimental

### 3.1. Materials

The excess activated sludge employed was collected from the aeration tank of the Ueda Sewage Treatment Works (Nagoya City, Japan), and concentrated at 1.0 wt% by decantation for 20 h in the refrigerator kept at 278 K. True density of solids in the sludge measured by the pycnometer was  $1.45 \times 10^3 \text{ kg/m}^3$ . Polyaluminum chloride (PACl, 250A, Taki Chem.) was employed as inorganic flocculants. Water used in water permeation through the filter cake was ultrapure, deionized water (minimum resistivity: 18 M $\Omega$  cm) prepared by purifying tap water through ultrapure water systems equipped with both Elix-UV20 and Milli-Q Advantage for laboratory use (Millipore Corp.).

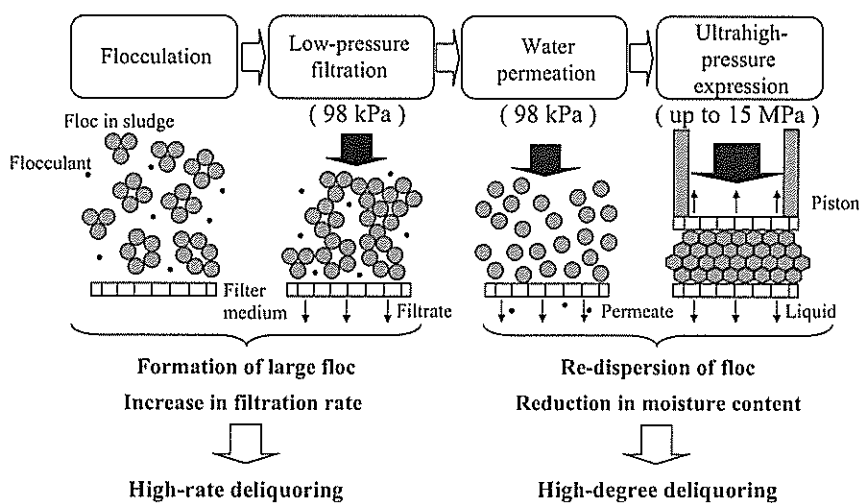


Fig. 1. Schematic view of deliquoring process developed.

### 3.2. Experimental apparatus and technique

The excess activated sludge concentrated at 1.0 wt% by decantation was flocculated with PACI by stirring at 300 rpm for 1 min. The particle size distributions before and after flocculation were measured by a laser diffraction particle size analyzer (SALD-2200, Shimadzu Corp.). The optimum dosage of PACI was determined from the comparative evaluation of the mean specific surface area size  $d_s$ .

Fig. 2(a) illustrates a schematic view of the experimental apparatus used in low-pressure filtration and water permeation through the filter cake formed. A specially designed deliquoring cell with an effective medium area of 9.6 cm<sup>2</sup> was utilized in this research. The cell essentially consists of a stainless-steel cylinder and stainless-steel top and bottom plates. A filter paper (No. 4A, Advantec Toyo Corp.) with a retention size of 1.0 μm was used as a filter medium. Low-pressure filtration was conducted in the dead-end mode by using excess activated sludge of 80 g flocculated with PACI under a constant pressure condition of 98 kPa adjusted automatically by a computer-driven electronic pressure regulator by applying compressed nitrogen gas.

Once filtration is completed, the amount of water which is equivalent to the volume of liquid contained in the filter cake formed in low-pressure filtration is permeated through the filter cake at the same constant pressure that one applied in low-pressure filtration, in order to re-disperse flocs in the cake. The filtrate in low-pressure filtration and the permeate in water permeation

through the filter cake were collected in a reservoir placed on an electronic balance connected to a personal computer to collect and record mass vs. time data. The weights were converted to volumes using density correlations. The amount of PACI contained in the permeate obtained during low-pressure filtration and water permeation was evaluated on the basis of the measurement of the electrical conductivity using the electric conductivity meter (DS-52, Horiba, Ltd.). The difference of the size distributions of flocs in the cake between before and after water permeation was measured by the laser diffraction particle size analyzer. The photomicrograph of flocs in the cake was taken by Digital HF Microscope (VH-8000, KEYENCE Corp.). The sample for the floc analysis after cake formation was prepared by adding the filtrate (water in the case of the cake after water permeation) to the cake and then by stirring at 100 rpm for 2 min. It should be noted that the stirring speed was set to a lower level than that in flocculation in order to avoid floc breakage.

The experimental apparatus used in ultrahigh-pressure expression is schematically shown in Fig. 2(b). Once water permeation was terminated, the top plate was removed from the deliquoring cell and alternatively the movable piston equipped with a filter paper of No. 4A as a filter medium was inserted in the cell cylinder. The liquid was squeezed out of the cake through the top and bottom filter media by application of a mechanical load through a piston by using a material testing machine (SC-20H (MNS-01), Tokyo Testing Machine Inc.). The cake was consolidated at constant pressures  $p_c$  ranging from 98 kPa to 15 MPa. It was suggested that the effect of the side wall friction in the deliquoring cell is negligible if the ratio of the cake thickness to cell cylinder did not exceed 0.6 (Grace, 1953; Tiller and Lu, 1972). In this study, the ratio of the cake thickness to cell cylinder is maintained at relatively low values ranging from 0.010 to 0.39 roughly in order to justify the assumption that the side wall friction is negligible. The time evolution of the cake thickness during constant-pressure consolidation of the cake was measured by a dial gauge fitted on the cell cylinder since the displacement of the cell cylinder was equal to the amount of change in the cake thickness. It should be also noted that the amount of change in the cake thickness is equal to the volume of liquid squeezed out of the cake per unit cross-sectional area. The equilibrium state was considered to be established when the reading of the dial gauge with the minimum scale value of 0.01 mm remained unchanged for 5 h. The residual moisture content in the compressed cake was measured using an infrared-ray moisture meter (FD-720, Kett Electric Lab.) at the end of consolidation in order to rate the degree of deliquoring on the basis of the cake moisture content including liquid inside the microorganism cells.

For comparison, a set of experiments where the flocculants were not employed were also carried out. Additionally, expression experiments were conducted at the same pressure as the one employed in water permeation in place of water permeation experiments.

## 4. Results and discussion

### 4.1. Flocculation

PACI was added to excess activated sludge at various values of the ratio  $R_f$  of added aluminum to the solid mass in sludge, and the particle size distribution was measured by the laser diffraction particle size analyzer to evaluate the flocculation performance of excess activated sludge. For laser diffraction measurements the sludge flocculated with PACI was diluted with the aqueous solution with the same PACI concentration in order to avoid the floc breakage. The mean specific surface area size  $d_s$  of particles

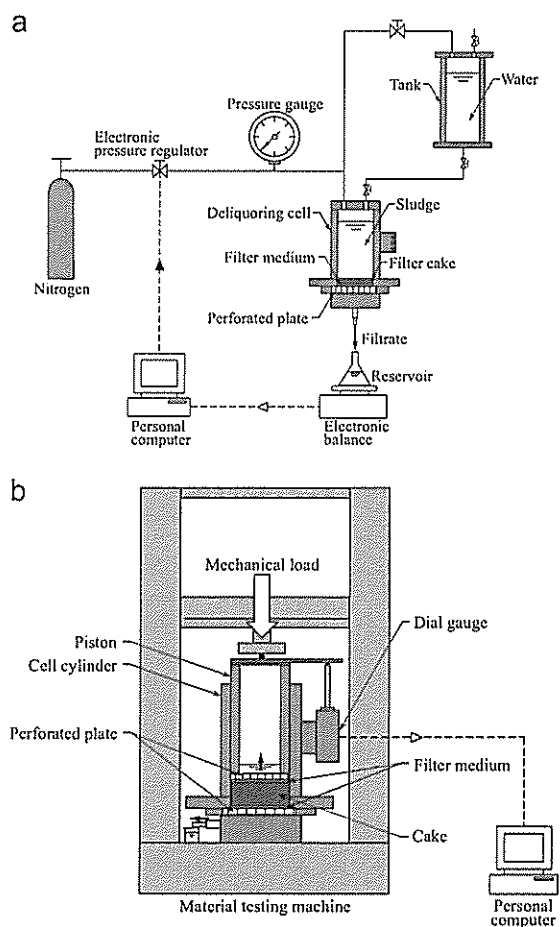


Fig. 2. Schematic view of experimental apparatuses: (a) apparatus for low-pressure filtration and water permeation through filter cake and (b) apparatus for ultrahigh-pressure expression.

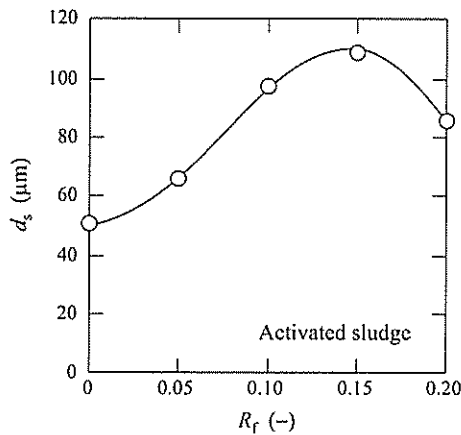


Fig. 3. Relation between mean specific surface area size and ratio of added aluminum to solid mass in sludge.

is plotted against the additive ratio  $R_f$  of PACI in Fig. 3. Whilst  $d_s$  initially increases with increasing  $R_f$ , it decreases by the excessive addition of the flocculant. It is clear that the optimum dosage of PACI where the value of  $d_s$  reaches a maximum is obtained at  $R_f$  of ca. 0.15. Thus, all experiments were carried out with this optimum dosage of PACI. In addition, it should be noted that inorganic flocculants such as PACI form relatively fragile flocs compared with organic flocculants.

#### 4.2. Low-pressure filtration

Typical data of low-pressure filtration of flocculated sludge conducted under the constant pressure condition of 98 kPa are plotted in Fig. 4 as the form of the filtrate volume  $v$  per unit medium area against the filtration time  $\theta$ . For comparison, the result for non-flocculated sludge is also included in the figure. It is obvious that the addition of PACI brings about a remarkable increase in the filtration rate because of the formation of highly permeable filter cake comprised of large flocs (Iritani et al., 2011). For instance, the filtration time is shortened by 93% to obtain the filtrate volume  $v$  of 6 cm by the addition of flocculants. This indicates that flocculation is extremely effective for the improvement of filterability of activated sludge in low-pressure filtration.

#### 4.3. Water permeation through filter cake

Fig. 5 shows the variation with time  $\theta$  of the moisture content  $R$  of the cake on the mass basis obtained from various operations to demonstrate the significance of water permeation through the filter cake. It should be noted that the moisture content of the filter cake decreases pronouncedly in a relatively short time by permeating water through the flocculated filter cake. This implies that the filter cake is efficiently compressed due to the re-dispersion of flocs in the filter cake because the flocculants in the cake are washed away by water permeation through the cake. Such reversible flocculation leads to the significant reduction in the moisture content of the cake. It is expected that the deliquoring of flocculated cake is accelerated in the course of floc breakage occurring during water permeation because the highly resistant skin layer is poorly formed next to the filter medium. In contrast, when the expression operation of the flocculated filter cake is performed in place of water permeation through the filter cake, there is a little reduction in the moisture content of the cake under the same pressure condition (98 kPa) as that employed in

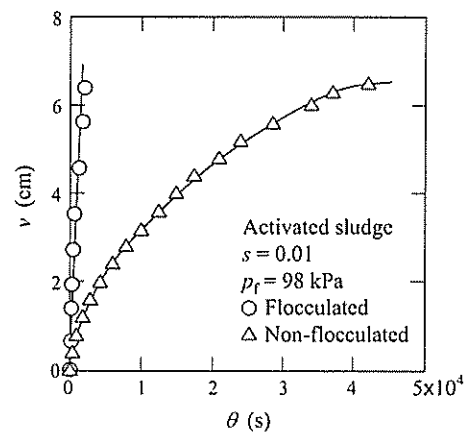


Fig. 4. Relation between filtrate volume per unit medium area and filtration time in low-pressure filtration.

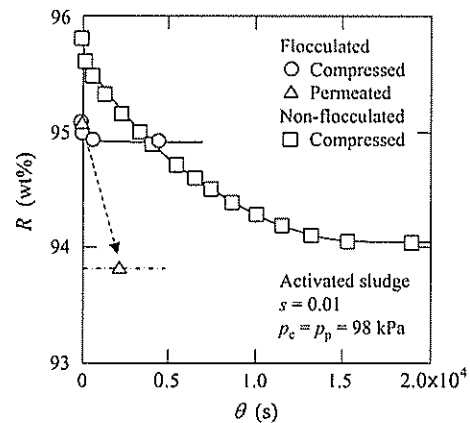


Fig. 5. Decrease in cake moisture content by water permeation through filter cake.

filtration, as shown in the figure. It takes long time to reduce the moisture content of the cake in the course of expression when the flocculants are not employed in low-pressure filtration.

Additionally, it should be stressed that ultrahigh-pressure expression of the cake was impossible except for the cake prepared by permeating water through the flocculated filter cake because a part of the cake leaked out of the narrowest clearance between the piston and cell cylinder. This is probably because the moisture content of the cake is significantly higher near the surface of the filter cake formed in filtration. If elastic diaphragm type of expression equipment which can withstand the ultrahigh-pressure is available, a comparison of ultrahigh pressure expression behaviors between permeated and non-permeated cakes may provide additional insights into the expression mechanisms.

The time variation of the amount of PACI contained in the permeate obtained during filtration and water permeation was measured in order to examine the role of water permeation through the filter cake. In Fig. 6, the aluminum concentration  $C_a$  is plotted against the permeate volume  $v$  per unit cross-sectional area during filtration and water permeation periods. The aluminum concentration  $C_a$  is kept at almost constant value ( $1.5 \times 10^{-6}$  kg/m<sup>3</sup>) throughout the course of filtration. This constant value nearly corresponds to the additive ratio  $R_f$  of aluminum (0.15). Once filtration is followed by water permeation, the aluminum concentration markedly decreases with the progress of water permeation, indicating that a large part of PACI contained in the cake is washed away.

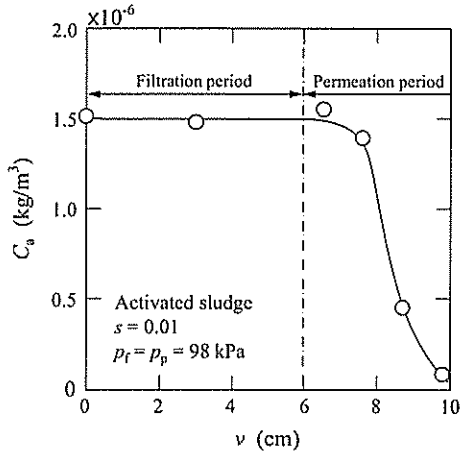


Fig. 6. Variation of aluminum concentration in permeate obtained during filtration and water permeation with permeate volume per unit cross-sectional area.

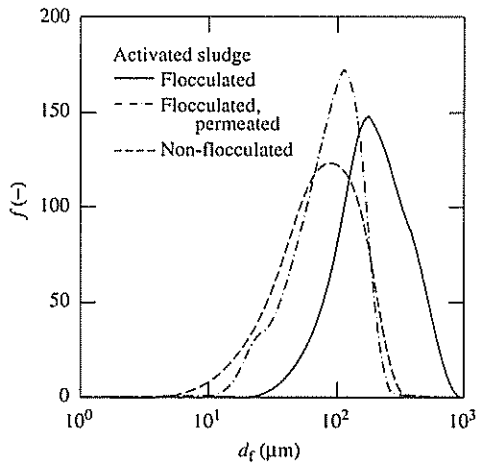


Fig. 7. Size distributions of flocs in cake prepared by different operations.

Fig. 7 compares the size distributions of flocs in the cake produced by different operations, where  $f$  is the frequency, and  $d_f$  is the diameter. Whilst the floc size in the flocculated filter cake is much larger than that in the non-flocculated cake, it pronouncedly decreases by permeating water through the cake and approach the floc size in the non-flocculated cake. It is shown from other experiments that the size distributions of flocs in the flocculated and non-flocculated cakes are nearly identical to those of flocs in the non-flocculated and flocculated sludge, respectively. Moreover, as for the effect of the osmotic pressure on the particle size, preliminary data obtained in our laboratory indicates that the particle size distribution of flocs in the sludge is nearly identical to that of flocs in the sludge in which the solvent is replaced by water through centrifugal decantation. Fig. 8 compares the photomicrographs of flocs in the cake before and after water permeation through the flocculated cake. It is obvious that large flocs produced by PACl addition are re-dispersed by permeating water through the flocculated cake.

#### 4.4. Cake moisture content attained by ultrahigh-pressure expression

In Fig. 9, the final moisture content  $R_c$  of the compressed cake on the mass basis obtained by ultrahigh-pressure expression is logarithmically plotted against the expression pressure  $p_c$  during

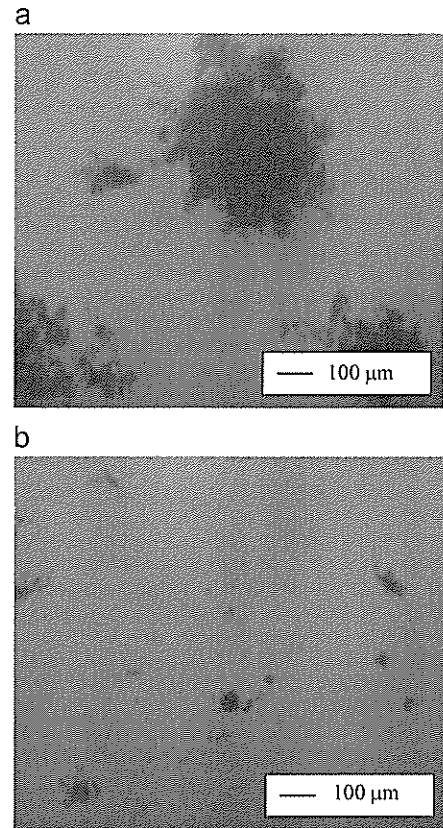


Fig. 8. Photomicrograph of flocs in cake: (a) before and (b) after water permeation.

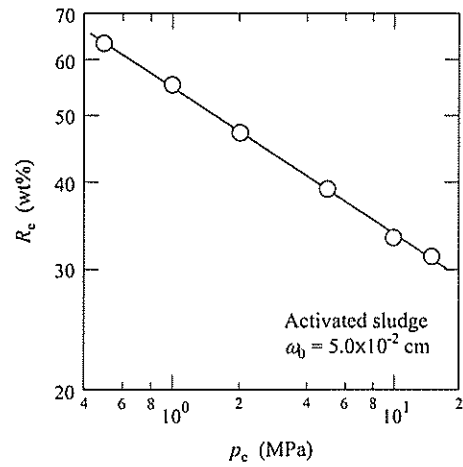


Fig. 9. Relation between final moisture content of compressed cake and expression pressure.

ultrahigh-pressure expression, where  $\omega_0$  is the total solid volume per unit cross-sectional area. It is found that the increase in the expression pressure results in the substantial decrease in the moisture content of the compressed cake. Of particular importance is the surprising result that the moisture content of the compressed cake is finally reduced to 31 wt% by expression under action of an ultrahigh pressure of 15 MPa. This finding leads to the surprising conclusion that the liquid contained within the microorganism cells is partially removed by the mechanical pressure when the ultrahigh pressure is applied to the compressed cake in the course of expression. The experimental data shown in

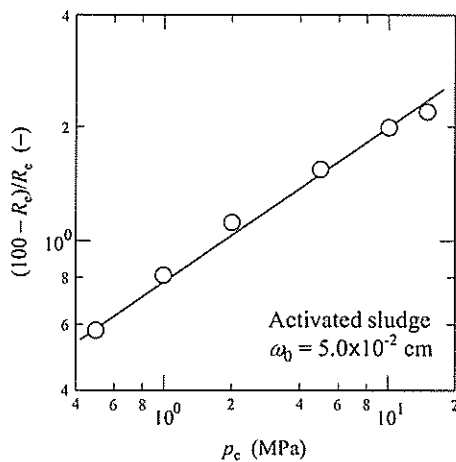


Fig. 10. Relation between  $(100 - R_e)/R_e$  and expression pressure.

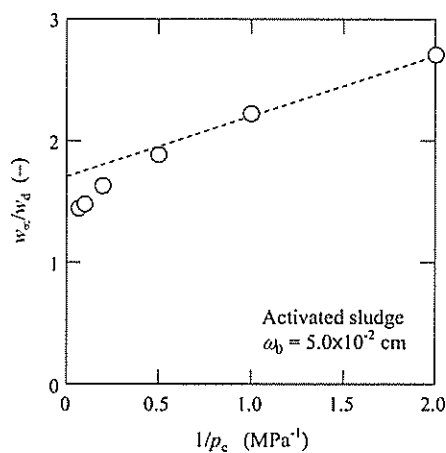


Fig. 11. Relation between  $w_\infty/w_d$  and reciprocal expression pressure.

Fig. 9 are illustrated in Fig. 10 in the form of a plot of  $(100 - R_e)/R_e$  vs.  $p_c$ . It is found that the plots show a linear relationship over a wide range of pressures.

In Fig. 11,  $w_\infty/w_d$  is plotted against the reciprocal expression pressure ( $1/p_c$ ), where  $w_\infty$  is the final wet cake mass per unit cross-sectional area, corresponding the expression pressure, and  $w_d$  is the dry cake mass per unit cross-sectional area (Nakakura et al., 1996). The final wet cake mass at the infinite pressure, which is related to the amount of the bound water, has been frequently evaluated from the ordinate intercept of the straight line of experimental data (Kawasaki et al., 1990a; Matsuda et al., 1992). However, the plots deviate from a linear relationship at more than 2 MPa pressures, and thus it is essential to measure the moisture content of the compressed cake from the real experiments in order to obtain the cake moisture content attained by ultrahigh pressure expression.

Several types of expressions can be utilized to relate the porosity  $\varepsilon$  or void ratio  $e$  (the volume of liquid per unit volume of solid) to the solid compressive pressure  $p_s$  as follows (Tiller and Cooper, 1962)

$$\varepsilon = \varepsilon_1 p_s^{-\lambda} \quad (1)$$

$$e = \frac{\varepsilon}{1 - \varepsilon} = E_0 - C_c \ln p_s \quad (2)$$

where  $\varepsilon_1$ ,  $\lambda$ ,  $E_0$ , and  $C_c$  are the empirical constants. The Terzaghi–Peck Eq. (2) has been frequently employed in the analysis of expression behaviors (Shirato et al., 1987; Iwata et al., 1991).

The porosity  $\varepsilon$  is related to the final moisture content  $R_e$  by

$$\varepsilon = \frac{e}{1 + e} = \frac{\rho_s R_e}{\rho_s R_e + \rho(100 - R_e)} \quad (3)$$

where  $\rho_s$  is the true density of solids, and  $\rho$  is the density of the liquid. It should be noted that the solid compressive pressure  $p_s$  throughout the compressed cake is equal to the applied expression pressure  $p_c$  on the assumption that the effect of the side-wall friction is negligible. Therefore, the data of  $R_e$  vs.  $p_c$  shown in Fig. 9 are converted into the data of  $e$  or  $\varepsilon$  vs.  $p_s$  based on Eq. (3).

Fig. 12((a) and (b)) shows the semi-logarithmic plot of  $e$  vs.  $p_s$  and the logarithmic plot of  $\varepsilon$  vs.  $p_s$ , respectively. As the liquid contained within the microorganism cells is partially removed in the course of expression,  $e$  and  $\varepsilon$  are rated on dry solid basis of microorganism cells for convenience. Whilst the semi-logarithmic plot of  $e$  vs.  $p_s$  cannot be represented by a linear relationship described by Eq. (2), the logarithmic plot of  $\varepsilon$  vs.  $p_s$  yields a straight line over a wide range of pressures in accord with Eq. (1). Therefore, the plot shown in Fig. 10 or Fig. 12(b) is available to examine the experimental data for ultrahigh-pressure expression of municipal excess activated sludge used in this study.

#### 4.5. Kinetics of ultrahigh-pressure expression

The semi-logarithmic plot of  $(1 - U_c)$  vs. the consolidation time  $\theta_c$  is available to evaluate the creep effect in the consolidation

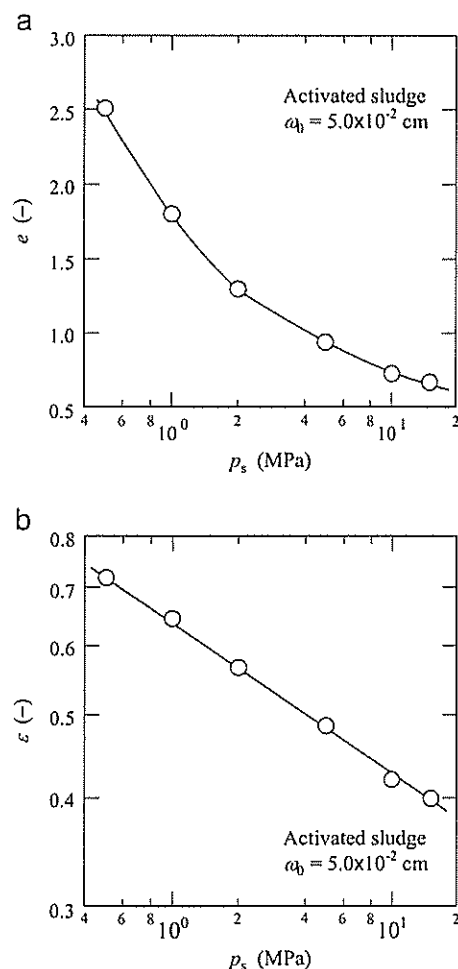


Fig. 12. Effect of solid compressive pressure on structure of compressed cake: (a) relation between void ratio and solid compressive pressure and (b) relation between porosity and solid compressive pressure.

process, where  $U_c$  is the average consolidation ratio indicating a measure of the degree of consolidation and is defined by Shirato et al. (1967, 1974)

$$U_c = \frac{L_1 - L}{L_1 - L_\infty} \quad (4)$$

where  $L_1$ ,  $L$ , and  $L_\infty$  are the thicknesses of the compressed cake at  $\theta_c=0$ ,  $\theta_c$ , and  $\infty$ , respectively. Fig. 13 depicts the typical results obtained in the ultrahigh-pressure expression experiment conducted at the pressure of 15 MPa. The plots can be approximated by three straight lines connecting the different slopes except for the very early stage of consolidation. The slope of the straight line becomes smaller in the range of larger consolidation time. This suggests that there exists a three-staged creep phenomenon with the different values of the creep constant. Therefore, it is expected that the experimental data are not able to be described by neither the modified Terzaghi model (Shirato et al., 1967) nor the Terzaghi–Voigt model (Shirato et al., 1974).

The data indicated in Fig. 13 are illustrated in Fig. 14 in the form of a plot of the average consolidation ratio  $U_c$  vs.  $\sqrt{\theta_c}$ . The experimental data are evaluated by the modified Terzaghi and multi-stage Voigt combined model developed in order to describe the multi-stage creep phenomenon. According to the model, the

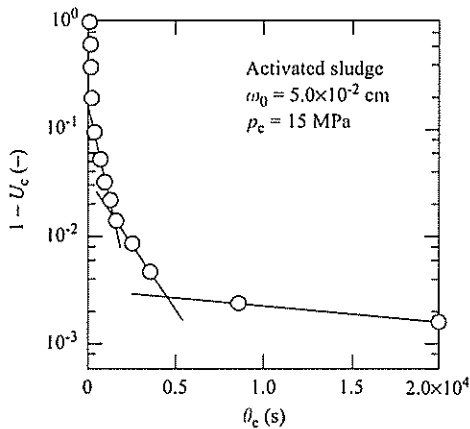


Fig. 13. Evaluation of creep effect.

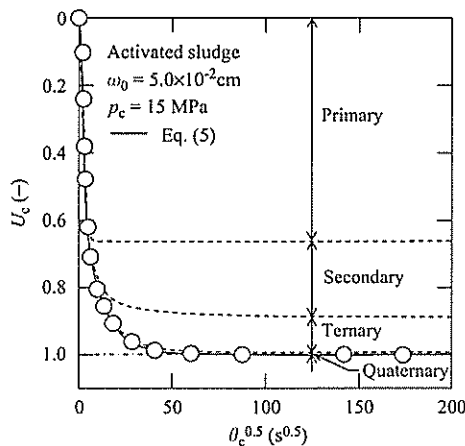


Fig. 14. Typical results for variation of average consolidation ratio with consolidation time.

time evolution of  $U_c$  is described as Iritani et al. (2010)

$$U_c = \frac{L_1 - L}{L_1 - L_\infty} = \left( 1 - \sum_{k=1}^K B_k \right) \left\{ 1 - \exp \left( -\frac{\pi^2}{4} \times \frac{i^2 C_e \theta_c}{\omega_0^2} \right) \right\} + \sum_{k=1}^K B_k (1 - \exp(-\eta_k \theta_c)) \quad (5)$$

where  $B_k$  and  $\eta_k$  are the creep constants of the  $k$ th stage creep, and  $i$  is the number of drainage surfaces. The term  $C_e$  is referred to as the modified consolidation coefficient and is defined by Shirato et al. (1967)

$$C_e = \frac{1}{\mu \alpha \rho_s (-de/dp_s)} \quad (6)$$

where  $\mu$  is the liquid viscosity, and  $\alpha$  is the local specific flow resistance of the compressed cake. Eq. (5) is derived based on the assumption that  $C_e$  is constant throughout the cake at any instant during consolidation although this assumption is not strictly valid (Shirato et al., 1967). Consequently, Eq. (5) may be used as an approximation with a proper mean value of  $C_e$  considered constant. The model is made up of series combination of the Terzaghi spring analogy and the multi-stage Voigt elements connected in series. The first term in Eq. (5) represents primary consolidation of filter cake based on the modified Terzaghi model, and the second term evaluates multi-stage creep effects. This equation is basically the same as the one for expression of agrofood presented by Lanoisellé et al. (1996), Grimi et al. (2010).

The solid line depicted in the figure represents the values calculated by using Eq. (5). Fairly good agreement with the experimental data can be obtained by accounting for the three-stage creep phenomenon. The dotted line represents the contribution of each consolidation stage to the overall consolidation. It is obvious that the fraction of the moisture removed during primary consolidation,  $A$ , defined as  $(1 - B_1 - B_2 - B_3)$ , accounts for the greatest proportion of consolidation, more than 60%, and that the fraction of the moisture removed during the third creep period,  $B_3$ , is extremely small.

The time variation of moisture content  $R$  of the compressed cake on the mass basis is obtained from the time variation of the cake thickness  $L$  based on the relation

$$R = \frac{100(L - \omega_0)\rho}{(L - \omega_0)\rho + \omega_0 \rho_s} \quad (7)$$

In Fig. 15,  $R$  is plotted against the consolidation time  $\theta_c$  during ultrahigh-pressure expression for a variety of expression pressures  $p_c$ . The experimental data are obtained from Eq. (7), using both the time variation of cake thickness  $L$  and the solid volume  $\omega_0$  per unit cross-sectional area measured with an infrared-ray moisture

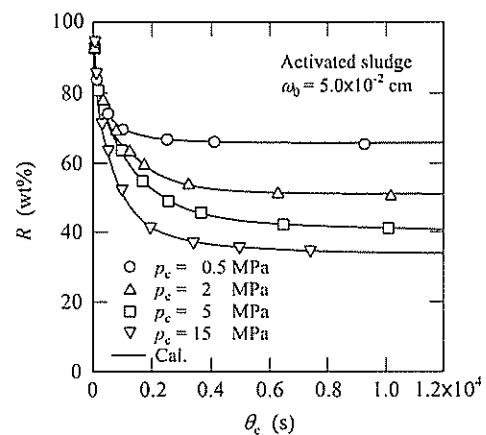


Fig. 15. Variation of cake moisture content with consolidation time.

meter. It is obvious that the increase in the expression pressure  $p_c$  leads to a dramatic improvement in expression performance. The solid lines in the figure are the calculations obtained from Eq. (7), using the time variation of the cake thickness  $L$  calculated from Eq. (5). The calculations compare favorably with the experimental data.

In Fig. 16, the fractions,  $A$ ,  $B_1$ ,  $B_2$ , and  $B_3$ , of the moisture removal are plotted against the expression pressure  $p_c$ . The fraction  $A$  constitutes the major portion of consolidation and increases with increasing expression pressure  $p_c$ . Conversely, the fraction  $B_1$  decreases with increasing  $p_c$ . This implies that the primary consolidation based on the Terzaghi spring analogy plays a more important role in controlling ultrahigh-pressure expression. The fraction  $B_2$  is kept at an almost constant value regardless of the value of  $p_c$ , and  $B_3$  is negligibly small.

The modified consolidation coefficient  $C_e$  is plotted as a function of the expression pressure  $p_c$  in Fig. 17. The coefficient  $C_e$  increases with increasing  $p_c$ , but  $C_e$  is less affected by  $p_c$  in the pressure range above 5 MPa. This may be attributed to the high compressibility of the cake in the ultrahigh-pressure range, as expected from the definition of  $C_e$  given by Eq. (6) (Iritani et al., 2003, 2008).

In Fig. 18, a set of creep constants,  $\eta_1$ ,  $\eta_2$ , and  $\eta_3$ , are plotted against the expression pressure  $p_c$ . It can be seen that each creep constant is maintained roughly constant irrespective of the

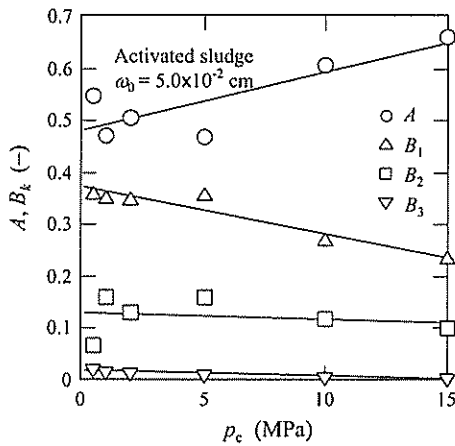


Fig. 16. Effect of expression pressure on ratio of consolidation of each stage to overall consolidation.

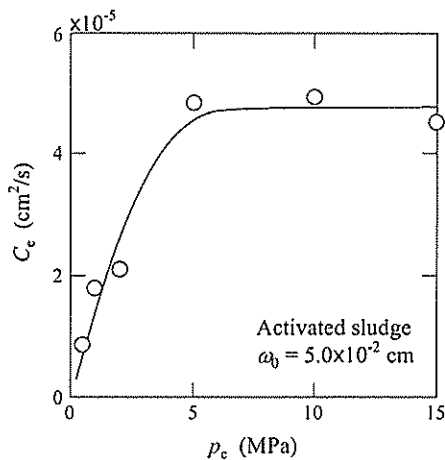


Fig. 17. Effect of expression pressure on modified consolidation coefficient.

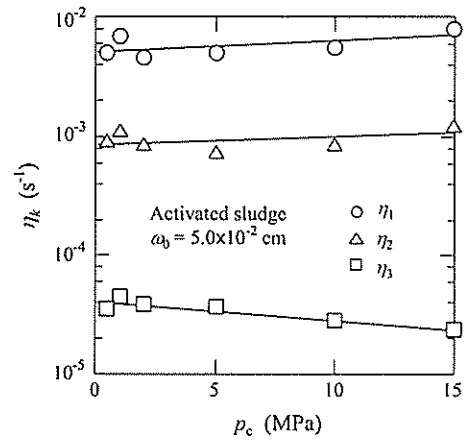


Fig. 18. Effect of expression pressure on creep constants.

pressure  $p_c$ . Each creep constant differs by more than one order of magnitude, thereby indicating that the creep phenomenon occurs in stages.

5. Conclusions

Ultrahigh-pressure expression combined with flocculation has been developed to achieve the high-rate and high-degree deliquoring of excess activated sludge. Flocculation of the sludge due to PACl addition brought about a marked increase in the filtration rate in low-pressure filtration. The moisture content of the compressed cake was finally reduced to 31 wt% by expression under action of an ultrahigh pressure of 15 MPa with the aid of pretreatment by water permeation through the filter cake, suggesting that the liquid contained within the microorganism cells was partially removed by the mechanical pressure. It was found from the analysis of ultrahigh-pressure expression that the equilibrium porosity in the compressed cake was empirically represented by a power function of the solid compressive pressure over a wide range of applied pressures from 0.5 to 15 MPa. Moreover, it was shown that the complicated kinetics of ultrahigh-pressure expression was accurately described on the basis of the modified Terzaghi and multi-stage Voigt combined model.

Nomenclature

- $A$  ratio of primary consolidation to overall consolidation
- $B$  creep constant
- $C_a$  aluminum concentration in permeate ( $\text{kg}/\text{m}^3$ )
- $C_c$  empirical constant in Eq. (2)
- $C_e$  modified consolidation coefficient ( $\text{m}^2/\text{s}$ )
- $d_f$  diameter (m)
- $d_s$  specific surface area size of particles (m)
- $E_0$  empirical constant in Eq. (2)
- $e$  void ratio of compressed cake
- $f$  frequency
- $i$  number of drainage surfaces
- $L$  thickness of cake (m)
- $L_1$  thickness of cake at  $\theta_c=0$  (m)
- $L_\infty$  thickness of cake at  $\theta_c=\infty$  (m)
- $p_c$  expression pressure (Pa)
- $p_f$  filtration pressure (Pa)
- $p_p$  water permeation pressure (Pa)
- $p_s$  solid compressive pressure (Pa)
- $R$  moisture content of cake on mass basis (wt%)

$R_c$	final moisture content of cake on mass basis (wt%)
$R_f$	ratio of added aluminum to solid mass in sludge
$s$	mass fraction of solids in sludge
$U_c$	average consolidation ratio
$\nu$	filtrate volume per unit medium area ( $\text{m}^3/\text{m}^2$ )
$w_\infty$	final wet cake mass per unit cross-sectional area, corresponding expression pressure (kg)
$w_d$	dry cake mass per unit cross-sectional area (kg)
$\alpha$	specific flow resistance of compressed cake (m/kg)
$e$	porosity of compressed cake
$\epsilon_1$	empirical constant in Eq. (1) ( $\text{kg}^4/\text{m}^4/\text{s}^{2\lambda}$ )
$\eta$	creep constant ( $\text{s}^{-1}$ )
$\mu$	liquid viscosity (Pa s)
$\theta$	time (s)
$\theta_c$	consolidation time (s)
$\lambda$	empirical constant in Eq. (1)
$\rho$	density of liquid ( $\text{kg}/\text{m}^3$ )
$\rho_s$	true density of solids ( $\text{kg}/\text{m}^3$ )
$\omega_0$	total solid volume per unit cross-sectional area ( $\text{m}^3/\text{m}^2$ )

## Acknowledgements

This work has been partially supported by Grant-in-Aid for Scientific Research from The Ministry of Education, Culture, Sports, Science and Technology, Japan and from The Ministry of the Environment, Japan, and by The Steel Foundation for Environmental Protection Technology. The authors wish to acknowledge with sincere gratitude the financial support leading to the publication of this article. The authors also wish to express their sincere appreciation to the Ueda Sewage Treatment Works for their generous contribution of the activated sludge used in this research.

## References

- Bergins, C., 2004. Mechanical/thermal dewatering of lignite. Part 2: A rheological model for consolidation and creep process. *Fuel* 83, 267–276.
- Chang, I.L., Lee, D.J., 1998. Ternary expression stage in biological sludge dewatering. *Water Res.* 32 (3), 905–914.
- Christensen, M.L., Keiding, K., 2007. Creep effects in activated sludge filter cakes. *Powder Technol.* 177, 23–33.
- Chu, C.P., Lee, D.J., Huang, C., 1998. The role of ionic surfactants in compression dewatering of alum sludge. *J. Colloid Interface Sci.* 206 (1), 181–188.
- Crimi, N., Vorobiev, E., Lebovka, N., Vaxelaire, J., 2010. Solid-liquid expression from denatured plant tissue: filtration-consolidation behavior. *J. Food Eng.* 96 (1), 29–36.
- Grace, H.P., 1953. Resistance and compressibility of filter cakes, Part I. *Chem. Eng. Prog.* 49 (6), 303–318.
- Huang, S., Chen, J.L., Chiang, K.Y., Wu, C.C., 2010. Effects of acidification on dewaterability and aluminum concentration of alum sludge. *Sep. Sci. Technol.* 45 (8), 1165–1169.
- Iritani, E., Mukai, Y., Katagiri, N., Yoshii, I., 2003. Formation of gel emulsion by filtration-consolidation of O/W emulsions. *J. Chem. Eng. Jpn.* 36 (5), 590–596.
- Iritani, E., Matsumoto, S., Katagiri, N., 2008. Formation and consolidation of filter cake in microfiltration of emulsion-slurry. *J. Membr. Sci.* 318, 56–64.
- Iritani, E., Sato, T., Katagiri, N., Hwang, K.J., 2010. Multi-stage creep effect in consolidation of tofu and okara as soft colloids. *J. Chem. Eng. Jpn.* 43 (2), 140–149.
- Iritani, E., Katagiri, N., Sano, Y., 2011. Properties of microfiltration of humic acid solution flocculated with PACl. *Kagaku Kogaku Ronbunshu* 37 (3), 246–250.
- Iwata, M., Igami, H., Murase, T., Yoshida, H., 1991. Analysis of electroosmotic dewatering. *J. Chem. Eng. Jpn.* 24 (1), 45–50.
- Kang, S.M., Kishimoto, M., Shioya, S., Yoshida, T., Suga, K., 1990a. Properties of extracellular polymer having an effect on expression of activated sludge. *J. Ferment. Bioeng.* 69 (2), 111–116.
- Kang, S.M., Kishimoto, M., Shioya, S., Yoshida, T., Suga, K., 1990b. Dewatering of extracellular polymer and activated sludges by thermochemical treatment. *J. Ferment. Bioeng.* 69 (2), 117–121.
- Kawasaki, K., Matsuda, A., Ide, T., Murase, T., 1990a. Measurement of cell density and floc property of excess activated sludge conditioned by freezing and thawing process, using centrifugal settling. *Kagaku Kogaku Ronbunshu* 16 (2), 401–403.
- Kawasaki, K., Matsuda, A., Murase, T., 1990b. The effect of freezing and thawing process on the expression characteristics and final moisture content of excess activated sludge. *Kagaku Kogaku Ronbunshu* 16 (6), 1241–1246.
- Kawasaki, K., Matsuda, A., Murase, T., 1996. The effect of bound water on filtration and consolidation characteristics of excess activated sludge treated by freezing and thawing treatment. *Kagaku Kogaku Ronbunshu* 22 (2), 294–300.
- La Heij, E.J., Kerkhof, P.J.A.M., Herwijn, A.J.M., Coumans, W.J., 1996a. Fundamental aspects of sludge filtration and expression. *Water Res.* 30 (3), 697–703.
- La Heij, E.J., Kerkhof, P.J.A.M., Kopinga, K., Pel, L., 1996b. Determining porosity profiles during filtration and expression of sewage sludge by NMR imaging. *AIChE J.* 42 (4), 953–959.
- Lanoiselle, J.L., Vorobiev, E.I., Bouvier, J.M., Piar, G., 1996. Modeling of solid/liquid expression for cellular materials. *AIChE J.* 42 (7), 2057–2068.
- Lee, D.J., Wang, C.H., 2000. Theories of cake filtration and consolidation and implications to sludge dewatering. *Water Res.* 30 (3), 1–20.
- Matsuda, A., Kawasaki, K., Mizukawa, Y., 1992. Measurement of bound water in excess activated sludges and effect of freezing and thawing process on it. *J. Chem. Eng. Jpn.* 25 (1), 100–103.
- Mihoubi, D., Vaxelaire, J., Zagrouba, F., Bellagi, A., 2003. Mechanical dewatering of suspension. *Desalination* 158, 259–265.
- Nakamura, H., Nishigaki, F., Matsuoka, T., Sanbuchi, M., Osasa, K., 1996. Dewatering of gels by mechanical compression. *Nippon Shokuhin Kagaku Kogaku Kaishi* 43 (6), 674–682.
- Petryk, M., Vorobiev, E., 2013. Numerical and analytical modeling of solid-liquid expression from soft plant materials. *AIChE J.* 59 (12), 4762–4770.
- Shirato, M., Murase, T., Kato, H., Fukaya, S., 1967. Studies on expression of slurries under constant pressure. *Kagaku Kogaku* 31 (11), 1125–1131.
- Shirato, M., Murase, T., Tokunaga, A., Yamada, O., 1974. Calculations of consolidation period in expression operations. *J. Chem. Eng. Jpn.* 7 (3), 229–231.
- Shirato, M., Iwata, M., Wakita, M., Murase, T., Hayashi, N., 1987. Constant-rate expression of semisolid materials. *J. Chem. Eng. Jpn.* 20 (1), 1–6.
- Tiller, F.M., Cooper, H., 1962. The role of porosity in filtration: Part V. Porosity variation in filter cakes. *AIChE J.* 8 (4), 445–449.
- Tiller, F.M., Lu, W.M., 1972. The Role of porosity in filtration VIII: Cake nonuniformity in compression-permeability cells. *AIChE J.* 18 (3), 569–572.
- Tiller, F.M., Yeh, C.S., 1987. The role of porosity in filtration. Part XI: Filtration followed by expression. *AIChE J.* 33 (8), 1241–1256.
- Tiller, F.M., Cleveland, T., Lu, R., 1999. Pumping slurries forming highly compactible cakes. *Ind. Eng. Chem. Res.* 38 (3), 590–595.
- Venter, M.J., Kuipers, N.J.M., de Haan, A.B., 2007. Modelling and experimental evaluation of high-pressure expression of cocoa nibs. *J. Food Eng.* 80, 1157–1170.
- Yoshida, H., 1993. Practical aspects of dewatering enhanced by electro-osmosis. *Drying Technol.* 11 (4), 787–814.

# 活性汚泥の圧搾による高度脱水における可逆凝集と超高压の複合効果<sup>†</sup>

入谷 英司<sup>1††</sup>・片桐 誠之<sup>1</sup>・鷺津 拓也<sup>1</sup>・黄 國楨<sup>2</sup>・鄭 東文<sup>2</sup>

<sup>1</sup>名古屋大学大学院工学研究科 化学・生物工学専攻, 〒464-8603 愛知県名古屋市千種区不老町

<sup>2</sup>淡江大学 化学工程與材料工学系, 台湾 25137 新北市淡水区英専路 151 號

キーワード: 超高压圧搾, 可逆凝集, 脱水, 活性汚泥, ケーク含水率

無機凝集剤のポリ塩化アルミニウム (PACl) と有機高分子凝集剤のクリフィックスを用いて, 余剰活性汚泥の高度脱水を行った。脱水は, 凝集スラリーの濾過, 濾過ケーキへの透水によるケーキ内の凝集フロクの再分散化, 超高压圧搾の一連のプロセスから構成される。クリフィックスの使用は, PACl の場合に比べ濾過速度を著しく増加させたが, 逆に圧搾速度は減少し, 特に低圧搾圧力の場合に, その傾向は顕著であった。圧搾圧力の増加によるケーキ含水率の低下は, クリフィックスより PACl の場合の方がより顕著であった。注目すべきは, 50 MPa の超高压を作用させると, ケーク含水率は圧搾終了時に 23.7 wt% まで減じたことである。Terzaghi 型の一次圧密とそれに続く主に二段階のクリープ現象を考えることにより, 平均圧密比や圧縮ケーキの平均含水率の経時変化などの超高压圧搾過程の動特性を良好に記述できた。その結果, クリフィックスの場合に, 特に低い圧搾圧力においてクリープ効果が著しいことがわかった。また, 修正圧密係数は圧搾圧力の増加とともに増大したが, ある限界圧搾圧以上では圧搾圧によらず一定値を示し, その値は, PACl, クリフィックスの場合にそれぞれ 5, 10 MPa 程度であった。

## 緒 言

現在, 我が国で年間 4 億 t を超える膨大な排出量の産業廃棄物の中で, 汚泥は 4 割を超える排出量割合を占め, その減量化が大きな課題となっている。機械的脱水法は, 乾燥などの熱的操作と比べ, 固液混合物の最も省エネルギー的な減量化法であり, 機械的脱水でできる限りの減容化を図り, 次段階のプロセスに繋げることが肝要である。しかしながら, 汚泥の種類や性状にもよるが, たとえば下水汚泥の機械的操作で得られる脱水ケーキの含水率は, 通常 80 wt% 前後であり, 更なる低含水率化は, 乾燥などの熱的操作に頼らざるを得ないのが現状である (Raynaud *et al.*, 2010)。

近年, 粗大で強固な凝集フロクを形成できる高分子凝集剤の高性能化が進みつつあり, 脱水速度の著しい向上が実現している一方, こうした強固な凝集フロク内に取り込まれた水分は, その分離除去が困難となり, 最終的に得られる脱水ケーキの含水率は比較的高くなってしまいう問題点がある (Qi *et al.*, 2011)。したがって, 凝集剤を使用せずに汚泥粒子が比較的分散した状態のまま機械的脱水操作を行った方が, 最終的に得られる脱水ケーキの含水率は低減されるものと予測されるが, その場合には, 汚泥スラリーが非常に難濾過性で, 高压縮性の濾過ケーキが形成され, 特に濾材近傍に生成する濾過抵抗が極度に大きくなり, いわゆるスキン層が脱水速度の律速となり, 脱水の進行を著

しく阻害することが知られている。より高い圧力を作用させればさせるほど, 特に濾過の初期段階でこのようなスキン層が形成されるため, 操作圧力の増加がケーキ含水率の低減化には直接繋がらない (Tiller and Green, 1973; Sorensen and Hansen, 1993; Tiller and Kwon, 1998)。したがって, 現状の技術では, 下水汚泥のような難脱水性有機汚泥の高効率な脱水は極めて困難な状況にあり, 汚泥の減量化や脱水汚泥の資源としての有効利用の観点から, 高速で低含水率の脱水ケーキを得る手法の開発が, 現在急務とされている。

そこで, 無機凝集剤による凝集スラリーを高速で濾過した後, 生成ケーキ層に純水を透過し, 無機凝集剤を洗い流してフロクを崩壊させ, 15 MPa におよぶ超高压を作用させてケーキの低含水率化を行う手法を開発した (Iritani *et al.*, 2014b)。本研究では, この手法の有効性や適用範囲をより明確にするため, 凝集剤に無機凝集剤のポリ塩化アルミニウム (PACl (polyaluminum chloride)) と有機高分子凝集剤でポリアクリル酸系, カチオン性のクリフィックスを用いて, 下水余剰汚泥を対象に一連の脱水実験を行い, 濾過, 純水透過, 圧密の各操作におけるそれぞれの凝集剤の作用効果を比較, 考察した。特に超高压を作用させた時の圧密速度や脱水度については, これまでまったく不明であり, 両者の凝集剤の作用効果の違いを比較することにより, 下水汚泥の機械的脱水操作のための基礎的指針を得る。

## 1. 実験装置および方法

試料には, 植田水処理センター (名古屋市) から採取した下水余剰汚泥を用い, 278 K に保たれた冷蔵庫内に静置して, 20 h のデカンテーションで約 2 倍に濃縮し, 固形分の質量分率  $s$  を 0.01

<sup>†</sup> 2014 年 5 月 19 日受理, 2014 年 6 月 24 日掲載決定

DOI: 10.1252/kakoronbunshu.40.396

<sup>††</sup> iritani@nuce.nagoya-u.ac.jp

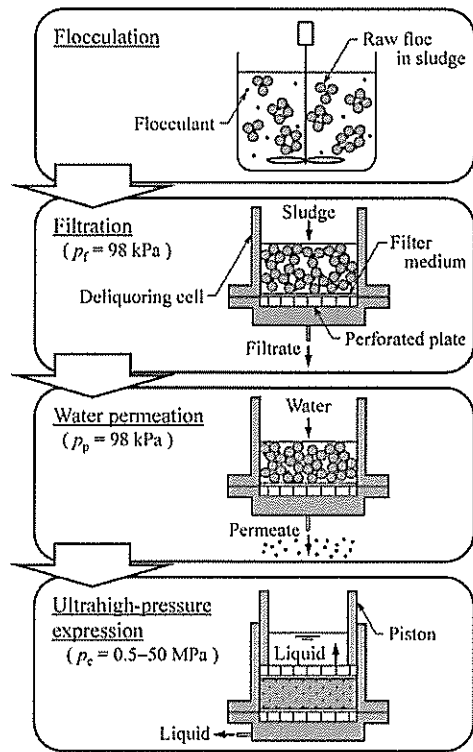


Fig. 1 Schematic diagram of deliquoring process developed in this research

の一定値に保って、実験に供した。この汚泥スラリーに、凝集剤として、無機凝集剤のPACI (250A, 多木化学), または有機高分子凝集剤でポリアクリル酸系, カチオン性のクリフィックス (CP-805, 栗田工業) を用いて凝集処理を行った後に、脱水実験に用いた。凝集処理前後のスラリー中の粒子の粒度分布を、レーザ回折式粒度分布測定装置 (SALD-2200, 島津製作所) で測定した。なお、ケーキへの透水に用いた純水には、超純水製造システム (Elix-UV20およびMilli-Q Advantage, ミリポア) で得た超純水を使用した。

ケーキ脱水のための一連のプロセスの流れをFigure 1にまとめた。凝集操作では、汚泥スラリーに所定量の凝集剤を添加し、ジャーテスター (入江商会) を用いて120 rpmで3 minの急速攪拌の後、50 rpmで10 minの緩速攪拌を行って凝集フロックを形成させた (Iritani *et al.*, 2011)。凝集処理した汚泥スラリーを用いて、窒素加压による濾過と材料試験機 (SC-50H, 東京試験機) による圧密の両操作が可能なセル断面積 $9.6\text{ cm}^2$ の超高压用圧搾セルを用いて、一連の濾過および圧密実験を行った (Iritani *et al.*, 2014b)。まず98 kPaの濾過圧力 $p_f$ で定圧濾過実験を行い、濾液質量の経時変化を電子天秤で測定し、濾液密度 $\rho$ の値を用いて、単位濾過面積あたりの濾液量 $v$ の経時変化に換算した。濾過終了後、直ちに濾過と同一圧力の98 kPaの透水圧力 $p_p$ で、ケーキの空隙体積に相当する量の純水を透過させた。次いで、セル上部のフランジを取り外して、下部に濾材を設けたピストンをセルシリンダに挿入し、材料試験機を用いて、0.5–50 MPaの圧搾圧力の範囲で、種々の荷重圧 $p_c$ を作用させ、両面排水で定圧圧密を行った。圧縮ケーキ厚さ $L$ の経時変化を、セルシリンダに取り付けたダイヤルゲージで測定した。圧密終了後のケーキ含水率 $R_c$ は、乾燥法に比べ簡便で精度の点でも遜色のない赤外線式水分計 (FD-720, Kett) で測定した。なお、ケーキ厚さの測定に用いたダイヤル

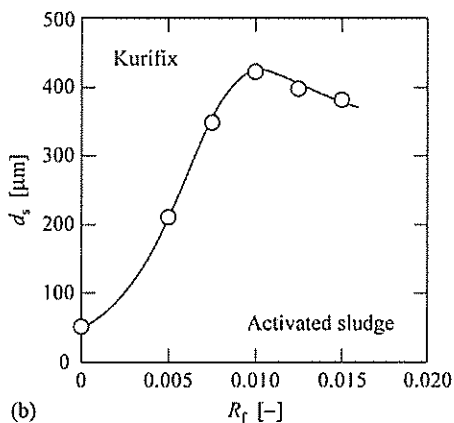
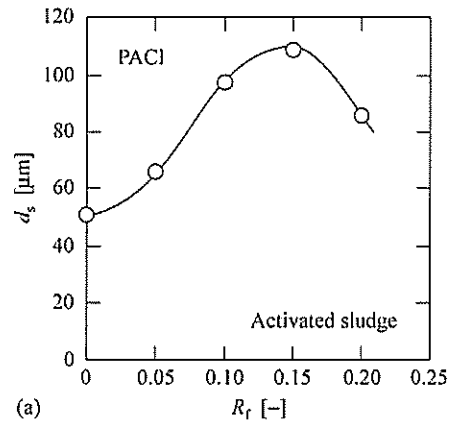


Fig. 2 Determination of optimum dosage of flocculants based on mean specific surface area size of flocs: (a) PACI and (b) Kurifix

ゲージの最小桁 (0.01 mm) が5 hの間変化しなくなった時点を圧密終了点と判断した。濾材には、保留粒子径が $1\text{ }\mu\text{m}$ の濾紙 (4A, ADVANTEC) を用いたが、圧搾圧が20 MPa以上では、濾紙が破損したため、JIS L 1096に準拠して求めた通気性が $0.3\text{ cm/s}$ 以下の濾布 (TRG803K, 岡山中尾フィルター) を使用した。また、圧搾圧が20 MPa以上では、圧搾圧を作用させると、シリンダとピストン間から汚泥の漏れが生じたため、段階的に圧搾圧を増加させて設定圧搾圧での圧密終了時のケーキ含水率を測定した。なお、比較のため、凝集処理を施していない汚泥スラッジの濾過および圧密実験、凝集濾過を行った後にケーキへの透水は行わず、透水圧力と同一の圧搾圧での圧密実験も行った。

## 2. 実験結果および考察

### 2.1 濾過性能に対する凝集効果

活性汚泥スラリーに無機凝集剤のPACI, または有機高分子凝集剤のクリフィックスを、種々に添加量を変化させて加え、スラリー中の粒子の粒度分布を測定した結果を、Figure 2に示した。図中の横軸の添加量 $R_f$ は、PACI, クリフィックスの場合に、それぞれ、スラリー中の固形分質量に対するアルミニウム質量、凝集剤質量として示した。いずれの凝集剤の場合も、添加量 $R_f$ の増加とともに生成フロックの面積平均径 $d_s$ は増大するが、PACIの場合には0.15の濃度比で、またクリフィックスの場合には0.01の濃度比で、それぞれ最大値を示し、過剰量添加すると、面積平均径はかえって減少し始める。この最適凝集域でPACIでは $100\text{ }\mu\text{m}$ 程度、クリフィックスでは、 $400\text{ }\mu\text{m}$ 程度の凝集フロックが得られ、

汚泥スラリーの平均径  $53 \mu\text{m}$  に比べると顕著な増大が見られ、また有機高分子凝集剤の凝集効果が、より顕著なことがわかる。荷電中和が主な凝集機構である PACI に比べ、クリフィックスでは荷電中和のほか、吸着架橋作用も加わり、より粗大なフロックが形成されるものと推察される。

Figure 2 に示した最適添加量の凝集剤を用いて得た凝集スラリーを  $98 \text{ kPa}$  の濾過圧力  $p_f$  で定圧濾過した結果を、Figure 3 に示し、凝集剤無添加の原液スラリーの結果と比較した。図には、単位濾過面積あたりの濾液量  $v$  が濾過時間  $\theta$  に対してプロットされている。また、図中の  $s$  は、スラリー中の固体の質量分率である。濾液量  $v$  が  $6 \text{ cm}$  となった時点までの平均濾過速度 ( $v/\theta$ ) を比較すると、クリフィックスによる凝集スラリーでは  $0.20 \text{ cm/s}$ 、PACI による凝集スラリーでは  $0.0061 \text{ cm/s}$ 、原液スラリーでは  $0.00019 \text{ cm/s}$  となった。凝集剤の添加により、濾過速度は著しく増大し、特にクリフィックスを用いた場合に、その効果は、より顕著であり、Figure 2 に示した凝集効果の傾向と一致している。

### 2.2 ケーク透水による脱水効果

スラリーを全量濾過した後、濾過圧力  $p_f$  と同一の圧力  $p_p (=p_f)$  で生成濾過ケークに純水を透過させ、透水前後のケークの含水率  $R$  を比較し、Figure 4 に示した。図中には、濾過終了後に透水を行わずに、濾過圧力  $p_f$  と同一圧力  $p_c (=p_p)$  で圧搾操作を行った場合、また凝集操作を行わずに、そのままスラリー原液を濾過、圧搾した場合の結果も、併せて示した。純水透過を行うと、PACI の場合には、 $2190 \text{ s}$  の透水時間で、ケークの含水率は、濾過ケークの  $95.1$  から  $93.8 \text{ wt}\%$  まで減少するのに対して、純水透過に代えて圧搾を行うと、ケーク含水率は  $94.9 \text{ wt}\%$  までしか減少しない。これは、純水透過を行うと、可逆凝集の機構でケーク中のフロックが崩壊し、粒子間隙の脱液が容易になるためと推察される (Sakohara *et al.*, 2000; O'Shea *et al.*, 2011)。一方、クリフィックスの場合には、純水透過を行っても、ケーク含水率は、濾過ケークの  $95.6$  から  $95.4 \text{ wt}\%$  までしか減少せず、圧搾操作と同様に、その脱液効果は小さい。架橋作用により生成した強固なフロックは純水透過では崩壊しないことを意味している。凝集剤を添加せずに、そのまま濾過、圧搾操作を行った場合には、圧搾操作により、ケーク含水率は濾過ケークの  $95.8$  から  $94.0 \text{ wt}\%$  まで減少し、最終含水率は透水ケークに匹敵するが、多大の圧搾時間を要し、たとえば  $94.1 \text{ wt}\%$  まで減少させるのに要する圧搾時間は  $13200 \text{ s}$  である。凝集剤による凝集フロックが形成されていない分、粒子間隙の脱液が容易ではあるが、凝集フロックに比べて、より微細な粒子を含むスラリーの濾過となるため、圧搾速度は著しく小さい。Figure 3 に示されたように、濾過操作にも長時間を要し、脱水度の観点からは問題ないものの、脱水速度の観点からは好ましい操作とは言えない。以上より、PACI を用いた場合に、純水透過を行うと、脱水速度と脱水度の向上を図ることができた。

なお、時間  $\theta=0$  でのプロットが濾過ケークの含水率に相当し、各操作での濾過ケークの含水率を比較すると、PACI、クリフィックスによる凝集濾過ケークでそれぞれ  $95.1$ 、 $95.6 \text{ wt}\%$ 、凝集剤未添加の濾過ケークで  $95.8 \text{ wt}\%$  であった。凝集剤未添加の場合に最も含水率が大きくなったのは、濾材近傍に緻密なケーク薄層が形成され、この部分での圧損が大きくなり、それ以外の大部分のケークでの圧縮圧力が小さくなったためと推察される (Tiller and Green, 1973; Sorensen and Hansen, 1993; Tiller and Kwon, 1998)。また、PACI に比べクリフィックスによる凝集ケークの方が、含水率が大きいのは、クリフィックスの方がより粗大な凝集

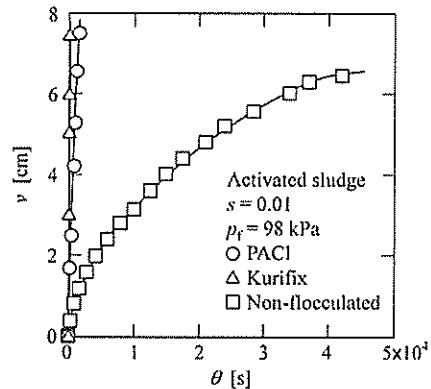


Fig. 3 Filtration performance in constant pressure filtration

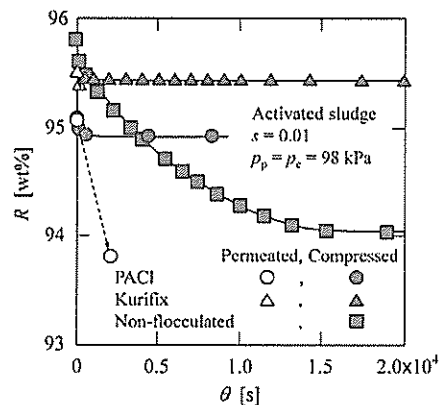


Fig. 4 Effect of water permeation through filter cake on decrease in cake moisture content

フロックが形成されるため、フロック密度関数の関係 (Tambo and Watanabe, 1979) からフロック密度が小さくなって、フロックは、より多くの液を含むようになり、その脱液が困難となるためと考えられる。

### 2.3 超高圧圧搾による脱水効果

凝集剤に PACI、またはクリフィックスを用い、濾過、純水透過を行った後に、圧力をさらに増大させて超高圧圧搾を行った場合の結果を Figure 5 に示した。図には、圧縮ケークの含水率  $R$  が圧密時間  $\theta_c$  に対してプロットされている。いずれの凝集剤の場合にも、圧搾圧力  $p_c$  の増加とともに、ケーク含水率は顕著に低下した。圧密の進行速度、すなわち含水率の低下速度は、クリフィックスに比べ PACI の方が著しく大きいことがわかる。これは、クリフィックスによる凝集フロックの方が、フロックが十分には崩壊せず、圧搾圧の作用下で脱液しにくくなるためと推察される。また、 $0.5 \text{ MPa}$  と圧搾圧が小さい場合には、凝集剤の違いによるケークの最終含水率にほとんど差異は見られないが、圧搾圧が増加すると、PACI の方が、より低いケーク含水率を示した。これもクリフィックスによる強固な凝集フロックの生成に起因するものと考えられる。PACI を用いると、 $15 \text{ MPa}$  の圧搾圧で含水率は  $31.4 \text{ wt}\%$  まで低下し、工業的には、通常  $80 \text{ wt}\%$  の脱水ケークが得られれば妥当とされていたことを考えると、この数値は驚異的であり、超高圧圧搾により微生物細胞内の水分も一部脱液されていることを示している。これまで機械的な脱水操作では、こうした細胞内水分を除去するのは困難であると言われていたが、凝集スラリーの高速濾過、生成濾過ケークへの透水によるケーク中の凝

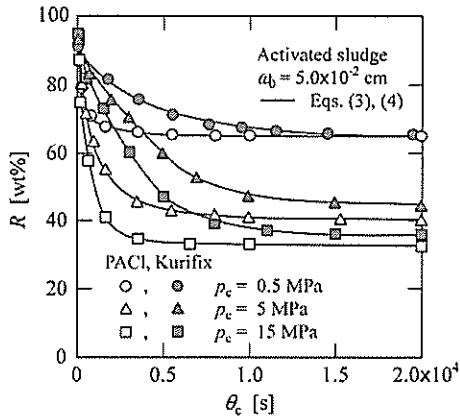


Fig. 5 Kinetics of moisture content of compressed cake formed during ultrahigh-pressure expression

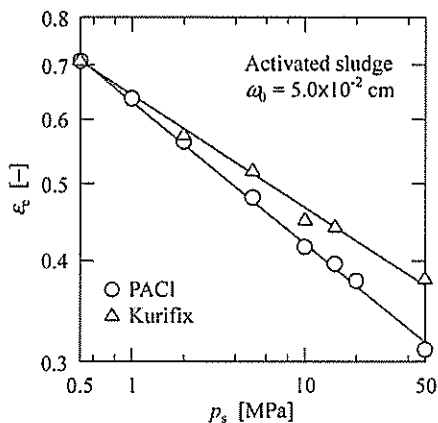


Fig. 6 Effect of solid compressive pressure on equilibrium porosity of compressed cake obtained by ultrahigh-pressure expression

集フロックの再分散化、超高压圧搾による高度脱液という一連の操作を通して、細胞内水分の除去も可能となった。これは、通常のプロセスで後に続く乾燥や焼却などの熱的操作への負担を大きく軽減できるため、その意義は大きい。

15 MPa以上の圧力を作用させて圧搾操作を行おうとすると、圧搾セルのシリンダとピストンの隙間から濾過ケーキが漏れ出てきたため、段階的に圧力を上げて漏れを防ぎ、圧搾圧力とそれに対応した圧縮ケーキの最終含水率を求めた。Figure 6には、このようにして求めたデータも加えて、超高压圧搾で得た圧縮ケーキの最終空隙率 $\epsilon_c$ と固体圧縮圧力 $p_s$ の関係を両対数プロットで示した。なお、ケーキの最終空隙率 $\epsilon_c$ と最終含水率 $R_c$ との間には、次式で示される関係がある。

$$\epsilon_c = \frac{\rho_s R_c}{\rho_s R_c + \rho(100 - R_c)} \quad (1)$$

ここで、 $\rho_s$ は固体粒子の密度、 $\rho$ は濾液の密度である。また、側壁摩擦が無視できるという仮定の下で、圧搾終了時では固体圧縮圧力 $p_s$ はケーキ内のどの部分でも圧搾圧力 $p_c$ に等しいとして求められる(Grace, 1953; Tiller and Lu, 1972)。プロットは、いずれの凝集剤を用いた場合にも、ほぼ直線関係を示し、次式で表された(Tiller and Cooper, 1962)。

$$\epsilon_c = \epsilon_1 p_s^{-\lambda} \quad (2)$$

ここで、 $\epsilon_1$ ,  $\lambda$ は実験定数である。直線勾配はPACIとクリフィックスの場合では異なり、0.5 MPaの低い圧縮圧力では、両者のプロットはほぼ一致するが、圧力の増加とともに、同一圧力での空隙率は、PACIの場合の方が、より小さくなる傾向を示した。本研究で行った最大圧縮圧の50 MPaでは、クリフィックスの場合の空隙率が0.380であったのに対して、PACIでは0.312の値を示し、Eq. (1)を用いて含水率の値に換算すると、23.7 wt%と驚異的に低い値を示した。圧縮圧力を増加させると、クリフィックスの場合の空隙率がPACIの場合ほど低下しなくなる現象は興味深く、この結果は、有機高分子凝集剤を利用すると、高い圧力を作用させても脱液できない水分の割合が増加することを示している。

次に、有機質スラリーに対して適川可能なTerzaghi-一般化Voigtモデルを利用して、超高压圧搾過程における圧密の動的挙動の解析を行った。このモデルは、修正Terzaghiモデルを表すバネ要素と直列に、Voigtモデルが複数個直列に繋がった要素を加えたものであり、このVoigtモデル群により、圧密過程で生じる多段階のクリープ現象を表現できる。本モデルでは、平均圧密比 $U_c$ の経時変化を、次式で表すことができる(Lanoisellé et al., 1996; Grimi et al., 2010; Iritani et al., 2010, 2014b)。

$$U_c = \frac{L_1 - L}{L_1 - L_\infty} = \left( 1 - \sum_{k=1}^K B_k \right) \left\{ 1 - \exp\left( -\frac{\pi^2}{4} \times \frac{i^2 C_c \theta_c}{\omega_0^2} \right) \right\} + \sum_{k=1}^K B_k \{ 1 - \exp(-\eta_k \theta_c) \} \quad (3)$$

ここで、 $L_1$ ,  $L$ ,  $L_\infty$ は、それぞれ圧密開始時、圧密時間 $\theta_c$ 、圧密平衡時の圧縮ケーキ厚さであり、したがって $U_c$ は全圧密量に対する時間 $\theta_c$ での圧密量の比となり、圧密の進行割合を示す。また、 $i$ は排水面の数(本研究では両面排水であるため、 $i=2$ )、 $C_c$ は一次圧密の進行速度を表す修正圧密係数、 $\omega_0$ は単位断面あたりの固体体積、 $B_k$ は全圧密量に対する $k$ 段目のクリープによる圧密量の比、 $\eta_k$ は $k$ 段目のクリープの進行速度を表す定数(Voigtモデルにおける遅延時間の逆数)である。

Figure 7(a)には比較的圧搾圧 $p_c$ が低い0.5 MPa, Figure 7(b)には高い圧搾圧の15 MPaでの平均圧密比 $U_c$ の経時変化を $U_c$ 対 $\sqrt{\theta_c}$ としてプロットし、PACIとクリフィックスの両者の圧密速度を比較した。いずれの圧搾圧においても、PACIの場合の方が、より早く圧密が進行するが、低い圧搾圧の0.5 MPaの場合の方が、その差異は、より顕著となる。また0.5 MPaでは全期間を通して差異が見られるが、15 MPaでは圧密後期の差異が大きくなるのが特徴的である。このことから、クリフィックスに比べ、PACIの場合の方が、脱水しやすい、より緩いフロックが形成されるが、高い圧搾圧を作用させると、フロックの崩壊はフロック強度にはそれほど依存しなくなるものと考えられる。しかしながら、高い圧搾圧での圧密後期における両者の挙動の差異は、クリフィックスの場合の方が、脱液されにくい水分の割合が多いことに起因すると推察される。図中の実線は、Eq. (3)のモデル式に基づき、実験データにフィッティングさせて得た計算値であり、本モデルにより良好に圧密挙動を記述できることがわかった。なお、このフィッティングでは、三段階のクリープを考慮したが、三段目のクリープ量は後述するように無視できるほど小さく、実質的には、主に二段階のクリープが生じていることが明らかとなった。

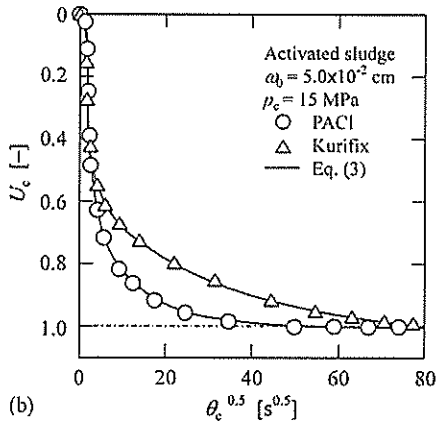
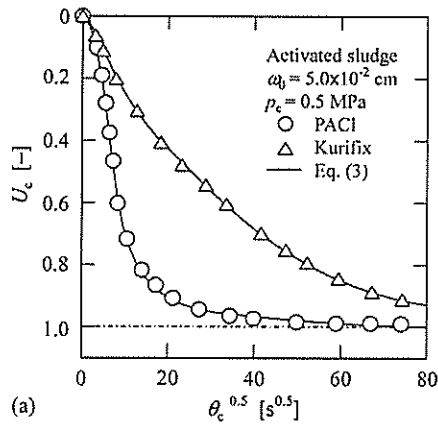


Fig. 7 Kinetics of average consolidation ratio: (a)  $p_c = 0.5$  MPa and (b)  $p_c = 15$  MPa

ケーキ含水率  $R$  とケーキ厚さ  $L$  との間には、次の関係がある。

$$R = \frac{100(L - \omega_0)\rho}{(L - \omega_0)\rho + \omega_0\rho_s} \quad (4)$$

したがって、 $\omega_0$  が既知なら、Eqs. (3), (4) を用いて含水率  $R$  の経時変化を計算することができる。Figure 5 の実線はこのようにして得た計算値であり、圧搾圧力や凝集剤の種類によらず、実験データを良好に記述できた。

Figure 8 には、一次圧密の割合  $A (= 1 - \sum_{k=1}^3 B_k, K=3)$  と各段におけるクリープ圧密の割合  $B_k (k=1-3)$  を圧搾圧力  $p_c$  に対してプロットした。PACI の場合には、Figure 8(a) に示すように、いずれの圧力においても一次圧密割合を表す  $A$  の寄与が最も大きく、低圧下での 50% 前後の値から、圧搾圧力  $p_c$  の増加とともに増大し、15 MPa では 66% となった。それに呼応して、一段目のクリープによる圧密割合を表す  $B_1$  は、圧搾圧力の増加とともに 36 から 24% まで減じた。また、二段目のクリープによる圧密割合を表す  $B_2$  は、圧搾圧力の影響をそれほど受けず、10-15% 程度の値を示した。三段目のクリープは、圧密終期のデータ解析より、その存在は確かに認められるものの、図に示すように圧密量の割合としては極めて小さい。したがって、この三段目のクリープ現象を無視してフィッティングを行っても、平均圧密比  $U_c$  やケーキ含水率  $R$  の経時変化をかなり精度良く記述できる。次に、クリフィックスの場合には、Figure 8(b) に示すように、0.5 MPa の低い圧搾圧では一次圧密の割合  $A$  は 16% と小さいが、圧搾圧  $p_c$  の増加とともに顕著に増大し、15 MPa の圧搾圧では 54% まで増大し、一次圧

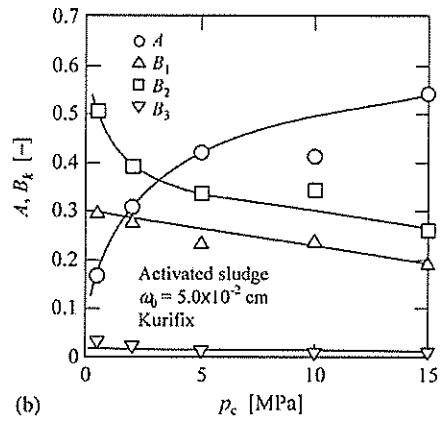
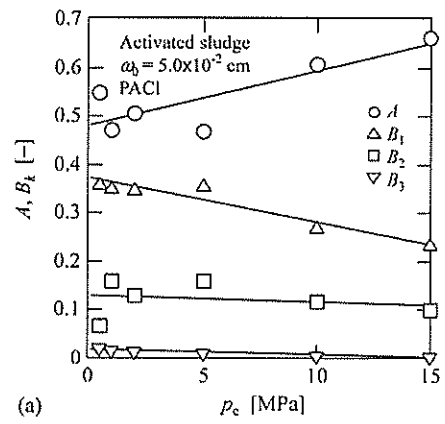


Fig. 8 Effect of applied expression pressure on ratio of consolidation of each stage to overall consolidation: (a) PACI and (b) Kurifix

密が最も支配的となった。一方、0.5 MPa で 51% と最も大きな寄与を示した二段目のクリープは、圧搾圧の増加とともに減少し、15 MPa では 26% まで減じた。一段目のクリープも、変化は、より緩慢であるが、同様な傾向を示し、0.5 から 15 MPa への増加により、クリープの割合は 30 から 20% へと減少した。なお、三段目のクリープの割合が些少であることは、PACI の場合と同様である。以上の結果を総合すると、クリフィックスの場合に、低い圧搾圧では、クリープ効果が顕著なことが、PACI の場合と比較して最も大きな相違である。これは、低い圧搾圧では、有機高分子凝集剤の架橋作用により得られた強固なフロックからの脱液が難しいため、一次圧密に比べてクリープの寄与が大きくなることを意味している。

次に、圧密速度を考察するため、Figure 9 には、フィッティングで得た修正圧密係数  $C_c$  を圧搾圧力  $p_c$  に対してプロットした。PACI、クリフィックスのいずれの場合にも、 $C_c$  は  $p_c$  の増加とともに増大するが、増加の仕方は次第に緩やかになり、やがて、ある圧搾圧以上では  $C_c$  は圧搾圧によらずほぼ一定値を示した。修正圧密係数  $C_c$  は次式で定義される (Shirato *et al.*, 1967)。

$$C_c = \frac{1}{\mu\alpha\rho_s(-de/dp_s)} \quad (5)$$

ここで、 $\mu$  は搾出液の粘度、 $\alpha$  は部分ケーキ比抵抗、 $e (= \varepsilon/(1 - \varepsilon))$ 、 $\varepsilon$  は部分空隙率はケーキの部分空隙比である。また、 $e$  と  $p_s$  の関係を表すのに、次式がよく利用される (Terzaghi and Peck, 1948)。

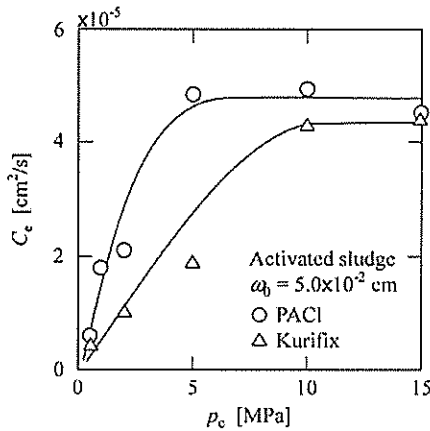


Fig. 9 Effect of applied expression pressure on modified consolidation coefficient

$$e = e_0 - C_c \ln p_s \quad (6)$$

ここで、 $e_0$ ,  $C_c$ は実験定数である。Equation (6)をEq. (5)に代入すると、次式を得る。

$$C_c = \frac{p_s}{C_c \mu \alpha p_s} \quad (7)$$

すなわち、 $\alpha$ が $p_s$ にほぼ比例して増加する高圧縮性ケーキの場合には、 $C_c$ は $p_s$ によらずほぼ一定値を示すことがわかる (Iritani *et al.*, 2003)。なお、圧密時の $\alpha$ ,  $p_s$ の値は実際にはケーキ内で分布があり、さらに圧密の進行に伴い変化するが、Eq. (3)の導出においては、クリープ効果も記述する必要上、 $C_c$ を一定としているため、実験データへのフィッティングから算出した $C_c$ 値は、圧密期間中の平均値を意味することとなる。このように $C_c$ 値を一定として圧密挙動を記述する解析解を導出し、 $C_c$ の値を議論する手法は、これまで数多く報告されている (Shirato *et al.*, 1967, 1974; Kawasaki *et al.*, 1990; Thelander, 1996; Chang and Lee, 1998; Mihoubi *et al.*, 2003; Bergins, 2004; Christensen and Keiding, 2007; Iritani *et al.*, 2007; Huang *et al.*, 2010)。以上のことから、Figure 9に示すように、圧搾圧が高くなると、ケーキの圧縮性が著しく増大するため、 $C_c$ は圧搾圧 $p_c$ の値によらず、ほぼ一定値を示すようになるものと推察される。多くの物質に対する濾過実験から、圧力が増加すると圧縮性が増大するという結果が得られており、本研究で得た圧搾実験の結果と、圧力の増加に伴う圧縮性の増大という点において、よく似た傾向が見られた (Iritani *et al.*, 2012, 2014a)。PACIとクリフィックスの両者を比較すると、Figure 9に示されるように、PACIの場合の方が、 $p_c$ に対する $C_c$ の増加傾向が顕著である。また、 $C_c$ が一定値を示すようになる限界圧は、PACIの場合の方が小さくなり、PACIの場合に5MPa程度、クリフィックスの場合に10MPa程度となる。このことは、PACIによって生成した凝集フロックが、圧搾圧を受けると、クリフィックスの場合より、より壊れやすいことを示唆している。

Figure 10には、Eq. (3)によるカーブフィッティングで用いた各段階でのクリープ速度定数 $\eta_k$  ( $k=1-3$ )を、圧搾圧力 $p_c$ に対してプロットした。各 $\eta_k$ の値は、圧搾圧力の影響をあまり受けないことが明らかとなった。また、 $\eta_1$ ,  $\eta_2$ ,  $\eta_3$ の順に、値は1オーダー程度ずつ小さくなり、段階的にクリープ現象が生じていることが示唆され、PACIとクリフィックスの間での差異はそれほど大き

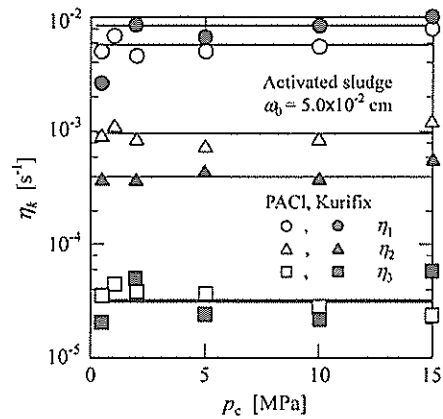


Fig. 10 Effect of applied expression pressure on creep constant in each stage

くないことがわかった。なお、Figure 8に示したように、三段目のクリープ量の割合 $B_3$ が些少であったことを思い起こすと、クリープ現象は、速度定数が大きく異なる二段階で主に生じていると考えてよい。この段階ごとのクリープ速度定数の大きな違いは、たとえば自由水と細胞内水分の脱液のしやすさの違いに由来するとも考えられるが、自由水とそれ以外の水分との定量化に基づく、より詳細な検討が必要とされる (Matsuda *et al.*, 1992; Kawasaki *et al.*, 1996)。

## 結 言

無機凝集剤のPACI、有機高分子凝集剤のクリフィックスを用いて、高速で余剰活性汚泥の凝集濾過を行った後に、凝集フロックを崩壊させるために濾過ケーキに透水し、超高压圧搾で高度に脱液して、できる限りの低含水率ケーキを得る手法を開発し、その有効性を検証した。PACIとクリフィックスを比較すると、凝集濾過ではクリフィックスを用いた場合の方が濾過速度はかなり大きくなったが、超高压圧搾では、PACIを用いた場合の方が圧搾速度は大きくなった。脱水度の観点からは、より高压の圧搾操作を行う場合には、PACIによるケーキの低含水率化の優位点が見られ、50MPaの圧搾圧力では、0.312の空隙率 (23.7wt%の含水率)の極めて高度に脱水された圧縮ケーキが得られた。また、超高压圧搾過程における脱液挙動を、Terzaghi-一般化Voigtモデルを適用して解析し、各段階での圧密量の割合や圧密速度定数を求め、PACIとクリフィックスによるこれらの値の違いや圧搾圧力の影響を明らかにし、考察を加えた。

【謝 辞】 本研究の一部は、文部科学省および環境省の科学研究費補助金、ならびに鉄鋼業環境保全技術開発基金の援助を受けて行われた。また、本研究で用いた汚泥は、植田水処理センターの提供を受けた。ここに記して謝意を表します。

## Nomenclature

$A$	= ratio of primary consolidation to overall consolidation	[-]
$B$	= creep constant	[-]
$C_c$	= empirical constant in Eq. (6)	[-]
$C_c$	= modified consolidation coefficient	[m²/s]
$d_p$	= specific surface area size of particles	[m]
$e$	= local void ratio of compressed cake	[-]
$e_0$	= empirical constant in Eq. (6)	[-]

$i$	= number of drainage surfaces	[-]
$L$	= thickness of compressed cake	[m]
$L_1$	= thickness of compressed cake at $\theta_c=0$	[m]
$L_\infty$	= thickness of compressed cake at $\theta_c=\infty$	[m]
$p_c$	= applied expression pressure	[Pa]
$p_f$	= applied filtration pressure	[Pa]
$p_p$	= water permeation pressure	[Pa]
$p_s$	= local solid compressive pressure	[Pa]
$R$	= moisture content of cake on mass basis	[wt%]
$R_c$	= equilibrium moisture content of cake on mass basis	[wt%]
$R_f$	= ratio of added aluminum or polymer to solid mass in sludge	[-]
$s$	= mass fraction of solids in sludge	[-]
$U_c$	= average consolidation ratio	[-]
$v$	= filtrate volume per unit effective membrane area	[m]
$\alpha$	= local specific flow resistance of compressed cake	[m/kg]
$\epsilon$	= local porosity of cake	[-]
$\epsilon_1$	= empirical constant in Eq. (2)	[kg <sup>4</sup> ·m <sup>-4</sup> ·s <sup>-24</sup> ]
$\epsilon_c$	= equilibrium porosity of compressed cake	[-]
$\eta$	= creep constant	[s <sup>-1</sup> ]
$\mu$	= liquid viscosity	[Pa·s]
$\theta$	= time	[s]
$\theta_c$	= consolidation time	[s]
$\lambda$	= empirical constant in Eq. (2)	[-]
$\rho$	= density of filtrate	[kg/m <sup>3</sup> ]
$\rho_s$	= density of solids	[kg/m <sup>3</sup> ]
$\omega_0$	= total solid volume per unit cross-sectional area	[m <sup>2</sup> /m <sup>2</sup> ]

### Literature Cited

- Bergins, C.; "Mechanical/Thermal Dewatering of Lignite. Part 2: A Rheological Model for Consolidation and Creep Process," *Fuel*, **83**, 267-276 (2004)
- Chang, I. L. and D. J. Lee; "Ternary Expression Stage in Biological Sludge Dewatering," *Water Res.*, **32**, 905-914 (1998)
- Christensen, M. L. and K. Keiding; "Creep Effects in Activated Sludge Filter Cakes," *Powder Technol.*, **177**, 23-33 (2007)
- Grace, H. P.; "Resistance and Compressibility of Filter Cakes, Part 1," *Chem. Eng. Prog.*, **49**, 303-318 (1953)
- Grimi, N., E. Vorobyev, N. Lebovka and J. Vaxelaire; "Solid-Liquid Expression from Denatured Plant Tissue: Filtration-Consolidation Behavior," *J. Food Eng.*, **96**, 29-36 (2010)
- Huang, S., J. L. Chen, K. Y. Chiang and C. C. Wu; "Effects of Acidification on Dewaterability and Aluminum Concentration of Alum Sludge," *Sep. Sci. Technol.*, **45**, 1165-1169 (2010)
- Iritani, E., Y. Mukai, N. Katagiri and I. Yoshii; "Formation of Gel Emulsions by Filtration-Consolidation of O/W Emulsions," *J. Chem. Eng. Jpn.*, **36**, 590-596 (2003)
- Iritani, E., N. Katagiri, K. M. Yoo and H. Hayashi; "Consolidation and Expansion of a Granular Bed of Superabsorbent Hydrogels," *AIChE J.*, **53**, 129-137 (2007)
- Iritani, E., T. Sato, N. Katagiri and K. J. Hwang; "Multi-Stage Creep Effect in Consolidation of Tofu and Okara as Soft Colloids," *J. Chem. Eng. Jpn.*, **43**, 140-149 (2010)
- Iritani, E., N. Katagiri and Y. Sano; "Properties of Microfiltration of Humic Acid Solution Flocculated with PACl," *Kagaku Kogaku Ronbunshu*, **37**, 246-250 (2011)
- Iritani, E., N. Katagiri and S. Kanetake; "Determination of Cake Filtration Characteristics of Dilute Suspension of Bentonite from Various Filtration Tests," *Separ. Purif. Tech.*, **92**, 143-151 (2012)
- Iritani, E., N. Katagiri, M. Tsukamoto and K. J. Hwang; "Determination of Cake Properties in Ultrafiltration of Nano-colloids Based on Single Step-up Pressure Filtration Test," *AIChE J.*, **60**, 289-299 (2014a)
- Iritani, E., N. Katagiri, T. Washizu and K. J. Hwang; "High-Level Deliquoring of Activated Sludge by Ultrahigh-Pressure Expression Combined with Flocculation," *Chem. Eng. Sci.*, **112**, 1-9 (2014b)
- Kawasaki, K., A. Matsuda and T. Murase; "The Effects of Freezing and Thawing Process on the Expression Characteristics and Final Moisture Content of Excess Activated Sludge," *Kagaku Kogaku Ronbunshu*, **16**, 1241-1246 (1990)
- Kawasaki, K., A. Matsuda and T. Murase; "The Effect of Bound Water on Filtration and Consolidation Characteristics of Excess Activated Sludge Treated by Freezing and Thawing Treatment," *Kagaku Kogaku Ronbunshu*, **22**, 294-300 (1996)
- Lanoisellé, J. L., E. I. Vorobyov, J. M. Bouvier and G. Piar; "Modeling of Solid/Liquid Expression for Cellular Materials," *AIChE J.*, **42**, 2057-2068 (1996)
- Matsuda, A., K. Kawasaki and Y. Mizukawa; "Measurement of Bound Water in Excess Activated Sludges and Effect of Freezing and Thawing Process on It," *J. Chem. Eng. Jpn.*, **25**, 100-103 (1992)
- Mihoubi, D., J. Vaxelaire, F. Zagrouba and A. Bellagi; "Mechanism Dewatering of Suspension," *Desalination*, **158**, 259-265 (2003)
- O'Shea, J. P., G. G. Qiao and G. V. Franks; "Temperature Responsive Flocculation and Solid-Liquid Separations with Charged Random Copolymers of Poly(*N*-Isopropyl Acrylamide)," *J. Colloid Interface Sci.*, **360**, 61-70 (2011)
- Qi, Y., K. B. Thapa and A. F. A. Hoadley; "Application of Filtration Aids for Improving Sludge Dewatering Properties—A Review," *Chem. Eng. J.*, **171**, 373-384 (2011)
- Raynaud, M., P. Heritier, J. C. Baudez and J. Vaxelaire; "Experimental Characterisation of Activated Sludge Behaviour during Mechanical Expression," *Process Saf. Environ. Prot.*, **88**, 200-206 (2010)
- Sakohara, S., T. Kimura and K. Nishikawa; "Flocculation Mechanism of Suspended Particles Utilizing Hydrophilic/Hydrophobic Transition of Thermosensitive Polymer," *Kagaku Kogaku Ronbunshu*, **26**, 734-737 (2000)
- Shirato, M., T. Murase, H. Kato and S. Fukaya; "Studies on Expression of Slurries under Constant Pressure," *Kagaku Kogaku*, **31**, 1125-1131 (1967)
- Shirato, M., T. Murase, A. Tokunaga and O. Yamada; "Calculations of Consolidation Period in Expression Operations," *J. Chem. Eng. Jpn.*, **7**, 229-231 (1974)
- Sorensen, P. B. and J. A. Hansen; "Extreme Solid Compressibility in Biological Sludge Dewatering," *Water Sci. Technol.*, **28**, 133-143 (1993)
- Tambo, N. and Y. Watanabe; "Physical Characteristics of Flocs—I. The Floc Density Function and Aluminum Floc," *Water Res.*, **13**, 409-419 (1979)
- Terzaghi, K. and R. B. Peck; *Soil Mechanics in Engineering Practice*, John Wiley, New York (1948)
- Theilander, H.; "The Expression and Washing of Lime Mud," *AIChE Symp. Ser. No. 311*, Vol. 92, pp. 89-98, AIChE, New York, U.S.A. (1996)
- Tiller, F. M. and H. Cooper; "The Role of Porosity in Filtration: Part V. Porosity Variation in Filter Cakes," *AIChE J.*, **8**, 445-449 (1962)
- Tiller, F. M. and W. M. Lu; "The Role of Porosity in Filtration VIII: Cake Nonuniformity in Compression-Permeability Cells," *AIChE J.*, **18**, 569-572 (1972)
- Tiller, F. M. and T. C. Green; "Role of Porosity in Filtration IX Skin Effect with Highly Compressible Materials," *AIChE J.*, **19**, 1266-1269 (1973)
- Tiller, F. M. and J. H. Kwon; "Role of Porosity in Filtration: XIII. Behavior of Highly Compactible Cakes," *AIChE J.*, **44**, 2159-2167 (1998)

# Combined Effect of Reversible Flocculation and Ultrahigh Pressure in High-Level Deliquoring Attained by Expression of Activated Sludge

Eiji IRTANI<sup>1</sup>, Nobuyuki KATAGIRI<sup>1</sup>, Takuya WASHIZU<sup>1</sup>, Kuo-Jen HWANG<sup>2</sup> and Tung-Wen CHENG<sup>2</sup>

<sup>1</sup>Department of Chemical Engineering, Nagoya University,  
Furo-cho, Chikusa-ku, Nagoya-shi, Aichi 464-8603, Japan

<sup>2</sup>Department of Chemical and Materials Engineering, Tamkang University,  
151 Yingzhuan Rd., Tamsui, New Taipei City 25137, Taiwan

**Keywords:** Ultrahigh-Pressure Expression, Reversible Flocculation, Deliquoring, Activated Sludge, Cake Moisture Content

High-level deliquoring of excess municipal activated sludge was accomplished by use of an inorganic flocculant, polyaluminum chloride (PACl), and an organic polymer flocculant, Kurifix. The deliquoring process consisted of filtration of flocculated sludge followed by ultrahigh-pressure expression combined with water permeation through the filter cake, resulting in the re-distribution of flocs in the filter cake. Whereas the use of Kurifix increased the filtration rate significantly more than PACl, it decreased the expression rate, particularly at low expression pressure. As the expression pressure increased, the cake moisture content decreased more remarkably in the case of PACl compared with Kurifix. Of particular interest is that an ultrahigh pressure of 50 MPa decreased the cake moisture content to 23.7 wt% at the end of expression. The kinetics of ultrahigh-pressure expression such as the variations with time of the average consolidation ratio and average cake moisture content was well elucidated by considering a Terzaghi type of primary consolidation followed by a mainly two-stage creep phenomenon. Consequently, the creep effect was marked in the case of Kurifix, particularly at low expression pressure. Moreover, the modified consolidation coefficient increased with the expression pressure and remained constant above a critical expression pressure, which depended on the flocculant: ca. 5 MPa for PACl and ca. 10 MPa for Kurifix.





## Synergy effect of ultrasonication and salt addition on settling behaviors of activated sludge



Eiji Iritani<sup>a,\*</sup>, Masako Nishikawa<sup>a</sup>, Nobuyuki Katagiri<sup>a</sup>, Kenji Kawasaki<sup>b</sup>

<sup>a</sup> Department of Chemical Engineering, Nagoya University, Furo-cho, Chikusa-ku, Nagoya 464-8603, Japan

<sup>b</sup> Department of Applied Chemistry, Ehime University, Bunkyo-cho 3, Matsuyama 790-8577, Japan

### ARTICLE INFO

#### Article history:

Received 11 December 2014

Received in revised form 20 February 2015

Accepted 22 February 2015

Available online 28 February 2015

#### Keywords:

Settling

Ultrasonication

Salt addition

Activated sludge

Reflocculation

### ABSTRACT

The batch sedimentation tests were conducted for the excess activated sludge treated by ultrasonication and addition of sodium chloride, and the settling behaviors such as the sedimentation velocity, the sludge volume, and the quality of the supernatant were examined for different values of the load power of ultrasonication, the sonication time, and the sodium chloride concentration. The ultrasonication pretreatment significantly increased the sedimentation velocity in the initial stage of sedimentation, and the effect was dramatically facilitated by the addition of sodium chloride even when the effect was unnoticeable in the pretreatment of the salt addition alone. The effect of ultrasonication was increased with increasing load power and sonication time and found to be evaluated by the specific ultrasonic energy dissipated into a liquid. The increase in the sedimentation velocity brought about by the pretreatment was caused by the increase in the floc size, and the sedimentation velocity was related to the median diameter of flocs, based on the Stokes law considering the effect of both the floc size and floc density. Moreover, the combined pretreatment markedly reduced the sludge volume, as compared to the pretreatments of ultrasonication alone and salt addition alone.

© 2015 Elsevier B.V. All rights reserved.

### 1. Introduction

The activated sludge process is extensively used in the world as the typical biological treatment of both wastewater and industrial effluents. A major issue of the operation of activated sludge systems is the removal of biological solids from the liquid phase followed by dewatering of these biosolids. Although settling is used as the initial step to increase the solids content, poor settleability of activated sludge is often problematic.

In many cases, chemical conditioning prior to solid–liquid separation is used in order to enhance the separation efficiency [1]. Flocculation of activated sludge leads to organic colloids aggregation, thereby improving the ability of sludge to settle [2]. However, the use of chemical flocculants such as salts and polyelectrolytes increases treatment costs and may also cause secondary environmental pollution. Thus, it is necessary to reduce the specific consumption of flocculants as much as possible.

Various physical and chemical pretreatments, in which sludge is disintegrated and microbial cells are destroyed, have been investigated to reduce the biosolids' volume generated from wastewater treatment plants, including ultrasonication [3–5], mechanical

disintegration (mills, homogenizers, etc.) [6], thermal hydrolysis [7], ozonation [8], acidification [9], alkaline addition [10], microwave irradiation [11], and their combined treatments [12]. These pretreatments enhance sludge biodegradability prior to anaerobic digestion or recycling in aeration tank. Among them, ultrasonication is a particularly attractive method because it cannot cause secondary environmental pollution as with other mechanical disintegration. However, these pretreatments frequently deteriorate sludge settleability and filterability mainly due to the floc breakage and the release of extracellular polymeric substances (EPS) from cells [13–16].

While ultrasonication has been used for the dispersion or collapse of flocculated particles in the liquid phase, Kakii et al. [17] revealed a really challenging fact that activated sludge disrupted by ultrasonication flocculated once again. This means that the ultrasonic pretreatment appears promising also as a means to improve the solid–liquid separation efficiency of activated sludge. In fact, on the basis of the results of the sedimentation velocity, capillary suction time (CST) and specific cake resistance in filtration, Feng et al. [18,19] indicated that ultrasonication with low specific energy is effective for enhancing sludge settleability and filterability. Vaxelaire et al. [20] reported based on the microscopic observations that numerous filaments of filamentous bacteria were

\* Corresponding author. Tel.: +81 52 789 3374; fax: +81 52 789 4531.  
E-mail address: [iritani@nuce.nagoya-u.ac.jp](mailto:iritani@nuce.nagoya-u.ac.jp) (E. Iritani).

### Nomenclature

$C_s$	concentration of sodium chloride in sludge (M)	$r$	correlation coefficient (–)
$D$	fractal dimension for self-similar structure (–)	SV	sludge volume defined as ratio of interface height $H$ to initial height $H_0$ (–)
$d_{50}$	median diameter of flocs (m)	SV <sub>300</sub>	sludge volume defined as ratio of interface height $H_{300}$ after 5 h (300 min) to initial height $H_0$ (–)
$d_f$	floc diameter (m)	TI	turbidity index defined as the ratio of the turbidity in the supernatant to the concentration of solids in sludge represented by the same unit (mg/L) as the turbidity (–)
$E$	specific ultrasonic energy dissipated into sludge (J/kg)	$t$	net ultrasonic exposure time (s)
$g$	acceleration of gravity ( $m/s^2$ )	$u_0$	sedimentation velocity during hindered settling period (m/s)
$H$	height of interface plane between sludge and supernatant (m)	$\theta$	sedimentation time (s)
$H_0$	initial height of sludge (m)	$\mu$	viscosity of supernatant (Pa s)
$H_{300}$	interface height after 5 h (300 min) (m)		
$I$	ultrasonic power dissipated into sludge (W)		
$M$	mass of sludge sample (kg)		
$P$	load power (W)		

cut by the ultrasonic pretreatment, leading to a better settling behavior.

Some research has been dedicated to the role of salt addition to the ultrasonicated sludge. Kakii et al. [17] reported that salt addition promoted reflocculation of ultrasonicated sludge. Yin et al. [21] found that ultrasonic pretreatment of activated sludge from petrochemical plant reduced the necessary flocculant dosage by approximately 25–50% because it decreased the specific cake resistance in filtration. Likewise, Hakata et al. [22] reported that the ultrasonic pretreatment with  $Al^{3+}$ -based coagulation improved the permeate flux in microfiltration of municipal wastewater treated by an activated sludge-lagoon process. In contrast, Feng et al. [19] demonstrated that sludge suffered from ultrasonication and cationic polymer addition provides no clear advantage over polymeric conditioning alone for improving sludge dewaterability. Dewil et al. [14] reported that the required dosage of flocculant increased proportionally with the level of ultrasonic energy to reach the same dryness as the untreated cake in vacuum filtration. Therefore, it is of particular importance to reveal whether the combined pretreatment of ultrasonication and flocculant addition is effective for the improvement of solid–liquid separation efficiency of sludge.

In the present article, the combined pretreatment of ultrasonication and salt addition is examined in order to improve the solid–liquid separation efficiency. In particular, the paper focuses on the synergy effect of ultrasonication and salt addition on settling behaviors such as the sedimentation velocity, sediment volume, and supernatant quality under various operational conditions of the ultrasonic power, sonication time, and added salt concentration using excess activated sludge produced from municipal sewage treatment works.

## 2. Materials and methods

### 2.1. Materials

The excess activated sludge mixed liquor employed in this study was sampled at the Ueda Sewage Treatment Works (Nagoya City, Japan). The solid concentration ranged from 3.6 to 4.9 g/L, the mean value being 4.3 g/L, during the course of our experimental work. The sludge was concentrated at 5.0 g/L by decantation for 20 h in the refrigerator kept at 5 °C to minimize change in its property, and used in the experiments within 4 days. The true density of solids in the activated sludge measured by a pycnometer is  $1.45 \times 10^3 \text{ kg/m}^3$  [23]. It is reported that the original activated sludges contain approximately 6–7 kg bound water per kg of dry solid mass [24]. The viscosities of sludge and supernatant

were measured by using a capillary viscometer. The concentrations of  $Na^+$  and  $Cl^-$  in the sludge were measured by an ion chromatography system (Dionex ICS-1100/2100, Thermo Fisher Scientific Inc., USA). The electric conductivity was measured with a conductivity meter (DS-52, Horiba Ltd., Japan). The zeta potential of particles in the sludge was determined by a particle microelectrophoresis apparatus (Model Mark II, Rank Brothers Ltd., UK). The properties of the activated sludge used in the experiments are listed in Table 1. Sodium chloride was employed as inorganic flocculants.

### 2.2. Experimental apparatus and technique

The ultrasonic apparatus employed was an ultrasonic homogenizer (UP-200S, Dr. Hielsher GmbH, Germany) equipped with a tip with an operating frequency of 24 kHz and a nominal load power output ranging from 50 to 200 W. After the sludge sample was warmed to room temperature (20 °C), the ultrasonic tip was immersed in the sample of 80 g to a depth of approximately 5 mm above the bottom of a 100-mL beaker. The sample was processed with the tip for different total operating times by pulsed ultrasonic irradiation in which one cycle consisted of both the operating time of 0.5 s and the downtime of 0.5 s in order to avoid the rise in temperature as far as possible. Thus, levels of sonication were varied by changing the load power and sonication time. The ultrasonicated sludge was adjusted to a variety of salt concentrations by the addition of the concentrated solution of sodium chloride. Thereafter, the sludge was conditioned by the rapid mixing at a speed of 150 rpm for 3 min using an agitator (Three-One Motor, BL 600, Shinto Scientific Co., Ltd., Japan) followed by the slow mixing at a speed of 50 rpm for 20 min to allow reflocculation to occur. This agitation condition was determined based on the results obtained for different agitation conditions.

Batch gravity sedimentation experiments were conducted using vertical Plexiglass cylinder with 2.9-cm internal diameter and 20-cm height in order to evaluate the settleability of the treated sludge. The settleability was evaluated by three criteria: the sedimentation velocity, the sludge volume, and the quality of the supernatant. Once the treated sludge of 80 g (corresponding to

Table 1  
Properties of activated sludge.

	Activated sludge
pH	6.9
Viscosity (mPa s)	2.62
$Na^+$ (mg/L)	26
$Cl^-$ (mg/L)	31
Electric conductivity (mS/m)	45.1
Zeta potential (mV)	–26.9

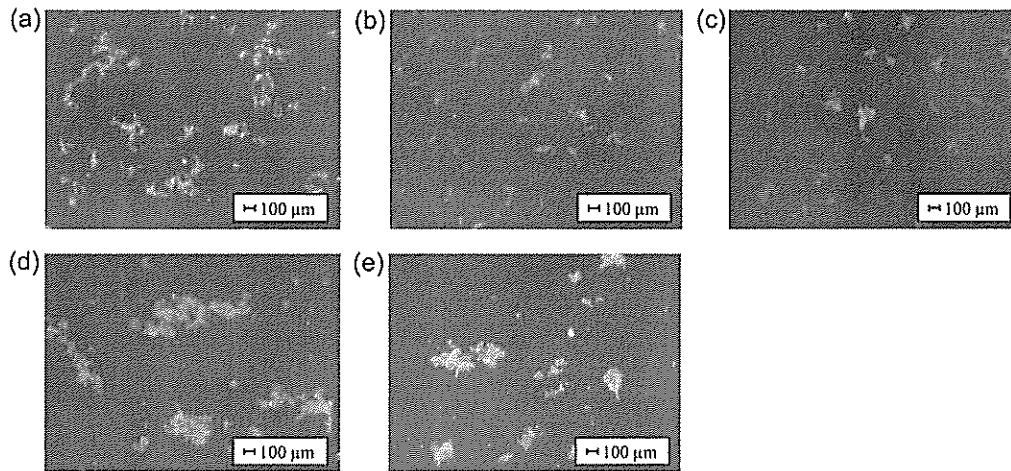


Fig. 1. Photomicrograph of floc structure in ultrasonicated sludge ( $P = 150 \text{ W}$ ,  $t = 75 \text{ s}$ ): (a) untreated sludge, (b) sludge immediately after ultrasonication, (c) ultrasonicated sludge after rapid mixing at 150 rpm for 3 min, (d) ultrasonicated sludge after slow mixing at 50 rpm for 20 min, and (e) ultrasonicated sludge after slow mixing at 50 rpm for 30 min.

the initial height  $H_0$  of 12.0 cm) was gradually poured into a graduated setting cylinder, the sedimentation experiment starts and the sedimentation height  $H$  of the interface plane between the top of settling bed suspension and the supernatant liquid was recorded by taking the photographs with the lapse of the specified sedimentation time  $\theta$  for 24 h. The liquid temperature was almost kept constant ( $20 \text{ }^\circ\text{C}$ ). The experiments were conducted more than twice in order to ensure the reproducibility of the results. The sedimentation velocity  $u_0$  was determined from the slope of the linear relationship between the sedimentation height  $H$  vs. the sedimentation time  $\theta$  during the initial stage of sedimentation. The sludge volume  $SV$  defined as the ratio of the interface height  $H$  to the initial height  $H_0$  was also determined for the specified sedimentation times.

After the sedimentation experiment is completed ( $\theta = 24 \text{ h}$ ), the supernatant containing fine particles and macromolecules was pipetted up to the surface of sedimented sludge. To evaluate the quality of the supernatant, the turbidity and total organic carbon

(TOC) in the supernatant were measured by the turbidimeter (ODYSSEY DR2500 spectrophotometer, Hach Co., USA) and TOC analyser (TOC-5050A, Shimadzu, Corp., Japan), respectively. The viscosity of the supernatant measured by using a capillary viscometer was ca.  $1 \text{ mPa s}$ , which was the same value as that of water. The sediment was diluted with the filtrate obtained by filtering the supernatant of the untreated sludge through a syringe filter with a  $0.45 \text{ }\mu\text{m}$  pore diameter (cellulose acetate) to remove any suspended solid particles, and then the photomicrographs of flocs were taken ( $\times 40$ ) with the digital photomicroscope (BA210EINT, Shimadzu Rika Corp., Japan). The floc size distribution by volume and the median diameter were determined from the feret diameters of at least 200 floc samples based on the photomicrographs. Alternatively, the floc size distribution was measured using a laser diffraction particle size analyzer (SALD-2200, Shimadzu Corp., Japan).

For comparison, the experiments were also carried out for the untreated sludge and the sludges conditioned by ultrasonication alone and salt addition alone, in addition to the sludge conditioned both by ultrasonication and by salt addition.

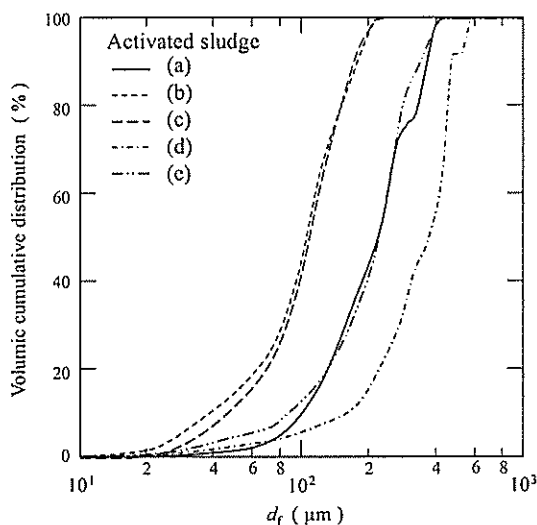


Fig. 2. Cumulative size distribution by volume of flocs in ultrasonicated sludge ( $P = 150 \text{ W}$ ,  $t = 75 \text{ s}$ ).

### 3. Results and discussion

#### 3.1. Microscopic observation and floc size measurement

In Fig. 1, the typical photomicrographs at  $40\times$  magnification of floc structure in the ultrasonicated sludge followed by different mixing operations are compared with the photomicrograph of floc structure in the untreated sludge. The corresponding cumulative size distributions by volume of flocs are illustrated in Fig. 2, where  $d_f$  is the floc diameter. The contrast between the floc size distributions shown in Fig. 2 and the photomicrographs shown in Fig. 1 reveals a better understanding of the change of floc structure induced by ultrasonication. The size distributions are based on the feret diameters measured from the photomicrographs of flocs since the measurements obtained using a laser diffraction particle size analyzer underestimates the real floc size probably as a result of floc breakage caused by the introduction of the sample into the measuring chamber. It should be noted that the particles less than  $10 \text{ }\mu\text{m}$  are ignored in the measurements because such small particles are mostly present in the supernatant after settling and have little influence on the sedimentation velocity. The cumulative size

distribution enables the volume median diameter of the flocs to be determined. The median diameter of the initial flocs in the raw untreated sludge is 220  $\mu\text{m}$  (Fig. 2). As shown in Fig. 1(a), the activated sludge is considerably heterogeneous because it consists of a large number of different microorganisms. Immediately after ultrasonication with the load power  $P$  of 150 W and the net ultrasonic exposure time  $t$  of 75 s, the flocs become much smaller than those in the untreated sludge due to floc disintegration (Fig. 1(a) and (b)), and the median diameter of flocs falls to 105  $\mu\text{m}$  (Fig. 2). Although the size distribution of the disrupted flocs in the ultrasonicated sludge remains almost unchanged by the following rapid mixing at 150 rpm for 3 min (Figs. 1(c) and 2), the flocs in the ultrasonicated sludge become significantly large after slow mixing at 50 rpm for 20 min following the rapid mixing (Fig. 1(d)) and the median diameter of flocs increased to a high value of 380  $\mu\text{m}$  (Fig. 2). The intracellular materials, such as proteins, and nucleic acids, released during the breakup of the bacterial cells act as an excellent flocculant. Due to the presence of positive charges, these compounds bind to the anionic sites of the bacteria and the polysaccharides, resulting in reflocculation [25]. However, the slow mixing of more prolonged period of 30 min following the rapid mixing disintegrates the flocs in the ultrasonicated sludge (Fig. 1(e)), and the median diameter decreases to almost the same size (220  $\mu\text{m}$ ) as that of untreated flocs (Fig. 2). This suggests that the flocs enlarged by ultrasonication are likely to be disrupted. It is, therefore, considered that the floc size is determined by a balance of both the growth and erosion of flocs resulting from the shearing action [17,25].

Fig. 3 shows the typical photomicrographs of floc structure in the sludge obtained by the combined pretreatment of ultrasonication and salt addition. The sludge ultrasonicated during 75 s with the power of 150 W was adjusted to the sodium chloride concentration  $C_s$  of 0.1 M due to salt addition immediately after ultrasonication. Fig. 4 illustrates the corresponding cumulative size distributions by volume of the flocs. Flocculation effect becomes more conspicuous when sodium chloride is added to the ultrasonicated sludge. Reflocculation of flocs disintegrated by ultrasonication occurs due to the action of sodium chloride once a rapid mixing is conducted, and the floc size increases to the same size as that of the untreated sludge (Figs. 3(a) and 4). It should be noted that the rapid mixing was carried out to mix the salt well with the sludge. The subsequent slow agitation for 20 min provokes the median size to further increase to 450  $\mu\text{m}$  (Figs. 3(b) and 4). Although the slow mixing time is prolonged until 30 min, the agitation does not cause significant disruption of the flocs grown (Figs. 3(c) and 4). Hence, it is inferred that salt addition to ultrasonicated sludge brings about not only the enlargement of the floc size but also the increase in the floc strength. The results obtained by the pretreatment of salt addition alone are also included in Figs. 3(d) and 4. Of particular interest is that salt addition to the ultrasonicated sludge greatly facilitates flocculation of activated sludge whereas the pretreatment of salt addition alone has little effect on flocculation in the sodium chloride concentration of 0.1 M (Fig. 3(b) and (d)). Consequently, it would be expected that the floc coarsening leads to the improvement of solid–liquid separation efficiency of activated sludge. In order to maintain the mixing condition constant, the rapid mixing at 150 rpm for 3 min followed by the slow mixing at 50 rpm for 20 min was adapted as the mixing condition for floc growth in all our subsequent experiments.

### 3.2. Batch sedimentation curve

In the batch sedimentation tests, the overall settling behaviors are examined by describing the sedimentation curve represented as the form of the height  $H$  of the interfacial plane between the

sludge and the supernatant normalized by the initial height  $H_0$  against the sedimentation time  $\theta$ . Fig. 5 illustrates the batch sedimentation curve of the sludge pretreated under various conditions. Although the particles less than about 10  $\mu\text{m}$  are mostly left in the supernatant without settling out, a distinct sedimentation interface of larger particles is observed. The sedimentation curve is based on the time variation of the height  $H$  of this interface. It is obvious that any sedimentation curve is roughly divided into two periods: the hindered settling period in which the interface between the sludge and the supernatant descends at a constant velocity depending on the sludge concentration and the subsequent sludge compression period in which the subsidence velocity of interface declines gradually. The sedimentation behaviors under various pretreatment conditions are compared from the viewpoint of the sedimentation velocity  $u_0$  during the hindered settling period and the sludge volume (SV), which is taken as a measure of thickening degree during the sludge compression period. In the untreated sludge, the sedimentation velocity  $u_0$  is 0.24 mm/min and the sludge volume  $SV_{300}$  defined as the ratio of the interface height  $H_{300}$  after 5 h (300 min) to the initial height  $H_0$  is 0.56, as shown in Fig. 5(a). In the salt added sludge with the sodium chloride concentration  $C_s$  of 0.1 M, the sedimentation velocity increased to 2.1 times that of the untreated sludge and  $SV_{300}$  reduced to 0.49. When the sludge is ultrasonicated during 75 s with the power  $P$  of 150 W, the sedimentation velocity increases to 3.2 times that of the untreated sludge and  $SV_{300}$  reduces to 0.42.

The figure clearly indicates that the sedimentation efficiency is surprisingly improved by adding the salt to the ultrasonicated sludge. The combined treatment increases the sedimentation to really 15.4 times that of the untreated sludge. The value of  $SV_{300}$  reduces to 0.31, and it takes only 27.4 min to attain the value of  $SV_{300}$  after 300 min obtained for the untreated sludge. It is demonstrated that an extraordinary improvement of the settling efficiency of excess activated sludge is brought about by ultrasonically-assisted flocculation based on the synergy effect of ultrasonication and salt addition. It is suggested that the fragmentation of particles caused by ultrasonication leads to the creation of more nuclei contributing to the floc development, enhancing the interaction between the particulates and/or the organic solutes and the salt [22]. Thus, cations increased by the salt addition reduce the number of negative charges at the surface of particle fragments due to charge neutralization, resulting in a marked flocculation effect.

Even though the sodium chloride concentration  $C_s$  in the sludge increases to 0.5 M, the sedimentation rate of the sludge treated by salt addition alone is comparable with that of the sludge with the concentration of 0.1 M, as shown in Fig. 5(b). However, the sludge volume markedly decreases with the progress of sedimentation, and  $SV_{300}$  decreases to 0.43 of a similar level to that of the sludge ultrasonicated during 75 s with the power  $P$  of 150 W. The salt addition to the ultrasonicated sludge increases the sedimentation rate to 25.2 times that of the untreated sludge and 10.3 times that of the sludge treated by the salt addition alone, and decreases  $SV_{300}$  to 0.27. Therefore, it takes only 6.2 min to attain the value of  $SV_{300}$  after 300 min obtained for the untreated sludge, and thus the sedimentation time is strikingly reduced in ca. one-fifty. This clearly indicates that the combined treatment of ultrasonication and salt addition is quite effective even under conditions of high salt concentrations. However, it should be noted that it is preferable to minimize the amount of salts added.

Fig. 5(c) and (d) illustrates the batch sedimentation curves of the sludge pretreated under different ultrasonication conditions from the condition ( $P = 150$  W and  $t = 75$  s) tested in Fig. 5(a). Although the flocculation effect becomes more remarkable with increasing power  $P$  and time  $t$ , it is considered desirable to minimize the ultrasonication exposure from an energy expenditure viewpoint.

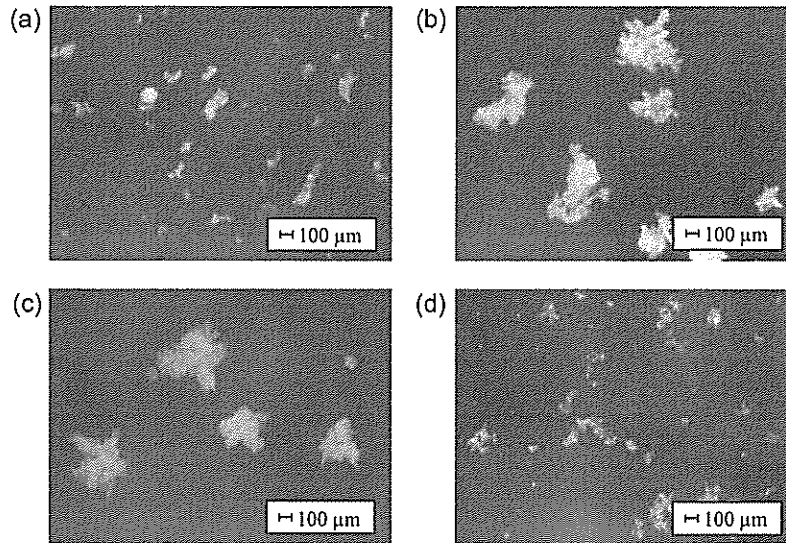


Fig. 3. Photomicrograph of floc structure in sludge obtained by combined pretreatment of ultrasonication ( $P = 150$  W,  $t = 75$  s) and salt addition ( $C_s = 0.1$  M): (a) sludge after rapid mixing at 150 rpm for 3 min, (b) sludge after slow mixing at 50 rpm for 20 min, (c) sludge after slow mixing at 50 rpm for 30 min, and (d) sludge treated by salt addition alone after slow mixing at 50 rpm for 20 min.

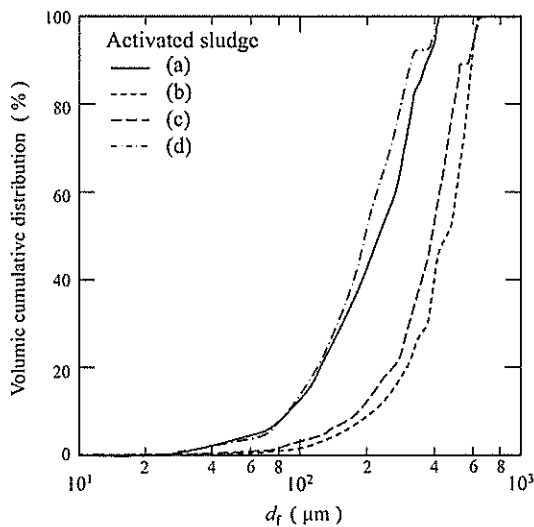


Fig. 4. Cumulative size distribution by volume of flocs in sludge obtained by combined pretreatment of ultrasonication and salt addition.

### 3.3. Effect of salt addition to ultrasonicated sludge on sedimentation rate and sludge volume

Fig. 6 expresses the effect of the sodium chloride concentration  $C_s$  in the ultrasonicated sludge on the sedimentation velocity  $u_0$  during the hindered settling period. It must be stressed, once again, that the sedimentation velocity  $u_0$  was determined from the slope of the linear relationship between  $H$  and  $\theta$ , as indicated by the dotted lines in Fig. 5. Accordingly, the time interval of calculating  $u_0$  is different depending to pretreatment conditions such as ultrasonication and salt addition. In general, as  $u_0$  increases, the time interval of hindered settling becomes shortened. The unsonicated sludge is used as a control. The increase in the sedimentation velocity with increasing salt concentration is insignificantly small for the unsonicated sludge since the flocculation effect of the monovalent cation ( $\text{Na}^+$ ) is unnoticeable. However, the salt addition to the

ultrasonicated sludge has a profound effect on the increase in the sedimentation velocity. The sedimentation velocity markedly increases with increasing salt concentration for the ultrasonicated sludge. Considering that the amount of salt added to the sludge should be minimized, it should be noted that  $C_s$  of 0.1 M have a substantial effect on settling enhancement in this ultrasonication condition ( $P = 150$  W,  $t = 75$  s). In Fig. 7, the sludge volume  $SV_{300}$  after 300 min is plotted against the sodium chloride concentration  $C_s$  in the sludge. The sludge volume gradually decreases as the salt concentration increases. The sludge volume at the salt addition to the ultrasonicated sludge reduces by more than 10% points than that at the salt addition to the untreated sludge, indicating the noticeable effect of ultrasonication on the reduction in the sludge volume.

### 3.4. Effect of ultrasonic energy in combined treatment on sedimentation velocity and sludge volume

The effect of ultrasonic energy on the settling behaviors are examined by conducting the batch sedimentation tests using the sludge ultrasonicated under conditions of the load power  $P$  ranging from 50 to 200 W and the net ultrasonic exposure time  $t$  ranging from 30 to 150 s. In order to examine the influence of ultrasonic irradiation quantitatively, the net ultrasonic power is evaluated by the ultrasonic power dissipated into a liquid not the load power [26]. The correlation between the net ultrasonic power  $I$  and the load power  $P$  obtained for the same ultrasonic homogenizer as that used in this study is given as [27]

$$I = 0.0171P^{1.47} + 15.2 \quad (40 \leq P \leq 200) \quad (1)$$

Thus, the effect of ultrasonication examined in this research is reviewed in the light of the ultrasonic energy dissipated in the sludge in order to comprehensively assess the effects of both the ultrasonic power  $I$  and ultrasonication time  $t$ . The specific ultrasonic energy  $E$  dissipated into a liquid is defined by [25,27,28]

$$E = It/M \quad (2)$$

where  $M$  is the mass of sludge sample.

Fig. 8 illustrates the plots of the sedimentation velocity  $u_0$  during the hindered settling period against the applied specific

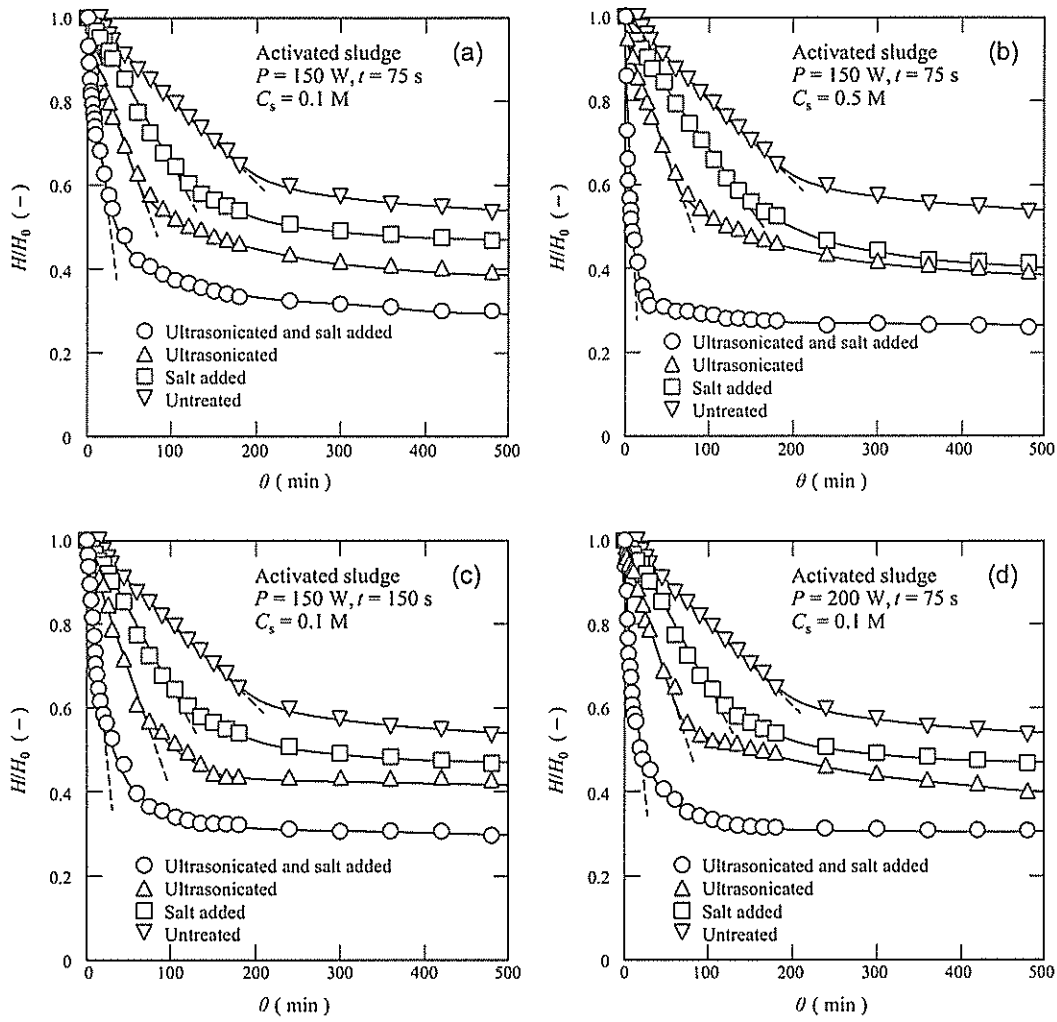


Fig. 5. Batch sedimentation curve: (a) effect of ultrasonication ( $P = 150$  W,  $t = 75$  s) and salt addition ( $C_s = 0.1$  M), (b) effect of ultrasonication ( $P = 150$  W,  $t = 75$  s) and salt addition ( $C_s = 0.5$  M), (c) effect of ultrasonication ( $P = 150$  W,  $t = 150$  s) and salt addition ( $C_s = 0.1$  M), and (d) effect of ultrasonication ( $P = 200$  W,  $t = 75$  s) and salt addition ( $C_s = 0.1$  M).

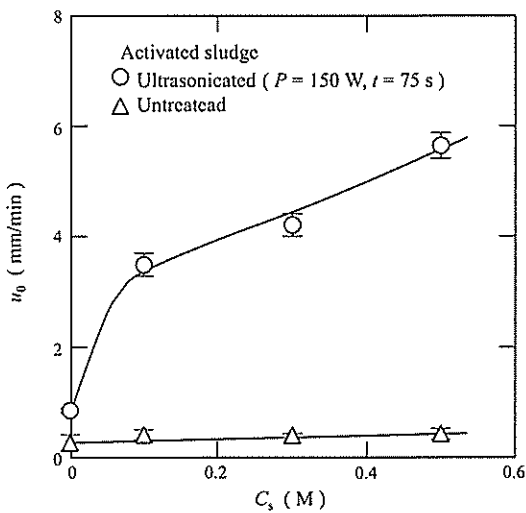


Fig. 6. Effect of sodium chloride concentration in sludge on sedimentation velocity.

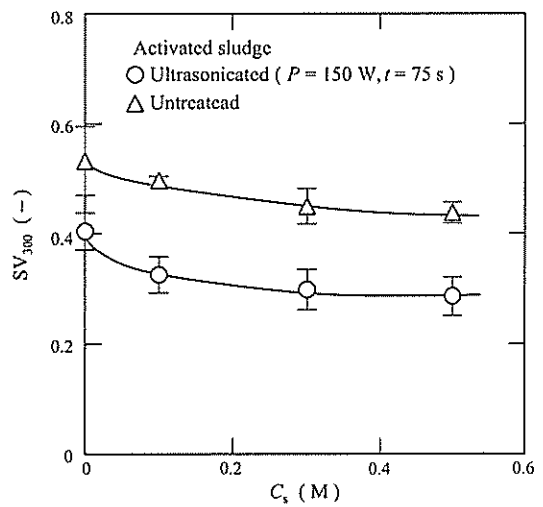


Fig. 7. Effect of sodium chloride concentration in sludge on sludge volume after 300 min.

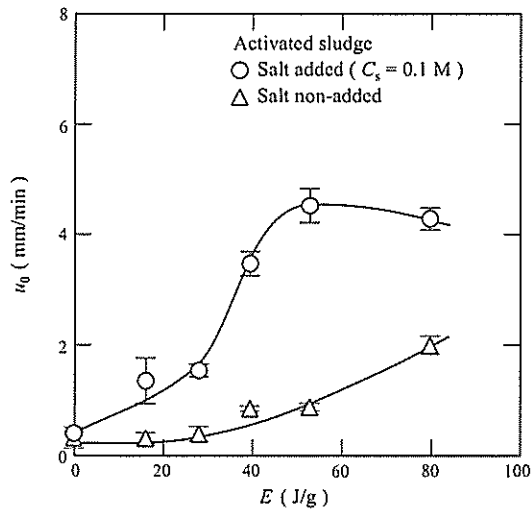


Fig. 8. Effect of specific ultrasonic energy on sedimentation velocity.

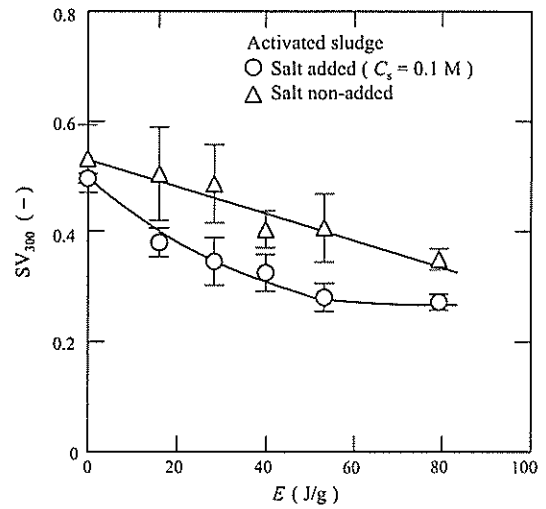


Fig. 9. Effect of specific ultrasonic energy on sludge volume after 300 min.

ultrasonic energy  $E$ . Since the salt added sludge with  $C_s$  of 0.1 M has an adequate effect on the elevation in the sedimentation velocity as shown in Fig. 6, the results for the sludge with  $C_s$  of 0.1 M are compared with those for the salt non-added sludge in Fig. 8. The sedimentation velocities for the salt added sludge are much higher than those for the salt non-added sludge in any ultrasonic energy. The increase in the sedimentation velocity with increasing ultrasonic energy is more profound for the salt added sludge. It should be noted that the ultrasonication effect for the salt added sludge is remarkable even in the low ultrasonic energy level. For instance, in the salt-added sludge, the sedimentation velocity at  $E$  of ca. 40 J/g corresponding to the condition of  $P$  of 150 W and  $t$  of 75 s increases to 15.4 times that of the untreated sludge. Considering that the amount of salt and the ultrasonic energy should be minimized, this condition is considered as a candidate for optimum conditions of settling enhancement. Although the synergy effect of the pretreatments of ultrasonication and salt addition on settling enhancement was confirmed in this study, more multifaceted approach is required for the optimization of the method. The sedimentation velocity considerably increases also for the salt non-added sludge when the specific ultrasonic energy  $E$  is increased to 80 J/g. However, as the floc disintegration was greatly accelerated at the energies of more than 80 J/g, a distinct settling interface was not observed.

In Fig. 9, the sludge volume  $SV_{300}$  after 300 min is plotted against the specific ultrasonic energy  $E$ . The sludge volume decreases with the increase in the specific ultrasonic energy. While the sludge volumes for the salt added sludge are considerably lower than those for the salt non-added sludge in any ultrasonic energy, the decreasing rate becomes gradual with increasing specific ultrasonic energy for the salt-added sludge. The sludge volume for the salt added sludge with the sodium chloride concentration of 0.1 M was decreased from 0.49 for the unsonicated sludge to 0.32 for the sludge conditioned with the specific ultrasonic energy of 40 J/g.

Fig. 10 illustrates the turbidity index  $TI$  (defined as the ratio of the turbidity in the supernatant to the concentration of solids in the sludge represented by the same unit (mg/L) as the turbidity) and  $TOC$  in the supernatant against the specific ultrasonic energy  $E$  for salt added (0.1 M) and non-added sludge samples. Although the turbidity index  $TI$  and  $TOC$  increase with increasing specific ultrasonic energy  $E$ , the increase in the turbidity index  $TI$  reaches nearly a plateau when the specific ultrasonic energy  $E$  exceeds

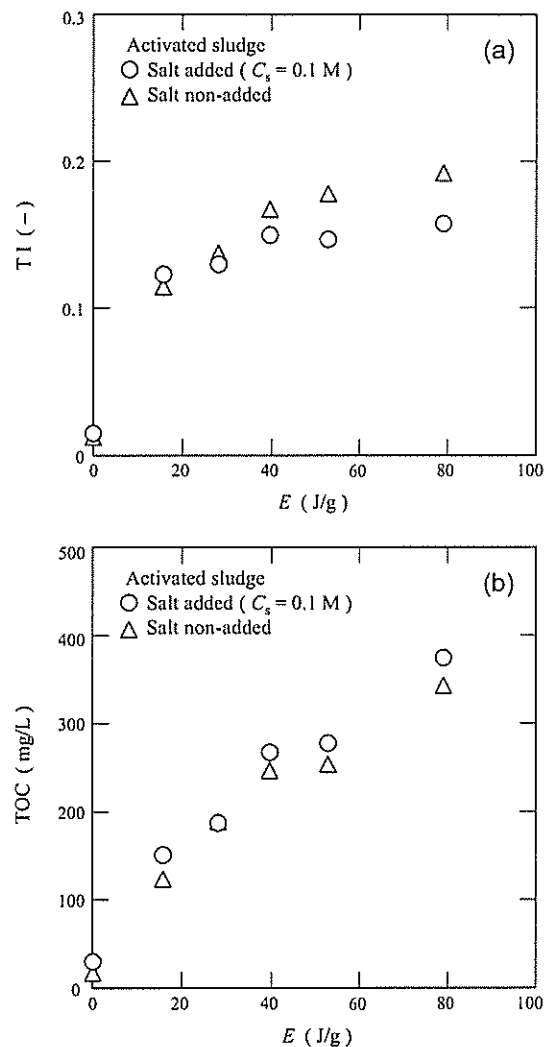


Fig. 10. Effect of specific ultrasonic energy on quality of supernatant: (a) turbidity index, and (b)  $TOC$ .

ca. 40 J/g. There is no distinct difference in the supernatant quality between salt added (0.1 M) and non-added sludge samples. Therefore, it is considered that ultrasonication particularly contributes to high concentration of non-flocculated and non-settled fine particles, and soluble organic matter in the supernatant, arising from the floc breakage [22,29]. Although the combined pretreatment is extremely effective in sludge thickening, the quality of the supernatant evaluated by turbidity and TOC was considerably deteriorated when ultrasonication was incorporated in the pretreatment. However, it would be expected that the ultrasonic pretreatment enhances biodegradability of contaminated supernatant prior to anaerobic digestion or recycling in aeration tank.

### 3.5. Relation between sedimentation velocity and floc size

It is well known that the sedimentation velocity of particles strongly depends on its size. In Fig. 11, the sedimentation velocity  $u_0$  during the hindered settling period is logarithmically plotted against the median diameter  $d_{50}$  of flocs in the sediment. It should be noted that the particles less than about 10  $\mu\text{m}$  are mostly left in the supernatant without settling out. Consequently, the sedimentation curve and the resulting sedimentation velocity are little influenced by such small particles. Therefore, such particles are ignored when the relation between the sedimentation velocity and the median diameter of flocs is evaluated. Plots show that the sedimentation velocity increases with the increase in the median diameter of flocs. Plots can be approximated by the straight line, as shown in the solid line in the figure, although there is some variation in the data. The value of slope is found to be ca. 1.66 (the correlation coefficient [30]  $r = 0.91$ ). According to the Stokes law applicable to settling of very dilute suspension, the sedimentation velocity increases directly with the square of the particle diameter [31]. In the case of flocs, the floc density decreases with the increase in the floc size [32], and hence the sedimentation velocity  $u_0$  is represented as

$$u_0 = \frac{d_f^{D-1} g}{18\mu} \quad (3)$$

where  $D$  is the fractal dimension for a self-similar structure,  $g$  is the acceleration of gravity, and  $\mu$  is the viscosity of the supernatant. The fractal dimension  $D$  in Eq. (3) is determined from the slope of the

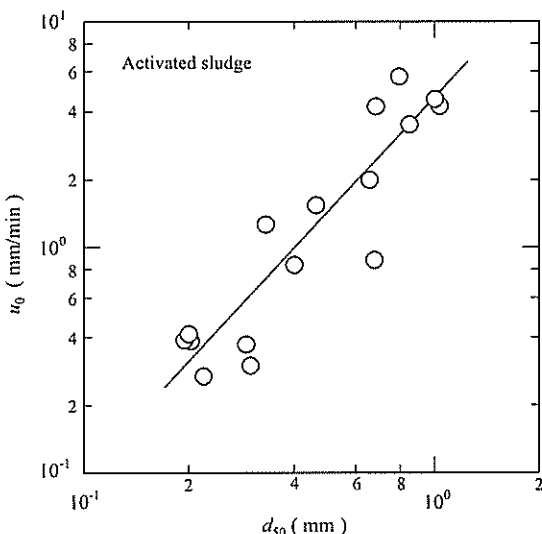


Fig. 11. Relation between sedimentation velocity and median diameter of flocs in sediment.

regression line in Fig. 11 and found to be ca. 2.66. This value is plausible because a lot of computer simulations show that the fractal dimension  $D$  may range from less than 1.7 to 3.0, depending on the condition of floc formation [33,34].

## 4. Conclusions

The effect of the pretreatments of ultrasonication and addition of sodium chloride was examined by conducting batch sedimentation experiments and the measurements of the floc size for excess activated sludge. The sedimentation velocity in the initial period of settling was increased due to the increase in the floc size with the increase in the specific ultrasonic energy dissipated into a liquid through the increase in the load power or the sonication time. The increase in the sedimentation rate was surprisingly noticeable when the sodium chloride was added to the ultrasonicated sludge. The sludge volume decreased significantly by the combined pretreatment of ultrasonication and salt addition.

## Acknowledgements

This work has been partially supported by Grants-in-Aid for Scientific Research from The Ministry of Education, Culture, Sports, Science and Technology, Japan and from The Ministry of the Environment, Japan. The authors wish to acknowledge with sincere gratitude the financial support leading to the publication of this article. The authors also wish to express their sincere appreciation to the Ueda Sewage Treatment Works for their generous contribution of the activated sludge used in this research.

## References

- [1] C.C. Wu, C. Huang, D.J. Lee, Effects of polymer dosage on alum sludge dewatering characteristics and physical properties, *Colloids Surf. A: Physicochem. Eng. Aspects* 122 (1997) 89–96.
- [2] V. Agradiotis, C.F. Forster, C. Carliell-Marquet, Addition of Al and Fe salts during treatment of paper mill effluents to improve activated sludge settlement characteristics, *Bioresour. Technol.* 98 (2007) 2926–2934.
- [3] X. Yin, P. Han, X. Lu, Y. Wang, A review on the dewaterability of bio-sludge and ultrasound pretreatment, *Ultrason. Sonochem.* 11 (2004) 337–348.
- [4] J. Laurent, M. Casellas, M.N. Pons, C. Dagot, Flocs surface functionality assessment of sonicated activated sludge in relation with physico-chemical properties, *Ultrason. Sonochem.* 16 (2009) 488–494.
- [5] A.R. Mohammadi, N. Mehrdadi, G.N. Bidhendi, A. Torabian, Excess sludge reduction using ultrasonic waves in biological wastewater treatment, *Desalination* 275 (2011) 67–73.
- [6] J. Kopp, J. Müller, N. Dichtl, J. Schwedes, Anaerobic digestion and dewatering characteristics of mechanically disintegrated excess sludge, *Water Sci. Technol.* 36 (1997) 129–136.
- [7] Y.Y. Li, T. Noike, Upgrading of anaerobic digestion of waste activated sludge by thermal pretreatment, *Water Sci. Technol.* 26 (1992) 857–866.
- [8] S.T. Yan, L.B. Chu, X.H. Xing, A.F. Yu, X.L. Sun, B. Jurcik, Analysis of the mechanism of sludge ozonation by a combination of biological and chemical approaches, *Water Res.* 43 (2009) 195–203.
- [9] Y. Chen, S. Jiang, H. Yuan, Q. Zhou, G. Gu, Hydrolysis and acidification of waste activated sludge at different pHs, *Water Res.* 41 (2007) 683–689.
- [10] R.V. Rajan, J.G. Lin, B.T. Ray, Low-level chemical pretreatment for enhanced sludge solubilization, *Res. J. Water Pollut. Control Fed.* 61 (1989) 1678–1683.
- [11] B. Park, J.H. Ahn, J. Kim, S. Hwang, Use of microwave pretreatment for enhanced anaerobiosis of secondary sludge, *Water Sci. Technol.* 50 (2004) 17–23.
- [12] Y.C. Chiu, C.N. Chang, J.G. Lin, S.J. Huang, Alkaline and ultrasonic pretreatment of sludge before anaerobic digestion, *Water Sci. Technol.* 36 (1997) 155–162.
- [13] R.O. King, C.F. Forster, Effects of sonication on activated sludge, *Enzyme Microb. Technol.* 12 (1990) 109–115.
- [14] R. Dewil, J. Baeyens, R. Goutvriind, The use of ultrasonics in the treatment of waste activated sludge, *Chin. J. Chem. Eng.* 14 (2006) 105–113.
- [15] R. Dewil, J. Baeyens, R. Goutvriind, Ultrasonic treatment of waste activated sludge, *Environ. Prog.* 25 (2006) 121–128.
- [16] F. Wang, M. Ji, S. Lu, Influence of ultrasonic disintegration on the dewaterability of waste activated sludge, *Environ. Prog.* 25 (2006) 257–260.
- [17] K. Kakii, H. Kato, K. Ohara, Y. Kawai, M. Yoshida, M. Kuriyama, T. Shirakashi, Reflocculation of sewage activated sludge disrupted by ultrasonication, *J. Biosci. Bioeng.* 72 (1994) 371–377.
- [18] X. Feng, H. Ley, J. Deng, Q. Yu, H. Li, Physical and chemical characteristics of waste activated sludge treated ultrasonically, *Chem. Eng. Process.* 48 (2009) 187–194.

- [19] X. Feng, J. Deng, H. Ley, T. Bai, Q. Fan, Z. Li, Dewaterability of waste activated sludge with ultrasound conditioning, *Bioresour. Technol.* 100 (2009) 1074–1081.
- [20] S. Vaxelaire, E. Gonze, G. Merlin, Y. Gonthier, Reduction by sonication of excess sludge production in a conventional activated sludge system: continuous flow and lab-scale reactor, *Environ. Technol.* 29 (2008) 1307–1320.
- [21] X. Yin, X. Lu, P. Han, Y. Wang, Ultrasonic pretreatment on activated sewage sludge from petro-plant for reduction, *Ultrasonics* 44 (2006) e397–e399.
- [22] Y. Hakata, F. Roddick, L. Fan, Impact of ultrasonic pre-treatment on the microfiltration of a biologically treated municipal effluent, *Desalination* 283 (2011) 75–79.
- [23] E. Iritani, N. Katagiri, T. Washizu, K.J. Hwang, High-level deliquoring of activated sludge by ultrahigh-pressure expression combined with flocculation, *Chem. Eng. Sci.* 112 (2014) 1–9.
- [24] D.J. Lee, S.F. Lee, Measurement of bound water content in sludge: the use of differential scanning calorimetry (DSC), *J. Chem. Technol. Biotechnol.* 62 (1995) 359–365.
- [25] E. Gonze, S. Pillot, E. Valette, Y. Gonthier, A. Bernis, Ultrasonic treatment of an aerobic activated sludge in a batch reactor, *Chem. Eng. Process.* 42 (2003) 965–975.
- [26] S. Koda, T. Kimura, T. Kondo, H. Mitome, A standard method to calibrate sonochemical efficiency of an individual reaction system, *Ultrason. Sonochem.* 10 (2003) 149–156.
- [27] E. Iritani, N. Katagiri, Y. Wakamatsu, J.H. Cho, Influence of ultrasonic pretreatment on deliquoring properties in expression of carrots, *J. Chem. Eng. Jpn.* 47 (2014) 869–875.
- [28] G. Erden, A. Filibeli, Ultrasonic pre-treatment of biological sludge: consequences for disintegration, anaerobic biodegradability, and filterability, *J. Chem. Technol. Biotechnol.* 85 (2010) 145–150.
- [29] J. Bien, T. Kamizela, M. Kowalczyk, The contamination of supernatant after sedimentation of sonicated activated sludge, *Environ. Prot. Eng.* 33 (2) (2007) 53–60.
- [30] I. Guttman, S.S. Wilks, J.S. Hunter, *Introductory Engineering Statistics*, second ed., John Wiley & Sons, New York, 1971.
- [31] W.M. Lu, K.L. Tung, C.H. Pan, K.J. Hwang, The effect of particle sedimentation on gravity filtration, *Sep. Purif. Technol.* 33 (1998) 1723–1746.
- [32] N. Tambo, Y. Watanabe, Physical characteristics of flocs – I. The floc density function and aluminum floc, *Water Res.* 13 (1979) 409–419.
- [33] S.N. Rogak, R.C. Flagan, Stokes drag on self-similar clusters of spheres, *J. Colloid Interface Sci.* 134 (1990) 206–218.
- [34] H. Huang, Porosity-size relationship of drilling mud flocs: fractal structure, *Clays Clay Miner.* 41 (1993) 373–379.

# Influence of Ultrasonic Pretreatment on Deliquoring Properties in Expression of Carrots

Eiji IRITANI<sup>1</sup>, Nobuyuki KATAGIRI<sup>1</sup>, Yuta WAKAMATSU<sup>1</sup> and Jun-Hyung CHO<sup>2</sup>

<sup>1</sup>Department of Chemical Engineering, Nagoya University, Furo-cho, Chikusa-ku, Nagoya-shi, Aichi 464-8603, Japan

<sup>2</sup>Department of Paper Science and Engineering, Kangwon University, Chunchon 200-701, Korea

**Keywords:** Expression, Carrot, Ultrasonic Irradiation, Cake Moisture Content, Heating Effect, Pretreatment

The effect of the pretreatment of ultrasonic irradiation on the deliquoring properties in expression was investigated by using carrots as an example of vegetables. The results indicated that the ultrasonic pretreatment produced a noticeable improvement in deliquoring behaviors such as the deliquoring rate and cake moisture content due to the physical damage of cell tissue, although the carrots were maintained in the original shape before and after ultrasonic irradiation. The time variation of the cake moisture content during the course of expression was well described by the three-stage creep model combined with the modified Terzaghi model. It was necessary to heat carrots above 50°C during ultrasonic irradiation in order to attain a desired effect in expression since carrots lost cell turgor pressure rapidly through  $\beta$ -elimination reaction occurring at about 50°C. The ultrasonic pretreatment was well evaluated from the viewpoint of the ultrasonic energy dissipated in the sample. The cake moisture content after 24 h from the beginning of expression dramatically decreased from 69 to 47% by increasing the pressure from 0.5 to 10 MPa, indicating that the cake consisting of treated carrots behaved as the compressible material in the expression operation.

## Introduction

Deliquoring is a crucial issue in the food industry and has been widely used in preserving food, food waste treatment, dry food manufacturing, and boosting yield in juice production (Gallego-Juárez *et al.*, 2007). The methods for deliquoring may be generally classified into two main types: mechanical and thermal deliquoring methods. Whilst thermal deliquoring such as drying and evaporation can remove any kind of moisture from the product, the major drawback is its high energy requirement. Instead, mechanical deliquoring such as expression and centrifugation can reduce energy consumption dramatically compared to thermal deliquoring, and thus it is a potential method as energy conservation technology. Nevertheless, mechanical deliquoring is generally unable to remove the moisture strongly attached to solids and the moisture contained in solids. Particularly, it is often difficult to dehydrate vegetables because of the existence of hard plant's cell walls. The high consolidation pressure is required to destroy such hard cell walls and to remove as much of the moisture as possible from vegetables: for instance, the pressure in the range 1–5 MPa for carrots (Grimi *et al.*, 2010). Although consolidation mechanisms due to the expression of cellular materials are extremely complicated, a large number of studies (Buttersack, 1994; Kawasaki *et al.*, 1996; Lanouisellé *et al.*, 1996; Rebouillat *et al.*, 1996; Kamst

*et al.*, 1997; Schwartzberg, 1997; Christensen and Keiding, 2007; Venter *et al.*, 2007) have so far been reported with the consolidation model (Shirato *et al.*, 1967, 1974) developed for soils and mineral materials as a springboard.

Suitable sample conditioning processes prior to deliquoring are frequently conducted to yield higher performance in deliquoring of cellular materials by damaging the tissue. So far, several treatments have been put forward as the pretreatment or in combination: ultrasonic irradiation (Gallego-Juárez *et al.*, 2007; García-Pérez *et al.*, 2009; Ozuna *et al.*, 2011; Ruiz-Hernando *et al.*, 2013) and microwave (Hu *et al.*, 2006; Yu *et al.*, 2009) in mechanical separation and drying, thermal treatment (Ruiz-Hernando *et al.*, 2013), electric field (Chen *et al.*, 2011), pulsed electric field (Bouzzara and Vorobiev, 2003; Grimi *et al.*, 2007) and freezing-thawing (Kawasaki *et al.*, 1996; Grimi *et al.*, 2010) in mechanical separation, and radio frequency (Cohen and Yang, 1995) in drying. Among them, ultrasonic irradiation is thought to be a tool with a great potential as the pretreatment for cellular materials and applied to several fields such as osmotic dehydration (Cárcel *et al.*, 2007), extraction process (Riera *et al.*, 2004), sludge disintegration (Erden and Filibeli, 2010), and so forth. It is expected that the effect of ultrasonic irradiation is largely dependent on the process variables such as sample temperature, ultrasonic power, and sonication time.

In the present article, carrot deliquoring due to expression is examined, and the effect of ultrasonic irradiation as the pretreatment on deliquoring behaviors in expression is investigated. The existing consolidation model is applied in order to elucidate the consolidation kinetics in expression of carrots pretreated by ultrasonic irradiation. The pretreatment

Received on April 25, 2014; accepted on June 3, 2014

DOI: 10.1252/jcej.14we150

Correspondence concerning this article should be addressed to E. Iritani (E-mail address: iritani@nuce.nagoya-u.ac.jp).

performance is evaluated with varying the values of several operating parameters such as sample temperature, ultrasonic power, and sonication time. Moreover, the influence of consolidation pressure on the expression behaviors is examined.

## 1. Experimental

### 1.1 Materials

Carrot (*Daucus carota* ssp. *sativus*) was selected as a subject of the present study. Carrots of good quality were purchased in the Nagoya University cooperative, stored in a refrigerator at  $5 \pm 1^\circ\text{C}$  after they were sealed in plastic films to avoid moisture loss, and used in the experiments within a week of purchase. The production areas of carrots used varied seasonally (Aichi, Aomori, and Hokkaido areas), and a set of experiments were carried out using the carrots harvested at the same area. After skin, top and bottom ends of the carrots were removed, the carrots were cut into cubes 3 mm per side by using a vegetable slicer, which can cut into a minimum of 3 mm dices, just before use. The true density of solids was measured by a pycnometer. The initial moisture content of carrots measured using an infrared-ray moisture meter (FD-720, Kett Electric Lab.) was within 87–91 wt% on a wet basis. In order to diminish the effect of impurity, the water used in the preparation of sample was ultrapure, deionized water (minimum resistivity:  $18\text{ M}\Omega\text{ cm}$ ) prepared by purifying tap water through ultrapure water systems equipped with both Elix-UV20 and Milli-Q Advantage for laboratory use (Millipore Corp.).

### 1.2 Ultrasonic pretreatment

Fifteen grams of cubic carrots were placed into a 50 mL beaker, and 30 mL of water was added. The beaker containing the sample was placed in a water bath incubator (BT23, Yamato Scientific Co., Ltd.) in order to keep the sample temperature constant during the ultrasonic pretreatment. The ultrasonic apparatus was an ultrasonic homogenizer (UP-200S, Dr. Hiesher GmbH) equipped with a probe with an operating frequency of 24 kHz and a load power ranging from 40 to 200 W. The ultrasonic probe was submerged in the sample to a depth of 1 cm above the bottom of the beaker. The sample was processed with the probe for the specified total operating time by pulsed ultrasonic irradiation in which one cycle consisted of both the operating time of 0.5 s and the downtime of 0.5 s in order to avoid a rise in temperature. The temperature inside of the sample was measured using a thermocouple before and after sonication, and it was confirmed that the temperature rise due to sonication was negligible. For comparison, the sample was prepared by heating in the water bath incubator without sonication. The ultrasonic power dissipated into a liquid was measured according to the method of Koda *et al.* (2003). The ultrasonic power  $I$  is given as

$$I = \left( \frac{dT}{dt} \right) C_p M \quad (1)$$

where  $T$  is the sample temperature,  $t$  is the net ultrasonic exposure time,  $C_p$  and  $M$  are the heat capacity and mass of

water, respectively. The term  $dT/dt$  represents the rate of increase in temperature. Accordingly, the ultrasonic power  $I$  corresponding to a specified load power can be calculated from the measurement of the initial temperature rise of water under sonication by using a thermocouple.

### 1.3 Deliquoring due to expression

The expression experiments of treated and untreated carrots were conducted using the so-called compression–permeability cell (C–P cell) (Grace, 1953; Okamura and Shirato, 1955), which comprised of a cell cylinder and a piston with a cross-sectional area of  $9.62\text{ cm}^2$ , as an expression cell, as shown in Figure 1. The sample was placed in the cell cylinder and the movable piston was inserted in the cell. The liquid was then squeezed out of the sample through the top and bottom filter cloths (TRG803K, Okayama Nakao Filter Media Corp.) by exerting a mechanical load through the piston by the use of a material testing machine (SC-20H(MNS-01), Tokyo Testing Machine Inc.). The semi-solid cake pre-consolidated in the C–P cell under a pressure  $p_1$  of 0.1 MPa was consolidated for 24 h at constant pressures  $p_2$  ranging from 0.5 to 10 MPa. The time evolution of the cake thickness during constant pressure consolidation of pre-consolidated cake was measured by a dial gauge fitted on the cell cylinder. The residual moisture content in the compressed cake was measured using the infrared-ray moisture meter at the end of expression.

## 2. Results and Discussion

### 2.1 Effect of ultrasonic irradiation

Typical deliquoring behaviors due to expression of carrots with and without the pretreatment of ultrasonic irradiation are compared in Figure 2(a). Expression experiments are conducted under the condition of the consolidation pressure of 0.5 MPa for the semi-solid cake pre-consolidated under a pressure of 0.1 MPa. In the case of the treated carrots, ultrasound is irradiated for the net ultrasonic exposure time  $t$  of 15 min under the conditions of the load power  $P$  of 40 W and the sample temperature  $T$  of  $50^\circ\text{C}$ . The temporal variation of moisture content  $R$  of the compressed cake on the

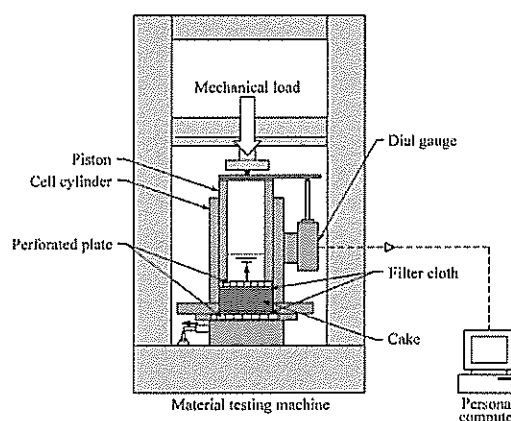
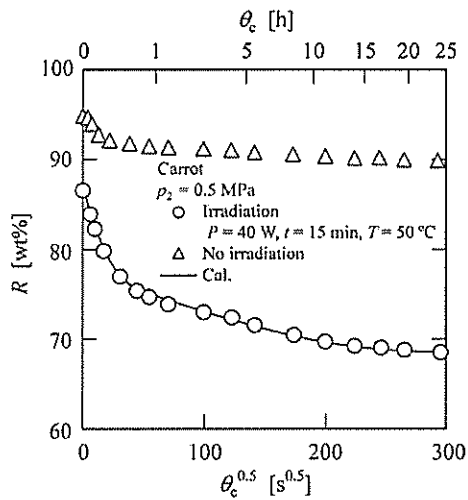
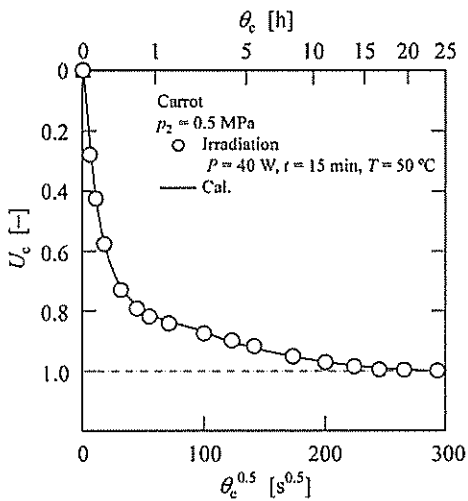


Fig. 1 Schematic view of expression apparatus



(a) Time variation of cake moisture content in expression



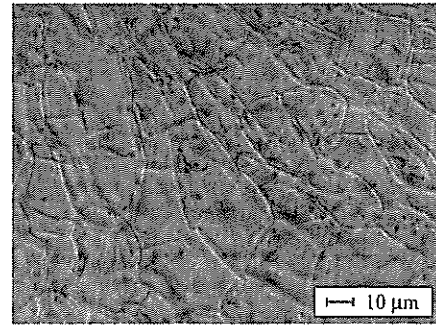
(b) Time variation of average consolidation ratio in expression

Fig. 2 Effects of ultrasonic pretreatment

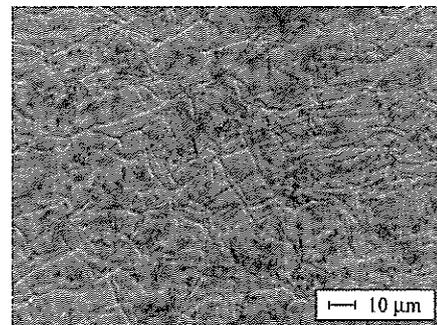
mass basis is plotted in the figure in the form of  $R$  against  $\sqrt{\theta_c}$  and  $\theta_c$ , where  $\theta_c$  is the consolidation time. The time variation of  $R$  is calculated from that of the cake thickness  $L$  based on the relation:

$$R = \frac{100(L - \omega_0)\rho}{(L - \omega_0)\rho + \omega_0\rho_s} \quad (2)$$

where  $\omega_0$  is the total solid volume per unit cross-sectional area,  $\rho$  is the density of the liquid, and  $\rho_s$  is the true density of solids. The decrease in the moisture content without ultrasonic irradiation is insignificant and continues to decrease from 95 to 90% little by little over the 24h tested. In contrast, the moisture content markedly decreases from 86 to 74% in 1h in the case of carrots pretreated with ultrasonic irradiation and reaches the low value of 69% in 24h tested. It should be noted that ultrasonic irradiation as the pretreat-



(a) Untreated with sonication



(b) Treated with sonication

Fig. 3 Photomicrographs of carrot surfaces

ment of expression produces a noticeable improvement in deliquoring behaviors. Ultrasonic irradiation causes cavitation in the liquid phase containing cubic carrots and brings about hydro-shear strength and sonochemical effects, leading to an improvement in expression properties synergistically. Whilst the carrots are maintained in the original cubic shape before and after ultrasonic irradiation, the cell tissue is subject to physical damage, as shown in the photomicrograph of Figure 3. This facilitates the deliquoring from the cell interior due to mechanical expression following ultrasonic irradiation.

The time variation of the average consolidation ratio  $U_c$  indicating a measure of the degree of consolidation is also shown in the case of pretreated carrots in Figure 2(b) as the form of  $U_c$  against  $\sqrt{\theta_c}$  and  $\theta_c$ . It takes only 37.4min to attain  $U_c$  of 0.8. On the basis of the multi-stage creep model combined with the modified Terzaghi model, the solid line depicted in Figure 2(b) represents the values calculated by (Lanoisellé *et al.*, 1996; Grimi *et al.*, 2010; Iritani *et al.*, 2010).

$$U_c = \frac{L_1 - L}{L_1 - L_\infty} = \left( 1 - \sum_{k=1}^K B_k \right) \times \left[ 1 - \sum_{N=1}^{\infty} \frac{8}{(2N-1)^2 \pi^2} \exp \left\{ -\frac{(2N-1)^2 \pi^2}{4} \cdot \frac{i^2 C_c \theta_c}{\omega_0^2} \right\} \right] + \sum_{k=1}^K B_k \{ 1 - \exp(-\eta_k \theta_c) \} \quad (3)$$

where  $L_1$  and  $L_\infty$  are the thicknesses of the compressed cake at  $\theta_c = 0$  and  $\infty$ , respectively,  $B_k$  and  $\eta_k$  are the creep constants of the  $k$ -th stage creep,  $i$  is the number of drainage surfaces, and  $C_c$  is the modified consolidation coefficient (Shirato *et al.*, 1967). The solid line shown in Figure 2(a) is the result of calculation derived by substituting the time variation of  $L$  calculated from Eq. (3) into Eq. (2). Fairly good agreement with the experimental data can be obtained by accounting for the three-stage creep phenomenon that the value of  $K$  in Eq. (3) is 3. The contributions  $A$  (defined as  $(1-B_1-B_2-B_3)$ ),  $B_1$ ,  $B_2$ , and  $B_3$  of each consolidation stage to the overall consolidation are 0.186, 0.259, 0.337, and 0.218, respectively. In contrast to the case of treated carrots, the experimental data of  $U_c$  for raw carrots are not shown in the figure since it is impossible to determine the value of  $L_\infty$  in Eq. (3) because of the gradually ever-changing cake thickness.

## 2.2 Effect of temperature

The effect of temperature of a sample controlled during ultrasonic irradiation on the deliquoring performance is investigated by changing the temperature of the liquid in the thermostat bath. The time evolutions of the moisture content  $R$  of the cake are plotted in Figure 4 for the different values of sample temperature  $T$  in ultrasonic pretreatment under the conditions of the load power  $P$  of 40 W and the sonication time  $t$  of 15 min. The data for carrots pretreated at 40°C show a similar trend to those for untreated carrots, and the ultrasonic pretreatment shows little improvement in deliquoring due to expression. Even when ultrasonic is irradiated with being heated to 47°C, the deliquoring behavior is closely similar to that of carrots treated at 40°C until about 6 h after the onset of expression. However, shortly thereafter, the moisture content  $R$  begins to decrease abruptly and eventually decreases to 70% range in 24 h. In the case of 50°C, the moisture content  $R$  decreases rapidly from the beginning of expression and finally reaches below 70% in 24 h.

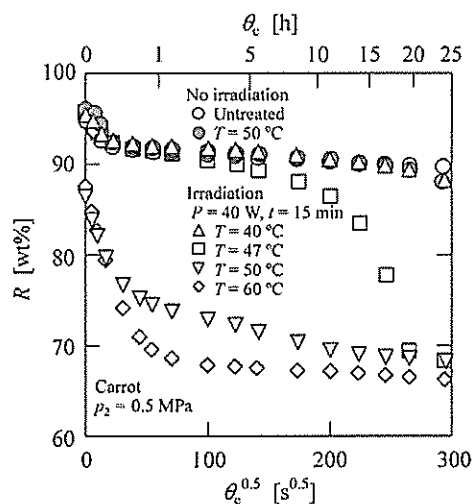


Fig. 4 Effect of sample temperature in ultrasonic pretreatment on time variation of cake moisture content in expression

Therefore, it is concluded that the sample temperature plays an extremely important role in accelerating the effect of ultrasonic pretreatment on the expression performance. It is necessary to heat the carrot above a minimum temperature threshold (around 50°C) in ultrasonic irradiation in order to attain a desired effect in expression. The loosening of the network of a cell wall biopolymer such as pectin, especially in the middle lamella between adjacent cells, at elevated temperature during ultrasonic irradiation may weaken the cell wall strength. Several studies have reported that carrots lose cell turgor pressure rapidly through thermal texture degradation due to  $\beta$ -elimination reaction when the tissue internal temperature reaches 50°C (Greve *et al.*, 1994; Sila *et al.*, 2006; Day *et al.*, 2012). It is obvious that such changes in pectin structure due to heating during ultrasonic irradiation lead to a significant improvement in expression performance obtained in this study. However, the expression performance of carrots pretreated by heating alone without ultrasonic irradiation is similar to that of raw carrots, as shown in Figure 4, and therefore the ultrasonic treatment in combination with heating is highly effective in improving the expression performance.

## 2.3 Effect of sonication time

In Figure 5, the variations with time of the cake moisture content  $R$  in expression are shown for the different values of the sonication time  $t$  in ultrasonic pretreatment under the conditions of the load power  $P$  of 40 W and the sample temperature  $T$  of 50°C. As the sonication time  $t$  increases from 5 to 15 min, the cake moisture content  $R$  significantly reduces, especially at comparatively-early times. However, a further increase in the sonication time  $t$  does not lead to a more significant improvement in the expression performance.

## 2.4 Effect of ultrasonic energy

Figure 6 shows the variations with time of the cake moisture content  $R$  in expression for the different values of the

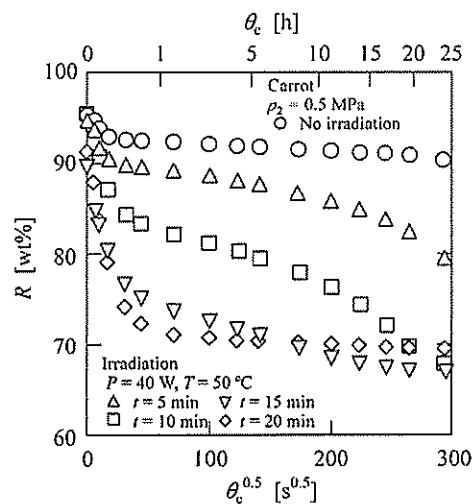


Fig. 5 Effect of sonication time in ultrasonic pretreatment on time variation of cake moisture content in expression

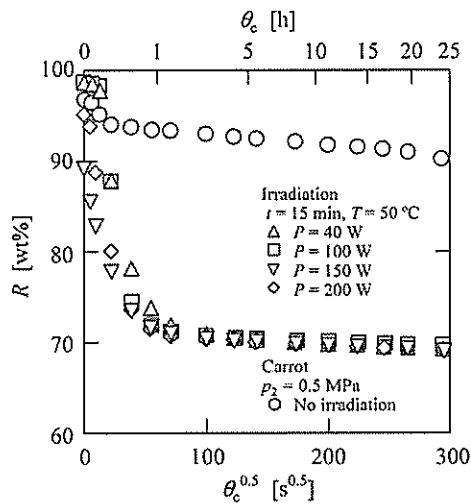


Fig. 6 Effect of load power in ultrasonic pretreatment on time variation of cake moisture content in expression

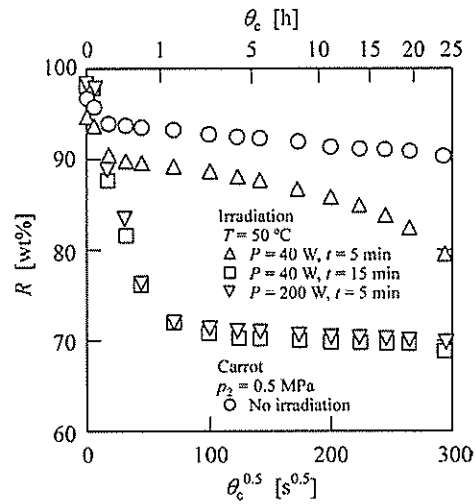


Fig. 8 Contribution of specific ultrasonic energy to expression performance

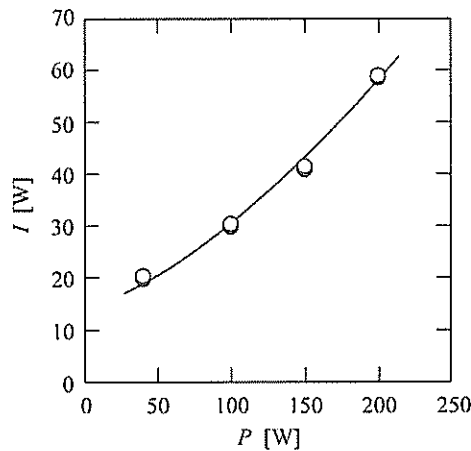


Fig. 7 Relation between load power and real power measured

load power  $P$  in ultrasonic pretreatment with the sonication time  $t$  of 15 min and the sample temperature  $T$  of 50°C. Although the load power  $P$  is increased from 40 to 200 W, a further improvement in the expression performance is not achieved by the increase in the load power, implying that there is a limited effect of the load power in ultrasonic pretreatment under the conditions used.

In order to examine the influence of ultrasonic irradiation quantitatively, the net ultrasonic power is evaluated by the ultrasonic power dissipated into a liquid, not the load power (Koda *et al.*, 2003). The relation between the load power  $P$  and the net ultrasonic power  $I$  measured is illustrated in Figure 7. Within the range of load power  $P$  tested, the relation is given as

$$I = 0.0171P^{1.47} + 15.2 \quad (40 \leq P \leq 200) \quad (4)$$

It has been reported that low density and long duration sonication is more efficient than high density and short duration in floc disintegration of biological sludge (Zhang

*et al.*, 2007; Xie *et al.*, 2009). Thus, the effect of ultrasonic pretreatment examined in this research is reviewed from the viewpoint of the ultrasonic energy dissipated in the sample in order to comprehensively assess the effects of both the ultrasonic power  $I$  and sonication time  $t$ . The specific ultrasonic energy  $E$  dissipated into a liquid is defined by (Erden and Filibeli, 2010)

$$E = It / W \quad (5)$$

where  $W$  is the mass of sample.

For instance, the specific ultrasonic energy  $E$  is 1140 kJ/kg in the ultrasonic pretreatment with the load power  $P$  of 40 W and the sonication time  $t$  of 15 min shown in Figure 6. Therefore, the expression behaviors were compared by varying the load power  $P$  and the sonication time  $t$ , keeping the specific ultrasonic energy  $E$  approximately constant. The results for the time variation of the cake moisture content  $R$  in expression are shown in Figure 8. The specific ultrasonic energy  $E$  is 1130 kJ/kg also in the ultrasonic pretreatment conducted at  $p$  of 200 W and  $t$  of 5 min. The result is remarkably similar to that obtained at the conditions of  $P$  of 40 W and  $t$  of 15 min. In contrast, when the load power  $P$  is reduced to 40 W, keeping the sonication time  $t$  at 5 min, a reduction in cake moisture content  $R$  is severely deteriorated. For practical purposes, it is important to elucidate the dependence of ultrasonic effect on the submergence depth of the ultrasonic probe, the container size, and the sample amount.

## 2.5 Effect of applied consolidation pressure

It is vitally important to elucidate the influence of the applied consolidation pressure on the expression behaviors, particularly in order to lower the cake moisture content associated with the elevated pressure. The time variations of the cake moisture content  $R$  in expression are illustrated in Figure 9 for the different values of the consolidation pressure  $p_2$ . As the pressure is increased, the lowering rate in  $R$

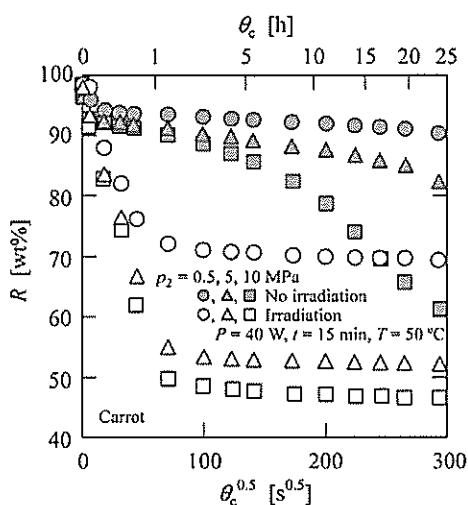


Fig. 9 Effect of consolidation pressure on time variation of cake moisture content in expression

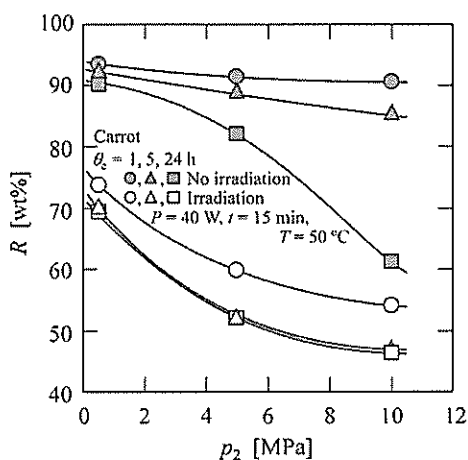


Fig. 10 Relation between cake moisture content at different consolidation times and consolidation pressure

for treated carrots in an early stage remarkably increases and the cake moisture content after 24 h undergoes a marked decrease. The cake moisture content  $R$  after 24 h dramatically decreases from 69 to 47% by increasing the pressure from 0.5 to 10 MPa. Thus, it is found that the cake consisting of treated carrots behaves as the compressible material in expression operation (Iritani *et al.*, 2007). In contrast, whilst the expression performance is improved with increasing pressure also in expression of raw carrots, the degree of deliquoring is less marked than that for treated carrots and the deliquoring rate is slightly improved particularly in early times.

In order to compare the cake moisture content  $R$  more clearly, the values of  $R$  at the consolidation time  $\theta_c$  of 1, 5, and 24 h are plotted in Figure 10 against the consolidation pressure  $p_2$ . Although the cake moisture content  $R$  for treated carrots remarkably decreases with the increase in the consolidation pressure,  $R$  at the consolidation time  $\theta_c$  of 5 h

is very close in value to that at  $\theta_c$  of 24 h for each pressure. It should be noted that the cake moisture content  $R$  for treated carrots at  $p_2$  of 0.5 MPa and  $\theta_c$  of 1 h corresponds to that for untreated carrots at  $p_2$  of ca. 7 MPa and  $\theta_c$  of 24 h. Accordingly, the use of ultrasonicated carrots in expression can significantly shorten the consolidation time required to reduce the cake moisture content at lower pressures.

## Conclusion

Liquid expression from carrots assisted with ultrasonic pretreatments was conducted to investigate the promoting effect of sonication on mechanical deliquoring of carrots, and the time variations of the moisture content in the compressed cake were measured during the course of expression conducted under the different values of applied consolidation pressure. The deliquoring rate of carrots was significantly enhanced by the pretreatment of ultrasonic irradiation, and the moisture content in the compressed cake was finally reduced to 47% at the pressure of 10 MPa. It turned out that the control of sample temperature was of extreme importance in sonication as the pretreatment and that the sample temperature should be kept to above 50°C. It was apparent from the model analysis that the deliquoring behavior was markedly influenced by the creep phenomenon. It was also found that the specific ultrasonic energy dissipated in the sample by the sonication treatment served as an indicator representing the degree of ultrasonic pretreatment. The elevated operating pressure was highly effective in reducing the cake moisture content as the result of the compressibility of the carrot cake.

## Acknowledgements

This work has been partially supported by Grants-in-Aid for Scientific Research from the Ministry of Education, Culture, Sports, Science and Technology, Japan and from the Ministry of the Environment, Japan, and by the Steel Foundation for Environmental Protection Technology. The authors wish to acknowledge with sincere gratitude the financial support leading to the publication of this article.

## Nomenclature

$A$	= ratio of primary consolidation to overall consolidation	[—]
$B$	= creep constant	[—]
$C_c$	= modified consolidation coefficient	[m <sup>2</sup> /s]
$C_p$	= heat capacity of water	[J/kg]
$E$	= specific ultrasonic energy dissipated in sample	[J/kg]
$I$	= ultrasonic power dissipated into liquid	[W]
$i$	= number of drainage surfaces	[—]
$L$	= thickness of cake	[m]
$L_1$	= thickness of cake at $\theta_c = 0$	[m]
$L_\infty$	= thickness of cake at $\theta_c = \infty$	[m]
$M$	= mass of water	[kg]
$P$	= load power	[W]
$p_1$	= pre-consolidation pressure	[Pa]
$p_2$	= consolidation pressure	[Pa]
$R$	= moisture content of compressed cake on mass basis	[wt%]
$T$	= sample temperature	[°C]
$t$	= net ultrasonic exposure time	[s]

$U_c$	= average consolidation ratio	[—]
$W$	= mass of sample	[kg]
$\eta$	= creep constant	[s <sup>-1</sup> ]
$\theta_c$	= consolidation time	[s]
$\rho$	= density of liquid	[kg/m <sup>3</sup> ]
$\rho_s$	= true density of solids	[kg/m <sup>3</sup> ]
$\omega_0$	= total solid volume per unit cross-sectional area	[m <sup>3</sup> /m <sup>2</sup> ]

### Literature Cited

- Bouzzara, H. and E. Vorobiev; "Solid-Liquid Expression of Cellular Materials Enhanced by Pulsed Electric Field," *Chem. Eng. Process.*, **42**, 249–257 (2003)
- Buttersack, C.; "Two-Zone Model for Solid-Liquid Separation by Filtration and Expression," *Chem. Eng. Sci.*, **49**, 1145–1160 (1994)
- Cárceles, J., J. Benedito, C. Rosselló and A. Mulet; "Influence of Ultrasound Intensity on Mass Transfer in Apple Immersed in a Sucrose Solution," *J. Food Eng.*, **78**, 472–479 (2007)
- Chen, K., H. Lei, Y. Li, H. Li, X. Zhang and C. Yao; "Physical and Chemical Characteristics of Waste Activated Sludge Treated with Electric Field," *Process Saf. Environ. Prot.*, **89**, 327–333 (2011)
- Christensen, M. L. and K. Keiding; "Creep Effects in Activated Sludge Filter Cakes," *Powder Technol.*, **177**, 23–33 (2007)
- Cohen, J. S. and T. C. S. Yang; "Progress in Food Dehydration," *Trends Food Sci. Technol.*, **6**, 20–25 (1995)
- Day, L., M. Xu, S. K. Oiseth and R. Mawson; "Improved Mechanical Properties of Retorted Carrots by Ultrasonic Pre-Treatments," *Ultrason. Sonochem.*, **19**, 427–434 (2012)
- Erden, G. and A. Filibeli; "Ultrasonic Pre-Treatment of Biological Sludge: Consequences for Disintegration, Anaerobic Biodegradability, and Filterability," *J. Chem. Technol. Biotechnol.*, **85**, 145–150 (2010)
- Gallego-Juárez, J. A., E. Riera, S. de la Fuente Blanco, G. Rodríguez-Corral, V. M. Acosta-Aparicio and A. Blanco; "Application of High-Power Ultrasound for Dehydration of Vegetables: Processes and Devices," *Drying Technol.*, **25**, 1893–1901 (2007)
- García-Pérez, J. V., J. A. Cárceles, E. Riera and A. Mulet; "Influence of the Applied Acoustic Energy on the Drying of Carrots and Lemon Peel," *Drying Technol.*, **27**, 281–287 (2009)
- Grace, H. P.; "Resistance and Compressibility of Filter Cakes, Part I," *Chem. Eng. Prog.*, **49**, 303–318 (1953)
- Greve, L. C., K. A. Shackel, H. Ahmadi, R. N. McArdle, J. R. Gohlke and J. M. Labavitch; "Impact of Heating on Carrot Firmness—Contribution of Cellular Turgor," *J. Agric. Food Chem.*, **42**, 2896–2899 (1994)
- Grimi, N., I. Praporscic, N. Lebovka and E. Vorobiev; "Selective Extraction from Carrot Slices by Pressing and Washing Enhanced by Pulsed Electric Fields," *Separ. Purif. Tech.*, **58**, 267–273 (2007)
- Grimi, N., E. Vorobiev, N. Lebovka and J. Vaxelaire; "Solid-Liquid Expression from Denatured Plant Tissue: Filtration-Consolidation Behavior," *J. Food Eng.*, **96**, 29–36 (2010)
- Hu, Q. G., M. Zhang, A. S. Mujumdar, W. H. Du and J. C. Sun; "Effects of Different Drying Methods on the Quality Changes of Granular Edamame," *Drying Technol.*, **24**, 1025–1032 (2006)
- Iritani, E., N. Katagiri, K. M. Yoo and H. Hayashi; "Consolidation and Expansion of a Granular Bed of Superabsorbent Hydrogels," *AIChE J.*, **53**, 129–137 (2007)
- Iritani, E., T. Sato, N. Katagiri and K. J. Hwang; "Multi-Stage Creep Effect in Consolidation of Tofu and Okara as Soft Colloids," *J. Chem. Eng. Japan*, **43**, 140–149 (2010)
- Kamst, G. F., O. S. L. Bruinsma and J. deGraauw; "Solid Phase Creep during the Expression of Palm Oil Filter Cakes," *AIChE J.*, **43**, 665–672 (1997)
- Kawasaki, K., A. Matsuda and T. Murase; "The Effect of Bound Water on Filtration and Consolidation Characteristics of Excess Activated Sludge Treated by Freezing and Thawing Treatment," *Kagaku Kagaku Ronbunshu*, **22**, 294–300 (1996)
- Koda, S., T. Kimura, T. Kondo and H. Mitome; "A Standard Method to Calibrate Sonochemical Efficiency of an Individual Reaction System," *Ultrason. Sonochem.*, **10**, 149–156 (2003)
- Lanoisellé, J. L., E. I. Vorobyov, J. M. Bouvier and G. Piar; "Modeling of Solid/Liquid Expression for Cellular Materials," *AIChE J.*, **42**, 2057–2068 (1996)
- Okamura, S. and M. Shirato; "Liquid Pressure Distribution within Cakes in the Constant Pressure Filtration," *Kagaku Kagaku*, **19**, 104–110 (1955)
- Ozuna, C., J. A. Cárceles, J. V. García-Pérez and A. Mulet; "Improvement of Water Transport Mechanisms during Potato Drying by Applying Ultrasound," *J. Sci. Food Agric.*, **91**, 2511–2517 (2011)
- Rebouillat, S., H. G. Schwartzberg and D. Leclerc; "The Uni-Axial Compression of Solid-Liquid Materials under Constant Rate of Strain," *J. Chem. Eng. Japan*, **29**, 29–36 (1996)
- Riera, E., Y. Golbs, A. Blanco, J. A. Gallego, M. Blasco and A. Mulet; "Mass Transfer Enhancement in Supercritical Fluids Extraction by Means of Power Ultrasound," *Ultrason. Sonochem.*, **11**, 241–244 (2004)
- Ruiz-Hernando, M., G. Martínez-Elorza, J. Labanda and J. Llorens; "Dewaterability of Sewage Sludge by Ultrasonic, Thermal and Chemical Treatments," *Chem. Eng. J.*, **230**, 102–110 (2013)
- Schwartzberg, H. G.; "Expression of Fluid from Biological Solids," *Separ. Purif. Methods*, **26**, 1–213 (1997)
- Shirato, M., T. Murase, H. Kato and S. Fukaya; "Studies on Expression of Slurries under Constant Pressure," *Kagaku Kagaku*, **31**, 1125–1131 (1967)
- Shirato, M., T. Murase, A. Tokunaga and O. Yamada; "Calculations of Consolidation Period in Expression Operations," *J. Chem. Eng. Japan*, **7**, 229–231 (1974)
- Sila, D. N., C. Smout, F. Elliot, A. Van Loey and M. Hendrickx; "Non-Enzymatic Depolymerization of Carrot Pectin: Toward a Better Understanding of Carrot Texture during Thermal Processing," *J. Food Sci.*, **71**, E1–E9 (2006)
- Venter, M. J., N. J. M. Kuipers and A. B. de Haan; "Modelling and Experimental Evaluation of High-Pressure Expression of Cocoa Nibs," *J. Food Eng.*, **80**, 1157–1170 (2007)
- Xie, B., H. Liu and Y. Yan; "Improvement of the Activity of Anaerobic Sludge by Low-Intensity Ultrasound," *J. Environ. Manage.*, **90**, 260–264 (2009)
- Yu, Q., H. Lei, G. Yu, X. Feng, Z. Li and Z. Wu; "Influence of Microwave Irradiation on Sludge Dewaterability," *Chem. Eng. J.*, **155**, 88–93 (2009)
- Zhang, P., G. Zhang and W. Wang; "Ultrasonic Treatment of Biological Sludge: Floc Disintegration, Cell Lysis and Inactivation," *Bioresour. Technol.*, **98**, 207–210 (2007)

## 7. 知的財産権の取得状況

- ・特許

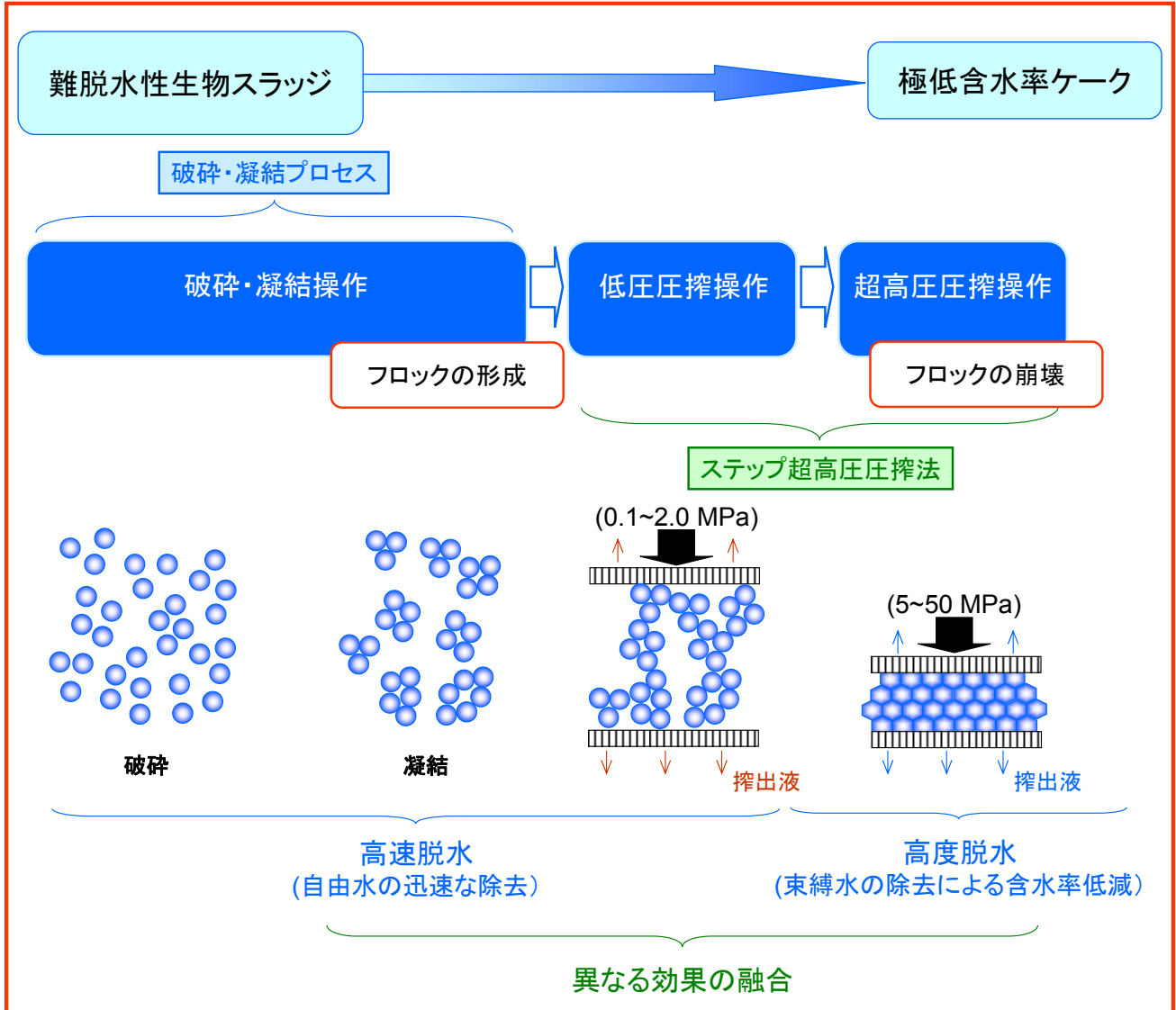
なし

- ・実用新案登録

なし

## 8. 研究概要図

# 3K123005 破碎・凝結プロセスを伴う 生物スラッジの超高压圧搾脱水法の開発



本研究では、高い脱水速度と高い脱水度の両者を同時に達成することが可能な難脱水性生物スラッジの脱水法として、破碎・凝結プロセスを伴う超高压圧搾脱水を提案し、その有効性を検証する。すなわち、スラッジを破碎して、一端フロックを崩壊させることによりフロック内の束縛水を放出させると共に、破碎方法によりスラッジ表面の特性をコントロールし、スラリー中のイオン、ポリマー等を利用して凝集剤を添加することなく緩く凝結した粗大フロックを形成させ、0.1 ~ 2.0 MPa の低圧下で圧搾して自由水を迅速に除去し脱水ケーキを得た後、圧力のステップ増加により 5 ~ 50 MPa の超高压を作用させてフロックを崩壊させつつ束縛水をさらに除去し極低含水率ケーキを得て、生物スラッジの高速減量化を図る。生物スラッジの破碎・凝結機構や超高压下におけるフロックの崩壊、ケーキの脱水機構の解明を行い、これらを総合して、最適な操作法を提示する。

## 9. 英文概要

- ・ 研究課題名

Development of Deliquoring Method of Biological Sludge by Ultrahigh-Pressure Expression Combined with Breakage/Aggregation Process

- ・ 研究番号

3K123005

- ・ 研究代表者名及び所属

Eiji Iritani, Nagoya University

- ・ 共同研究者名及び所属

Nobuyuki Katagiri, Nagoya University

- ・ 要旨

Sludge accounts for over 40 percent of industrial waste in Japan, and thus it is of the utmost importance to reduce the waste volume as much as possible. Dewatering by mechanical expression of residual sludge arising from wastewater treatment has become increasingly important due to the relatively low energy consumption compared to thermal drying which follows in the process sequences. Unfortunately, the dewatering rate and moisture content of the compressed cake produced by mechanical expression of biological sludge are currently unsatisfactory.

In this study, a dewatering method by ultrahigh-pressure expression of biological sludge assisted with cell disruption and coagulation processes was developed as an innovative technique to overcome the defects of the conventional mechanical dewatering methods. The moisture content of the compressed cake was finally reduced to 27 wt% by expression under action of an ultrahigh pressure of 10 MPa. This new method shortened the dewatering time of activated sludge compared to the conventional method, and reduced the sludge volume by 99.3 %. The results derived from a series of experiments attained the research goals from the viewpoint of both the dewatering rate and the water content of the compressed cake. It was shown that the complicated kinetics of expression of activated sludge under the ultrahigh-pressure conditions was accurately described using the newly developed multi-stage creep model and that the model will be useful for evaluating the dewatering performance under various operating conditions.

- ・ キーワード

Biological Sludge, Dewatering, Expression, Ultrahigh Pressure, Disruption, Coagulation